Evaluation of the Catchment Parameter (CAPA) and Midgley and Pitman (MIPI) empirical design flood estimation methods.

Ruan Smal

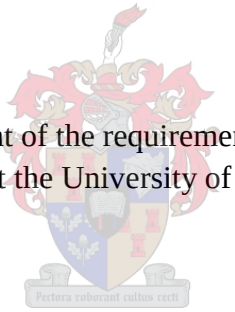

Thesis presented in partial fulfilment of the requirement for the degree of Master of Civil Engineering at the University of Stellenbosch

J.A. Du Plessis
2012 June

By submitting this electronically, I declare that the entirety of the work contained therein is my own, that I am the owner of the copyright thereof (unless to the extent otherwise stated) and that I have not previously in its entirety or in part submitted it for obtaining another qualification.

Date: 08/06/2012

Summary

The devastating effects floods have on both social and economic level make effective flood risk management an essential part of rural and urban development. A major part of effective flood risk management is the application of reliable design flood estimation methods. Research over the years has illustrated that current design flood estimation methods as a norm show large discrepancies which can mainly be attributed to the fact that these methods are outdated (Smithers, 2007).

The research presented focused on the evaluation and updating of the Midgley and Pitman (MIPI) and the Catchment Parameter (CAPA or McPherson) empirical design flood estimation methods. The evaluation was done by means of comparing design floods estimated by each method with more reliable probabilistic design floods derived from historical flow records.

Flow gauging stations were selected as drainage data points based on the availability of flow data and available catchment characteristics. A selection criterion was developed resulting in 53 gauging stations. The Log Normal (LN) and Log Pearson Type III (LP III) distributions were used to derive the probabilistic floods for each gauging station.

The flow gauging stations were used to delineate catchments and to quantify catchment characteristics using Geographic Information Systems (GIS) software and their associated applications.

The two methods were approximated by means derived formulas instead of evaluating and updating the two methods from first principles. This was done as a result of the constraints brought about by both time and the attainment of the relevant literature. The formulae were derived by means of plotting method inputs and resulted in graphs, fitting a trendline through the points and deriving a formula best describing the trendline.

The derived formulae and the catchment characteristics were used to estimate the design floods for each method. A comparison was then done between the design flood results of the two methods and the probabilistic design floods. The results of these comparisons were used to derive correction factors which could potentially increase the reliability of the two methods used to estimate design floods.

The effectiveness of any updating would be the degree (or level) in which the reliability of a method could be increased. It was proven that the correction factors did decrease the difference between the *'assumed and more reliable probabilistic design floods'* and the methods' estimates.

However, the increase in reliability of the methods through the use of the recommended correction factors is questionable due to factors such as the reliability of the flow data as well as the methods which had to be used to derive the correction factors.

Opsomming

Die verwoestende gevolge van vloede op beide ekonomiese en sosiale gebiede beklemtoon die belangrikheid van effektiewe vloed risiko bestuur vir ontwikellings doeleindes. ‘n Baie belangrikke gedeelte van effektiewe vloed risiko bestuur is die gebruik van betroubare ontwerp vloed metodes. Navorsing oor die laaste paar jaar het die tekortkominge van die metodes beklemtoon, wat meestal toegeskryf kan word aan die metodes wat verouderd is.

Die navorsing het gefokus op die evaluering en moontlike opdatering van die Midley en Pitman (MIPI) en die “Catchment Parameter” (CAPA of McPherson) empiriese ontwerp vloed metodes. Die evaluering het geskied deur middel van die vergelyking van die ontwerp vloed soos bereken deur die twee metodes en die aanvaarde, meer betroubare probabilistiese ontwerp vloede, bepaal deur middel van statistiese ontledings.

Vloei meetstasies is gekies as data-punte omrede die beskikbaarheid van vloei data en beskikbare opvanggebied eienskappe. ‘n Seleksie kriteruim is ontwikkel waaruit 53 meetstasies gekies is. Die Log Normale (LN) en Log Pearson Tipe III (LP III) verspreidings is verder gebruik om die probabilistiese ontwerp vloede te bereken vir elke meetstasie. Die posisie van die meetstasies is ook verder gebruik om opvanggebiede te definieer en opvanggebied eienskappe te bereken. Geografiese inligtingstelsels (GIS) is vir die doel gebruik inplaas van die oorspronlik hand metodes.

Die twee metodes is benader deur die gebruik van afgeleide formules inplaas van ‘n eerste beginsel benadering. Dit is gedoen as gevolg van die beperkings wat teweeggebring is deur beide tyd en die beskikbaarheid van die relevante litratuur wat handel oor die ontwikkeling van die twee metodes. Die formules is verkry deur middel van die plot van beide insette en resultate in grafieke, die passing van tendenslyne en die afleiding van formules wat die tendenslyne die beste beskryf.

Die afgeleide formules saam met die opvanggebied eienskappe is toe verder gebruik om die ontwerp vloede van elke meet stasie te bepaal, vir beide metodes. The resultate van die twee metodes is toe vergelyk met die probabilistiese ontwerp vloede. Die resultate van hierdie vergelyking is verder gebruik om korreksie faktore af te lei wat moontlik die betroubaarheid van die twee metodes kon verhoog.

Die doeltreffendheid van enige opdatering sal die mate wees waarin die betroubaarheid van n metode verhoog kan word. Gedurende die verhandeling is dit bewys dat die korreksie faktore wel n vermindering teweebring in die verskil tussen die ontwerp vloede van die aanvaarde meer betroubare probabilistiese ontwerp vloede van beide metodes.

Die toename in betroubaarheid van die metodes deur die gebruik van die voorgestelde korreksie faktore is egter bevraagteken as gevolg van faktore soos die betroubaarheid van die vloei data self asook die metodologie wat gevolg is om die korreksie faktore af te lei.

Acknowledgements

God

Professor A. Görgens (Aurecon)

Professor W.J.R. Alexander (University of Pretoria)

Professor J.C. Smithers (University of KwaZulu-Natal)

Mr J.P. Odendaal (SRK)

Mr A.G. Chemaly (Aurecon)

Miss Z. Els (Aurecon)

Abbreviations

A_e	Effective catchment area (km^2)
ARF	Area reduction factor
C	Catchment coefficient
C_1	Rational method rural runoff coefficient
C_2	Rational method urban runoff coefficient
C_3	Rational method lakes runoff coefficient
CAPA	Catchment Parameter design flood estimation method
CDF	Cumulative distribution function
CN	Curve number
C_p	Runoff coefficient for annual exceedance probability
C_t	Lag Coefficient
D	Duration (hours)
DWAF	Department of Water Affairs and Forestry
FS_DWAF	Flood Studies directorate of the Department of Water Affairs and Forestry
GEV	General Extreme Value distribution
GIS	Geographic Information Systems
HRU	Hydrological Research Unit (of the University of Witwatersrand)
i_p	Average rainfall intensity for annual exceedance probability
k	Storm runoff factor
K	Flood routing factor
L	Longest watercourse (km)
L_c	Centre of gravity of catchment length (km)
LM	L-Moment
LN	Log Normal Distribution
LP III	Log Pearson Type III distribution
M	CAPA lumped parameter
MAP	Mean Annual Precipitation (mm)
MIPI	Midgley and Pitman design flood estimation method
MLP	Maximum Likelihood Procedure
MM	Method of Moment
P	Annual Probability of exceedance (%)
PDF	Probability density function
P_e	Effective storm rainfall
PWM	Probability weighted moments
Q_P	Peak flow for a given annual exceedance probability (m^3/s)
Q_S	Mean annual flood (m^3/s)
RMF	Regional maximum flood (m^3/s)
S	Soil water retention
S_A	Mean catchment slope (m/m)
S_L	Mean river slope (m/m)
SUH	Synthetic Unit Hydrograph
t_c	Time of concentration (hours)
UN	United Nations
W_p	Standardised variant
τ	Correction factor (dependent on the Area)
$\alpha\beta\gamma$	Rational method weighting factors with $\alpha + \beta + \gamma = 1$

Table of Contents

1 INTRODUCTION 1
2 RESEARCH OBJECTIVES AND METHODOLOGY 4
2.1 RELEVANCE 4
2.2 IMPORTANCE 4
2.3 REASONS FOR TOPIC AND METHODOLOGY 4
2.4 OBJECTIVES 5
2.5 METHODOLOGY 6
2.5.1 Literature Review 6
2.5.2 Data Assembly 6
2.5.3 Evaluation and updating of the MIPI and CAPA methods 7
3 LITERATURE REVIEW 8
3.1 KEY CONCEPTS 8
3.1.1 Design flood estimation methodology 8
3.1.2 Drainage Point 9
3.1.3 Elevation Data 9
3.1.3.1 Contours 9
3.1.3.2 Elevation points 9
3.1.3.3 Sources of Elevation Data 9
3.1.4 Catchments 9
3.1.5 Precipitation 10
3.1.5.1 Rainfall Measurement 10
3.1.5.2 Mean Annual Precipitation MAP 11
3.1.6 Runoff 11
3.1.7 Effective Catchment Area (A_e) 12
3.1.8 Mean Catchment Slope (S_A) 12
3.1.9 Longest Watercourse (L) 12
3.1.10 Mean River Slope (S_L) 13
3.1.11 Time of Concentration (t_c) 13
3.1.12 Centre of Gravity of Catchment Length (L_C) 14
3.1.13 Land Surface Cover 14
3.1.13.1 Vegetation 14
3.1.13.2 Soil cover 14
3.1.14 Area Reduction Factor ARF 15
3.1.15 Flow Gauging 15
3.2 DETERMINISTIC DESIGN FLOOD ESTIMATION METHODS 15
3.3 STATISTICAL ANALYSIS 16
3.4 EMPIRICAL DESIGN FLOOD ESTIMATION METHODS FOR SOUTH AFRICA 22
3.5 MIPI METHOD 23
3.6 CATCHMENT PARAMETER (CAPA) METHOD 25
4 QUANTIFICATION OF CATCHMENT CHARACTERISTICS BY MEANS OF GIS 28
4.1 CATCHMENT CHARACTERISTICS QUANTIFICATION PROCESS 28
4.1.1 Drainage points 29
4.1.2 Rasters 29
4.1.3 Digital Estimation Model (DEM) 30
4.1.4 Hydrologically Correct DEM 30
4.1.5 Flow Direction Raster 31
4.1.6 Flow Accumulation Raster 32
4.1.7 Slope 33
4.1.8 Snap Drainage Point 34
4.1.9 Watershed 35
4.2 CATCHMENT CHARACTERISTICS CALCULATIONS 36
4.2.1 Projections 36
4.2.2 Catchment Area 37
4.2.3 Longest Water Course 38
4.2.4 Slope 38
4.2.5 MAP 38
5 DATA COLLECTION AND PROCESSING 40

5.1 DATA COLLECTION PROCESS 40
5.1.1 DEM generation 43
5.1.2 Quantification of Catchment Characteristics 45
5.1.3 Annual maximum flood peak analysis 47
6 RELIABILITY OF DATA 49
6.1 DATA QUALITY AND GOOD PRACTICE 49
6.2 FLOOD PEAK DATA 49
6.3 RAINFALL DATA 51
6.4 GIS GENERATED DATA 52
7 MIPI COMPARISON 54
7.1 METHOD DELINEATION 54
7.2 METHOD EVALUATION 57
7.3 REGIONAL EVALUATION AND UPDATING 57
7.3.1 Region 1 59
7.3.2 Region 2 60
7.3.3 Region 3 62
7.3.4 Region 4 63
7.3.5 Region 5 65
7.3.6 Region 6 66
7.3.7 Region 7 67
7.3.8 Proposed Update for the MIPI Method 68
7.3.9 Evaluation of the proposed updates 69
8 CAPA COMPARISON 71
8.1 DELINEATION OF THE CAPA "M" DIAGRAM 71
8.2 EVALUATION OF CAPA METHOD QUANTIFIED BY Q_S 73
8.3 UPDATING OF THE QUANTIFIED CAPA Q_S 76
8.4 DELINEATION AND EVALUATION OF THE CAPA METHOD DESIGN FLOODS 78
8.5 UPDATING OF THE CAPA DESIGN FLOODS 80
9 CONSIDERATIONS WHEN UPDATING METHODS ESTIMATION OF DESIGN FLOODS 86
9.1 DATA COLLECTION AND EVALUATION 86
9.1.1 Annual flood peak records 86
9.1.2 Catchment characteristics or other input data 87
9.2 METHOD DELINEATION AND EVALUATION 87
9.3 UPDATING OF METHODS OF ESTIMATION OF DESIGN FLOODS 88
10 CONCLUSION 89
11 RECOMMENDATIONS 91
12 REFERENCES 92
A. Appendix A A-1
B. Appendix B B-1
C. Appendix C C-1
D. Appendix D D-3
E. Appendix E E-1
F. Appendix F F-1
G. Appendix G G-1

List of Figures

FIGURE 1: METHODS CATEGORISATION (SMITHERS, 2003) 5
FIGURE 2: HISTOGRAM 16
FIGURE 3: FREQUENCY DISTRIBUTION 17
FIGURE 4: CUMULATIVE DISTRIBUTION 17
FIGURE 5: DIFFERENT MEANS 18
FIGURE 6: DIFFERENT VARIANCE 19
FIGURE 7: DIFFERENT SKEWNESS 19
FIGURE 8: MIPI DIAGRAM (US, 2006) 24
FIGURE 9: HOMOGENOUS FLOOD REGIONS (SANRAL, 2007) 25
FIGURE 10: CAPA 'M' DIAGRAM TO DETERMINE MEAN ANNUAL FLOOD 27
FIGURE 11: ELEVATION RASTER (DEM) WITH 11 COLOUR BANDS 29
FIGURE 12: CROSS SECTION THROUGH A SINK 31
FIGURE 13: DIRECTION CODING 31
FIGURE 14: ELEVATION RASTER MATRIX AND CORRESPONDING FLOW DIRECTION RASTER MATRIX 32
FIGURE 15: FLOW DIRECTION RASTER AND CORRESPONDING DEPRESSIONLESS DEM 32
FIGURE 16: FLOW ACCUMULATION RASTER AND CORRESPONDING FLOW DIRECTION RASTER 33
FIGURE 17: SLOPE RASTER EN CORRESPONDING DEM 34
FIGURE 18: INCORRECT POSITIONING OF DRAINAGE POINT ON FLOW ACCUMULATION RASTER 34
FIGURE 19: MEASURE FUNCTION 35
FIGURE 20: CORRECT AND INCORRECT SNAP DISTANCES ON A FLOW ACCUMULATION RASTER 35
FIGURE 21: WATERSHED FOR A SNAPPED DRAINAGE POINT 36
FIGURE 22: ZONAL STATISTICS TABLE 39
FIGURE 23: SOUTH AFRICAN FLOW GAUGES 40
FIGURE 24: EXCLUDED GAUGES BASED ON THE FIRST SELECTION CRITERIA 42
FIGURE 25: SELECTED GAUGES 43
FIGURE 26: UPSTREAM QUATERNARIES FOR SELECTED GAUGES 44
FIGURE 27: QUATERNARIES FOR J3H004 AND THE SURROUNDING FOUR CONTOUR MAPS 45
FIGURE 28: DEPRESSIONLESS DEMS 46
FIGURE 29: FLOW ACCUMULATION RASTERS 46
FIGURE 30: CATCHMENTS FOR SELECTED GAUGES 47
FIGURE 31: PERCENTAGE DIFFERENCE IN CATCHMENT AREAS 52
FIGURE 32: MIPI DIAGRAM (RIGHT-HAND SIDE OF FIGURE 8) 54
FIGURE 33: MIPI DIAGRAM (LEFT-HAND SIDE OF FIGURE 8) 56
FIGURE 34: ORIGINAL AND ITERATED REGIONAL LINES FOR REGION 1 60
FIGURE 35: ORIGINAL AND ITERATED REGIONAL LINES FOR REGION 2 61
FIGURE 36: ORIGINAL AND ITERATED REGIONAL LINES FOR REGION 3 63
FIGURE 37: ORIGINAL AND ITERATED REGIONAL LINES FOR REGION 4 64

FIGURE 38: ORIGINAL AND ITERATED REGIONAL LINES FOR REGION 5 66
FIGURE 39: OLD, CALCULATED AND PROPOSED REGIONAL LINES FOR REGION 7 68
FIGURE 40: PROPOSED UPDATE FOR THE MIPI DIAGRAM 69
FIGURE 41: EVALUATION OF THE PROPOSED UPDATES FOR THE MIPI DESIGN FLOODS COMPARED TO THE ORIGINAL MIPI METHOD DIFFERENCES. 70
FIGURE 42: LUMPED PARAMETER M VS. CONSTANT C 73
FIGURE 43: CAPA PERCENTAGE DIFFERENCES 73
FIGURE 44: DIFFERENCE IN Q_S PLOTTED AGAINST RANKED MAP CHARACTERISTICS. 74
FIGURE 45: DIFFERENCE IN Q_S PLOTTED AGAINST RANKED CATCHMENT AREA CHARACTERISTICS. 74
FIGURE 46: DIFFERENCE IN Q_S PLOTTED AGAINST RANKED LONGEST WATERCOURSE CHARACTERISTICS. 75
FIGURE 47: DIFFERENCE IN Q_S PLOTTED AGAINST RANKED MEAN CATCHMENT CHARACTERISTICS. 75
FIGURE 48: ORIGINAL QS DIFFERENCES COMPARED TO UPDATED QS DIFFERENCES 78
FIGURE 49: MAP VS. DWAF FACTOR 79
FIGURE 50: PATTERN IDENTIFIED BETWEEN DIFFERENCES AND K_P (10 YEAR RECURRENCE INTERVAL) 80
FIGURE 51: K_P VALUES PLOTTED AGAINST MAP FOR THE 5 YEAR RECURRENCE INTERVAL. 81
FIGURE 52: K_P VALUES PLOTTED AGAINST MAP FOR THE 10 YEAR RECURRENCE INTERVAL. 82
FIGURE 53: K_P VALUES PLOTTED AGAINST MAP FOR THE 20 YEAR RECURRENCE INTERVAL. 82
FIGURE 54: K_P VALUES PLOTTED AGAINST MAP FOR THE 50 YEAR RECURRENCE INTERVAL. 82
FIGURE 55: K_P VALUES PLOTTED AGAINST MAP FOR THE 100 YEAR RECURRENCE INTERVAL. 83
FIGURE 57: COMPARISON BETWEEN THE ORIGINAL AND UPDATED DIFFERENCES FOR THE 1:5 YEAR RECURRENCE INTERVAL 84
FIGURE 58: COMPARISON BETWEEN THE ORIGINAL AND UPDATED DIFFERENCES FOR THE 1:10 YEAR RECURRENCE INTERVAL 84
FIGURE 59: COMPARISON BETWEEN THE ORIGINAL AND UPDATED DIFFERENCES FOR THE 1:20 YEAR RECURRENCE INTERVAL 84
FIGURE 60: COMPARISON BETWEEN THE ORIGINAL AND UPDATED DIFFERENCES FOR THE 1:50 YEAR RECURRENCE INTERVAL 85
FIGURE 61: COMPARISON BETWEEN THE ORIGINAL AND UPDATED DIFFERENCES FOR THE 1:100 YEAR RECURRENCE INTERVAL 85

List of Tables

TABLE 1: PEOPLE AFFECTED IN SOUTH AFRICA BY NATURAL DISASTERS 1
TABLE 2: CORRECTION FACTORS FOR TIME OF CONCENTRATION 13
TABLE 3: VALUES OF K_P FOR VARIOUS PROBABILITIES OF EXCEEDANCE 27
TABLE 4: AFRICA ALBERS EQUAL ALBERS *MODIFICATIONS* 37
TABLE 5: ABSCISSA VALUES (Y) FOR MIPI RECURRENCE INTERVALS AND REGION INTERSECTIONS 56
TABLE 6: STATISTICAL CHARACTERISTICS OF THE FLOOD MAGNITUDE DIFFERENCES IN PERCENTAGE 57
TABLE 7: REGION 1 DIFFERENCES IN PERCENTAGE 59
TABLE 8: ORIGINAL AND ITERATED Y-VALUES FOR REGION 1 59
TABLE 9: REGION 2 DIFFERENCES IN PERCENTAGE 60
TABLE 10: ORIGINAL AND ITERATED Y-VALUES FOR REGION 2 61

TABLE 11: REGION 3 DIFFERENCES IN PERCENTAGE 62
TABLE 12: ORIGINAL AND ITERATED Y-VALUES FOR REGION 3 62
TABLE 13: REGION 4 DIFFERENCES IN PERCENTAGE 63
TABLE 14: ORIGINAL AND ITERATED Y-VALUES FOR REGION 4 64
TABLE 15: REGION 5 DIFFERENCES IN PERCENTAGE 65
TABLE 16: ORIGINAL AND ITERATED Y-VALUES REGION 5 65
TABLE 17: REGION 6 DIFFERENCES IN PERCENTAGE 66
TABLE 18: REGION 7 DIFFERENCES IN PERCENTAGE 67
TABLE 19: ORIGINAL AND ITERATED Y-VALUES FOR REGION 7 67
TABLE 20: PROPOSED NEW ABSCISSA Y VALUES FOR THE MIPI METHOD 68
TABLE 21: STATISTICAL CHARACTERISTICS COMPARISON BETWEEN UPDATED AND ORIGINAL MIPI DIFFERENCES 69
TABLE 22: CALCULATED CONSTANT B AND C 72
TABLE 23: ABSOLUTE DIFFERENCE AVERAGES FOR CLUSTER 1 AND 3 AND THE DERIVED CORRECTION FACTORS. 76
TABLE 24: VALUES OF KP FOR VARIOUS RECURRENCE INTERVALS (US, 2006) 78
TABLE 25: CALCULATED FACTORS C AND B FOR DIFFERENT RECURRENCE INTERVALS 79
TABLE 26: STATISTICAL CHARACTERISTICS FOR THE DIFFERENCES BETWEEN THE CAPA AND PROBABILISTIC DESIGN FLOODS 80
TABLE 27: DERIVED K_P VALUES 83
TABLE 28: COMPARISON OF STATISTICAL CHARACTERISTICS BEFORE AND AFTER UPDATING 83
TABLE 29: CORRECTION FACTOR FOR Q_S 85
TABLE 30: DERIVED K_P VALUES 85
TABLE 31: GAUGE SPECIFIC DATA IN QUATERNARIES A TO D A-1
TABLE 32: GAUGE SPECIFIC DATA IN QUATERNARIES E TO R A-2
TABLE 33: GAUGE SPECIFIC DATA IN QUATERNARIES S TO X A-3
TABLE 34: DISTRIBUTION SPECIFIC PROBABILISTIC FLOODS IN QUATERNARIES A TO D B-1
TABLE 35: DISTRIBUTION SPECIFIC PROBABILISTIC FLOODS IN QUATERNARIES E TO R B-2
TABLE 36: DISTRIBUTION SPECIFIC PROBABILISTIC FLOODS IN QUATERNARIES S TO X B-3
TABLE 37: MIPI DESIGN FLOOD EVALUATION FOR REGION 1 TO 3 ..... C-1
TABLE 38: MIPI DESIGN FLOOD EVALUATION FOR REGION 4 TO 7 ..... C-2
TABLE 39: EVALUATION OF THE PROPOSED MIPI UPDATES FOR REGION 1 TO 3 ..... D-3
TABLE 40: EVALUATION OF THE PROPOSED MIPI UPDATES FOR REGION 4 TO 7 ..... D-4
TABLE 41: EVALUATION AND UPDATING OF Q_S FOR SLOPES BETWEEN 0 AND 0.043 M/M E-1
TABLE 42: EVALUATION AND UPDATING OF Q_S FOR SLOPES BETWEEN 0.063 AND 0.545 M/M E-2
TABLE 43: EVALUATION OF THE CAPA DESIGN FLOODS FOR GAUGES WITHIN QUATERNARIES A TO C F-1
TABLE 44: EVALUATION OF THE CAPA DESIGN FLOODS FOR GAUGES WITHIN QUATERNARIES D TO Q F-2
TABLE 45: EVALUATION OF THE CAPA DESIGN FLOODS FOR GAUGES WITHIN QUATERNARIES R TO X F-3
TABLE 46: EVALUATION OF THE UPDATED CAPA DESIGN FLOODS WITHIN QUATERNARIES A TO C G-1
TABLE 47: EVALUATION OF THE UPDATED CAPA DESIGN FLOODS WITHIN QUATERNARIES D TO Q G-2
TABLE 48: EVALUATION OF THE UPDATED CAPA DESIGN FLOODS WITHIN QUATERNARIES R TO X G-3

1 Introduction

South Africa has borne witness to seventy four (74) natural disasters between 1920 and August 2006 (EM-DAT, 2007) which met at least one of the following four criteria:

- 10 or more people reported killed
- 100 or more people reported affected
- Declaration of a state of emergency or a
- Call for international assistance

The seventy four (74) natural disasters consist of: floods (26), wind storm (17), droughts (8), earthquakes (8), epidemics (6), wild fires (7), extreme temperatures (1) and slides (1). To provide an indication of the distribution of these disasters and the magnitude of the devastation they caused, Table 1 summarises the number of people either killed, injured, affected in other ways, left homeless, as well as the total number affected.

Table 1: People affected in South Africa by natural disasters

Disaster	Killed	Injured	Affected	Homeless	Total Affected
Drought	-	-	17,475,000	-	17,475,000
Earthquake	70	163	1,285	-	1,448
Epidemic	271	-	99,633	-	99,633
Extreme Temperature	30	-	-	-	-
Flood	1,161	49	142,116	32,085	174,250
Slides	34	-	-	-	-
Wind Storm	194	983	614,150	8,700	623,833
Wild Fires	68	505	1,000	4,250	5,755
Total	1,828	1,700	18,333,184	45,035	18,379,919

From Table 1 it is clear that droughts affected the greatest number of people followed by wind storms. This is due to the fact that droughts occur over large parts of the country and normally for long periods of time. Wind storms, on the other hand, affected a large number of people due to the fact that they were spread over large areas. These wide spread areas sometimes included cities and towns which increased the number of people affected.

Table 1 further illustrates that floods accounted for more than 60% of deaths caused in South Africa over the 86 years between 1920 and 2006. On the basis of the data presented in Table 1, floods have caused more deaths than all other natural disasters combined. This is recognised as a worldwide trend and the United Nations has supported these findings by stating that:

> "…… *of all the natural phenomena capable of producing disasters, flooding is by far the most significant in causing loss of life. The severity of such disasters is often increased several fold by the after effects such as diseases and starvation*" (UN, 1976).

Verification of the devastation by floods caused in South Africa is best illustrated by the February-March 2000 floods. These floods have been described as the worst humanitarian disasters to affect the subcontinent (Alexander, 2001).

According to The International Conference on Total Disaster Risk Management held in 2003 (ADRC, 2007) a flood (which is also classified as a *hydro meteorological hazard)* can be defined as:

> *"overflowing by water of the normal confines of a stream or other bodies of water, or accumulation of water by drainage over areas which are not normally submerged"* (ADRC, 2007).

Flooding occurs when water flows or ponds over areas that are not normally subjected to these conditions. In order for this to happen, an influx of water is required into an area which exceeds the volume of water which the area is able to drain without overtopping regular flow confines.

The main cause of this arises from abnormal precipitation (rainfall) over the catchment (a catchment being an area of land that drains water to a drainage point) feeding the area. Other minor causes also include the melting of snow, release of water from dams, and the malfunction of large water supply structures such as pipes and reservoirs.

Civil engineers, along with scientists, are primarily responsible for minimising these effects, which largely shifts the responsibility onto them to protect vulnerable and unsuspecting civilians. This is accomplished through risk management, as the magnitude and random occurrence of flood events make it impossible to completely prevent floods. Risk management is achieved through the effective design and construction of flood routing and retention structures, as well as the implementation of early warning systems and the identification and marking of flood prone areas

In order to apply effective flood risk management a thorough understanding of the processes that cause floods is required as well as a knowledge of the magnitude of the expected flood peaks and the associated risk, knowledge of the appropriate flood hydrological methods to determine the magnitude, and knowledge of the procedures that can be implemented to reduce the associated risks (Alexander, 2001).

In South Africa, flood hydrology has come in leaps and bounds over the last 90 years. During 1919 the Department of Irrigation (now the Department of Water Affairs, DWA) issued the first paper on flood hydrology in South Africa titled *'Maximum flood curves'* in its Professional paper series (US, 2006). This design flood estimation method was the only acknowledged method for flood determination in South Africa at that time. It was developed over the next 50 years transforming the method from a pure empirical method to a statistically based method (Alexander, 1990).

The most comprehensive studies on flood hydrology in South Africa to date were carried out by the Hydrological Research Unit (HRU) of the University of the Witwatersrand at the request of the South African Institution of Civil Engineering. Their first report was published in 1969 (US, 2006).

Some methods proposed in the report, as well as in some of the follow up HRU reports were actually developed a few years before the first report was published (US, 2006). Recent reviews of design flood estimation by Smithers and Schulze (Smithers, 2003) indicate that, relative to other countries, little new research into techniques for design flood estimation has been conducted in South Africa since the early 1970s.

Further research done in 1990 for the South African Department of Transport, on the accuracy of existing design flood estimation methods, showed that there were unacceptably large discrepancies in the results of the methods currently being used and recognised (Smithers, 2003).

Further research carried out on the Mkomaas River in Natal, South Africa, later confirmed these large discrepancies. Alexander concluded that there are serious deficiencies in some of the design flood methods, and that these were primarily related to a lack of understanding of the properties of the flood producing rainfall event (Alexander, 2001).

Despite the unacceptably large discrepancies and importance of reliable design flood estimation in flood risk management, the design flood estimation methods that were proposed and developed in the 1970's and earlier, are still being used today i.e. 2012. There are exceptions where a few methods have in some or other way been updated during the last three decades.

2 Research Objectives and Methodology

2.1 Relevance

Reliable design flood estimations are essential in order to apply effective flood risk management. Given the necessity for reliable design flood estimations, a gloomy picture was sketched in Section 1 concerning the reliability of most design flood estimation methods used in South Africa.

There has been a need to address the deficiencies in the reliability of design flood estimation methods for many years, if not for at least two (2) decades. This could have be done either by updating existing South African design flood estimation methods, or through the development of new more reliable design flood estimation methods.

2.2 Importance

The foremost way in which the reliability of existing design flood estimation methods can be improved or more reliable methods developed is through in-depth research into the numerous factors that influence the reliability of the methods.

This thesis is intended to evaluate the reliability of two empirical methods and to suggest possible amendments to the methods which could potentially increase their reliability. The research has identified numerous factors which influence the reliability of the two design flood estimation methods. The findings arising from this research can be used to:

(a) increase the reliability of the two methods; and
(b) contribute towards future research in methods for the estimation of design floods.

2.3 Reasons for Topic and Methodology

The categorisation of flood analyses methods has been attempted by numerous experts and researchers (Smithers, 2003). Figure 1 illustrates the categorisation as presented by Smithers. Design flood estimation methods are primary categorised into three main categories, namely:

- Statistical
- Deterministic
- Empirical

The research in this thesis has focused on two empirical design flood estimation methods, along with statistical methods and analyses. Both of these categories form part of the stream discharge analyses categories illustrated in Figure 1. Deterministic design flood estimation methods fell outside the scope of this thesis and were not considered in detail.

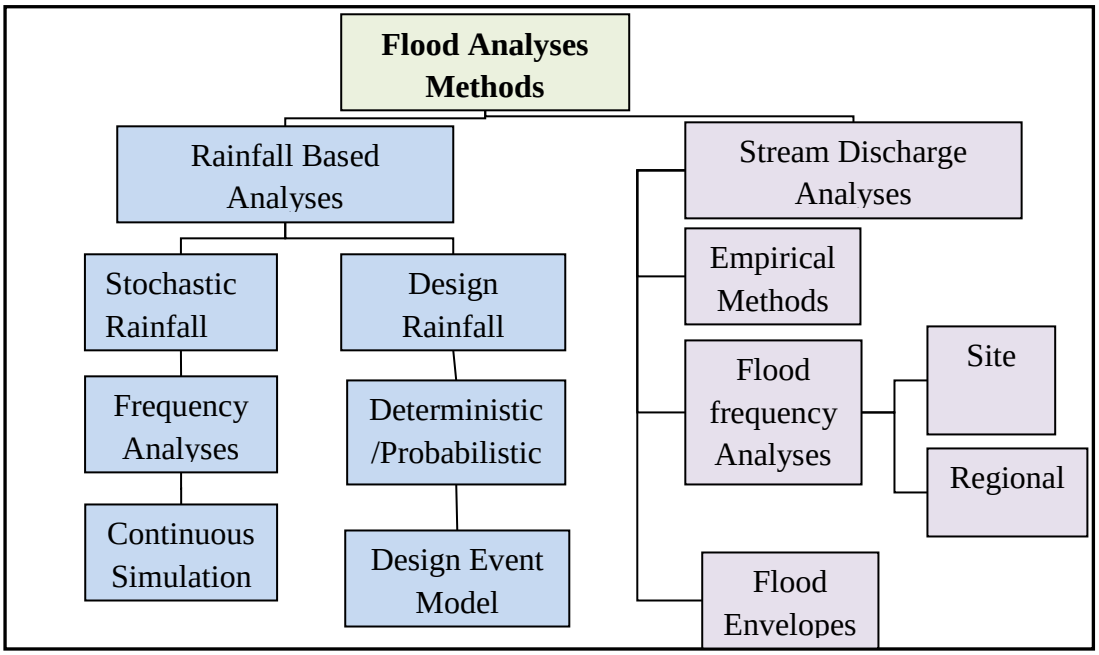

Figure 1: Methods Categorisation (Smithers, 2003)

The concern regarding the reliability of design estimation methods has already been highlighted in Section 1. Despite these concerns raised by numerous experts and DWA, the methods were still being applied and recognised in South Africa

The successful updating of design food estimation methods was necessary. Research completed since the development of design flood estimation methods helped to identify numerous facts about flood hydrology – especially shortcomings in the design flood estimation methods – which helped with the improvement and updating of these design estimation methods (US, 2007).

The other major factor which contributed to the improvement and updating of these methods was access to longer data records. Records consist of more than 30 years of additional flow data, which greatly improved the reliability of the dataset which could be used to calibrate the design flood estimation methods (US, 2007). The application of computers and specialised software also considerably decreased the time required to compute and apply data.

2.4 Objectives

The broader objective of this research is to help address the current shortcoming experienced in design flood estimation methods used in South Africa. The main objective of the study was to identify factors which would require consideration during the updating of the two considered empirical design flood estimation methods. This could potentially assist in the development of methodologies to update flood design methods.

The main objective was achieved by means of satisfying the secondary objective, namely that of evaluating and updating two empirical design flood estimation methods, and addressing their apparent deficiencies. The two methods which were considered included the Catchment Parameter (CAPA) and the Midgley and Pitman (MIPI) design flood estimation methods, which are add are addressed in much greater detail in later sections of this thesis.

2.5 Methodology

The proposed methodologies followed during this research included the following phases.

2.5.1 Literature Review

The research commenced with an in-depth review of key concepts which were also reported on. These key concepts included conventional concepts and principles used in hydrology and design flood estimation methods. This approach also served as an aid to obtain an improved understanding of the most commonly used design flood estimation methods and concepts.

The main design flood estimation methods commonly used and applied in South Africa were also considered, although the main focus was on the methods and groups of methods which formed part of the research.

Research was also done on the application of GIS software packages to delineate catchments and quantify catchment characteristics. The literature review of GIS software packages was also used for the quantification of catchment characteristics as part of the data assembly process.

2.5.2 Data Assembly

Data assembly focused on the collection of information and was used to derive the necessary data to evaluate and improve the reliability of the two empirical design flood estimation methods. This data included the position of flow gauging stations as well as flow records from which the annual maximum flood peaks could be derived.

Two important factors that required special consideration were the reliability of flow records and denaturalisation of flow records as a result of upstream influences. Relevant information regarding these influential factors was collected, evaluated and used to derive selection criterion for suitable gauging stations. This was done in order to increase the reliability of the flow data used as well as to minimise the impact of denaturalised data on the research.

The selection criterion was used to select a sample of gauging station with a sound distribution over South Africa. The *'soundness of distribution'* was improved by ensuring that each of the 22 primary drainage regions had at least one gauging station. This concluded the selection process which yielded 53 gauging stations.

Flow records of each of the 53 gauging stations were then statistically analysed to estimate the probabilistic floods for each gauge. This was done by means of applying the Log Normal and Log Pearson Type III distributions and selecting the best fitting distribution. This concluded the derivation of probabilistic floods against which the methods were evaluated and updated.

With the positions of the gauging stations known GIS was used to delineate the catchment for the each gauging station and to quantify the catchment area. GIS was used to quantify all the applicable catchment characteristics (see 3.1.4 titled *'Catchments'*).

2.5.3 Evaluation and updating of the MIPI and CAPA methods

The evaluation of the MIPI and CAPA methods commenced with the delineation of each method. Errors associated with computing values from graphs, utilised by both methods, were initially addressed by deriving formulae which the graphs could surrogate with. These formulae, along with the quantified catchment characteristics, were then used to derive the design floods for each method.

These design floods were then evaluated against the floods determined using probabilistic methods. The results from this evaluation were noted and patterns identified which aided in updating of the MIPI and CAPA methodology. The lack of available information on the original methodology and data used to develop the methods necessitated the use of derived formulae instead of updating the methods from first principles.

The entire thesis was dissected (or scrutinised) with the aim of confirming the correctness of suggested improvements: It was concluded by making recommendation on factors which would require special consideration and possible methodologies which should be followed when attempting to improve the reliability of design flood estimation methods through updating.

3 Literature Review

As was stated in Section 2 titled *'Methodology'*, the purpose of this part of the research was to collect all relevant information from literature reviewed. The first step focused on outlining of key concepts relevant to flood hydrology and design flood estimation methods. This was followed by focussing on two design flood estimation methods. Special attention was given towards the CAPA and MIPI design flood estimation methods as well as the statistical analyses of records of annual flood peaks.

3.1 Key Concepts

It is important to understand the building blocks (or key concepts) of existing methods of design flood estimation as well as concepts used in the wider field of flood hydrology. This section (section 3.1) focused on key design flood estimation concepts and the methodologies normally followed in design flood estimation.

3.1.1 Design flood estimation methodology

The design flood estimation process starts at the point in a catchment where a design flood is required for planning, design (e.g. spillways for dams, bridges, river engineering, drainage and stormwater structures) and, disaster management or flood risk management. This point of a catchment is normally referred to as the drainage point. A selection is then made on the type of design flood estimation method(s) which will be used in the analyses depending on the data available at that particular drainage point.

The estimation of design floods from statistical analyses (probabilistic floods) of annual peak flood records is considered to be the most reliable method. This is however only possible if reliable flow records are available at the drainage point or a point just up- or downstream of the drainage point.

The absence of flow records necessitates the use of either deterministic or empirical design flood estimation methods. All these methods require some or other catchment characteristics inputs which first need quantification. The first step in the use of these methods is to delineate the catchment which can either be done manually, or through the application of software. Given the known boundaries (watershed) of the catchment enables the user to quantify the other required catchment characteristics using manual methods or by means of appropriate GIS type software.

The catchment characteristics are used as *'input'* into the methods to estimate design floods for given recurrence intervals. Comparison of the results of the different methods results as well as calibration (if possible) can be used to increase the reliability of estimated design floods.

3.1.2 Drainage Point

Design flood estimation is always done at a specific drainage point, also known as the catchment outlet. This point is then used as reference from which the catchment can then be delineated.

3.1.3 Elevation Data

Catchment delineation requires the identification of watersheds which is identified from elevation data, normally contours, which is used to derive and quantify other catchment characteristics.

3.1.3.1 Contours

Contours are defined as lines that connect points with the same elevation. These lines are normally spaced at specific elevation intervals. Contours can be generated via either an analogue or digital processes which could include interpolation between elevation points.

3.1.3.2 Elevation points

An elevation point is defined as an elevation at a certain horizontal coordinate point. Elevation points are generally reference points which were determined for trigonometrical calculations. More recently, satellite radar is used to determine elevation points at predetermined intervals and provides the user with a grid of elevation points for use in GIS applications related to hydrological studies.

3.1.3.3 Sources of Elevation Data

The Chief Directorate of Surveys and Mapping is the South African Government institution responsible for mapping and surveys in South Africa and all data associated with it, including elevation data. Contours and elevation points are made available by them to the public in numerous forms which includes orthographical maps, ground photos with contours draped on to them or shape files for GIS application.

Elevation data is also available from numerous other sources such as providers of GIS application software. The only other source worth mentioning is NASA (NASA, 2007). Elevation data in the form of elevation points and DEM can be downloaded from their website. Contours were used as the primary elevation data during the research for this thesis.

3.1.4 Catchments

The catchment for a drainage point can only be accurately defined if the set of elevation data covers the catchment draining towards the drainage point. A catchment is defined as the area where precipitation resulting in runoff accumulates and drains to and through the particular drainage point.

When manually done, the boundaries of a catchment are normally identified on contour maps by plotting watersheds which separate areas that drain through the same drainage point from areas that will not drain through the drainage point.

GIS software can also be used to determine catchment areas, as well as most of the other catchment characteristics. The use of GIS and the methodology employed by this software will be discussed in further detail in section 4.

All, if not most, methods of design flood estimation that have been developed make use of one or more catchment characteristics that influence the drainage characteristics of catchment. These characteristics can only be quantified once the catchment has been identified. In most research studies, research programmes and actual methods of flood determination, some of the parameters that influence the drainage characteristics of a catchment include:

- The effective catchment area (A_e).
- Mean catchment slope (S_A).
- Longest watercourse (L).
- Mean river slope (S_L).
- Centre of gravity of catchment length (L_C).
- Land surface cover.
- Time of concentration (t_c).
- Precipitation characteristics which include:
    - Rainfall intensity
    - Rainfall distribution over time
    - Aerial distribution of rainfall
    - Direction of storm movement

3.1.5 Precipitation

Precipitation is the process where water in any form (rain, snow, hail) falls to the surface of the Earths, with rainfall being primarily responsible for the occurrences of floods in South Africa. The severity of a flood is primarily determined by the intensity, duration and distribution of the flood-producing rainfall event.

Rainfall characteristics play a major role in floods and thus design flood estimation. The collection of precipitation data is therefore just as important as reliable flow records to enable design floods to be estimated (or determined) with reasonable accuracy.

3.1.5.1 Rainfall Measurement

Rainfall can be measured using numerous different methods, for example, the most acceptable method used to date was (and still is) manually-recording rain gauges (24hr rainfall data). The data collected through this method is of great value and the primary source of rainfall data in South Africa. It is predicted that the use of radar and satellite will

replace this method in the future. These two methods of measurement have the advantage of providing real-time and areal estimation instead of only point rainfall.

The use of rainfall data is essential in design flood estimation, and is incorporated into almost all design flood estimation methods through one or other characteristic calculated from rainfall data. For the purpose of this thesis, the most important concept relating to rainfall data is mean annual precipitation (MAP) of a catchment.

3.1.5.2 Mean Annual Precipitation MAP

Rainfall stations in and around a catchment area are primarily used to determine the MAP of that particular catchment. The most commonly used data to determine the MAP is that obtained by assembling rainfall data from 24h rainfall at stations in and around the catchment using the Thiessen Polygon Method. Special care should be given to rainfall stations outside the catchment, for example, any two adjacent stations where rainfall differs considerably due to their topographical positions. Stations which exhibit such differences and are outside a catchment should be excluded from the data set to be used.

The Thiessen Polygon Method subdivides the catchment into areas by bisecting lines which connect the selected rainfall station. Each area is allocated to the station located inside the area. These areas i.e. obtained from sub-division of the main catchment area are calculated (or measured) and expressed as a fraction of the total catchment area. These fractions are then multiplied by the MAP of the corresponding station and summed to determine the MAP for the catchment.

GIS can also be used to quantify the MAP of a catchment: This was used in the research for this thesis and is described in Section 4.

3.1.6 Runoff

When the rate of rainfall exceeds the interception requirements and the rate of infiltration, water starts to accumulate on the surface, rainfall being the flood producing water source in this event. Surface water accumulates in small depressions and hollows (detention) found on the surface. After exceeding these detention capacities, water starts to flow down slopes in a thin film over the surface.

The collective name for these thin films and different sizes of streams is runoff. Runoff can be the result of various different events with precipitation being the major producer of runoff (US, 2007). Other major contributors towards runoff are groundwater in one or other form. An important factor in estimation of design floods is the area over which runoff is generated. This area is known as the effective catchment area.

3.1.7 Effective Catchment Area (A_e)

The effective catchment area (A_e) and flood producing rainfall are the two most important catchment characteristics used in design flood estimation. The area of a catchment consists of the total area of the catchment as defined by the boundaries (watersheds) of the catchment.

The effective catchment area, on the other hand, is the area of the catchment which contributes to the peak runoff of the catchment. Ineffective areas are most often surface depressions such as pans and lakes as well as areas separated by artificial and geological barriers.

The use of the total catchment area instead of effective area is widely applied in South Africa for the estimation of design floods and when using the various methods to determine floods. This is theoretically incorrect, however in many instances the difference between the actual catchment area and the effective catchment area is insignificant and the use of $A_e = A$ is therefore acceptable.

The use of scale representations of catchments is necessary to calculate the effective catchment area. When manually done a planimeter can be used but the most common (or modern) practise is to use GIS, or similar, software to calculate the effective area.

3.1.8 Mean Catchment Slope (S_A)

The manual procedure to calculate the mean catchment slope is to superimpose a grid of at least 50 squares over the catchment on a topographical or contour map. For each grid intersection, a point is drawn as perpendicular as possible to the two adjacent contours. The horizontal distance of each line is measured and converted to the actual distance by scaling the length of the line. The interval between the contours, which represents the height difference, is then divided by the actual horizontal distance to determine the slope for the specific point in the catchment. The mean catchment slope is the calculated by averaging all the slopes calculated at each grid intersection.

Alternatively GIS application can also be used to determine the mean catchment slope. This method of slope calculation is explained in section 4.1.7.

3.1.9 Longest Watercourse (L)

The distance travelled by runoff which takes the longest time to reach the drainage point of a catchment area is known as the longest watercourse. The route travelled consists of a natural channel (L_1) and over land flow (L_2). L_2 is the longest distance between the upstream end of the natural channel, which forms part of the longest watercourse, and the catchment boundary.

These distances can be accurately measured using GIS. Alternatively topographical maps can be used to determine these lengths. Flow paths are also normally well-documented on topographical maps and can be of great help in defining the longest watercourse.

In order to effectively apply the longest watercourse measurement, the slope of the watercourse needs to be quantified. The slope of the watercourse is the main factor that influences the rate of flow and is referred to as the mean river slope.

3.1.10 Mean River Slope (S_L)

The mean river slope is the average slope of the longest watercourse and can be calculated using various methods. The 10-85 method involves use of the difference in elevation and the length between two points to approximate the mean river slope. These points are 10% and 85% of the longest watercourse length, respectively, measured from the drainage point. Other methods include the Equal area method and Taylor-Schwarz method.

The mean river slope and longest watercourse characteristics can be incorporated into various formulas to calculate the time of concentration of a catchment.

3.1.11 Time of Concentration (t_c)

Time of concentration is the approximate time that it will take for a particle of water to travel the entire route of the longest watercourse (US, 2007). Various equations have been developed and proposed. The University of the Witwatersrand recommends use of the United States Bureau of Reclamation equation (US, 2007) where:

$$t_c = \tau \, [\, 0.87 \, L^2 / 1000 \, S_L]^{0.385} \qquad \textbf{Equation 1}$$

With:

- t_c - Time of concentration (hour)
- τ - Correction factor (dependent on size of A)
- L - Length of natural channel (km)
- S_L - Mean channel slope (m/m)

For South African conditions experience has shown that the proposed equation produces to small t_c values for smaller catchments and vice versa Kovacs developed a set of correction factors (unpublished) to overcome this problem (US, 2007). These values area listed in Table 2.

Table 2: Correction factors for time of concentration

A (km^2)	τ
< 1	2
1 - 100	2 - 0.5 log A
100 - 5 000	1
5 000 - 100 000	2.42 - 0.385 log A
> 100 000	0.5

It was found, through a derivation and test done for this research, that the more simplistic Equation 2 produced values of t_c similar to those used in the equation of the US Bureau of Reclamation.

$$t_c = \tau /15 \ (L^{0.77} / S_L^{0.385}) \qquad \textbf{Equation 2}$$

3.1.12 Centre of Gravity of Catchment Length (L_C)

The centre of gravity of a catchment length is the distance measured from the drainage point to a point on the longest watercourse opposite the centre of gravity of the catchment area. The centre of gravity can be determined by GIS application, alternatively the balancing point of a paper cut scaled representation of the catchment area can be found.

3.1.13 Land Surface Cover

Another characteristic influencing runoff over a catchment is the land surface cover. The two main land surface characteristics which influence the runoff and flow is vegetation and soil type.

3.1.13.1 Vegetation

Vegetation is responsible for water retention in a catchment, and also has an influence on the runoff rate of a catchment. This characteristic is normally used in the calculation of runoff coefficients which are used in the deterministic methods of flood estimation. Vegetation can be categorised in four main categories which include:

- Forest.
- Dense bush and woods.
- Thin bush and cultivated land.
- Grassland and bare surfaces.

These categories are mainly grouped on the basis of their ability to obstruct the runoff giving more time for part of the runoff to infiltrate, which in turn is controlled by the soil cover.

3.1.13.2 Soil cover

Soil cover is mainly categorised according to permeability. The four main categories include:

- Very permeable.
- Permeable.
- Semi-permeable.
- Impermeable.

Each category has its own characteristic which should carefully be examined before classification is done for a catchment. Information on soil cover can be obtained for South Africa from standard 1:250 000 soil maps. The identification of Dolomitic areas is a very

important consideration (or factor): These areas may absorb as much as 90 percent of the runoff for underground storage.

3.1.14 Area Reduction Factor ARF

The rainfall associated with flood producing storms is almost never spread evenly in time and distribution over a catchment. It is therefore necessary to reduce the point rainfall depth accordingly by applying an Area Reduction Factor (ARF).

3.1.15 Flow Gauging

Flow gauging is the process where the depth of flow (stage) of a stream or river is measured and the discharge calculated through the use of stage-discharge relationships. A flow gauging station is best defined as follows:

> *"A gauging station is a site on a river (or stream) which has been selected, equipped and operated to provide the basic data from which systematic records of water levels and discharge may be derived. Essentially it consists of a natural or artificial river cross-section where a continuous record stage can be obtained and where a relation between stage and discharge can be determined."* (Lambie, 1978)

The primary measurement taken at a flow gauging station is the stage. These measurements are taken continuously. The discharge is then calculated by applying the stage-discharge relationship calculated especially for each measurement point. This relationship simply provides a discharge quantity given a certain stage measurement and is a function of the dimensions of the structure or river section at the point.

3.2 Deterministic design flood estimation methods

Deterministic design flood estimation methods are used in cases where no flow records or very few flow records exist. Deterministic methods have been developed (or derived) on the basis where it has been assumed that the statistical properties for both floods and storm rainfall are the same, and can therefore be applied in such instances. This assumption is used in more complex conceptual rainfall-runoff models. In essence these rainfall-runoff models are the translation of rainfall and catchment characteristics into design floods. The most commonly used deterministic methods in South Africa are listed below.

- Rational method.
- Direct Runoff Hydrograph.
- Synthetic Unit Hydrograph (SUH).
- SCS-SA method.

. Although they were further research, they were exclude form this thesis. Instead more focus was given on the remaining two design flood estimation categories.

3.3 Statistical Analysis

The main focus of flood analyses is to estimate design floods. Floods, however, are natural, random occurrences, and estimated magnitudes thereof cannot be calculated with absolute certainty. It is, however, possible to quantify the measure of uncertainty through applying concepts and methods of probability to historical flood peaks observed at flow gauging stations. Annual flood peaks and their use in probability analyses will be dealt with later in the section.

Statistical analyses provide powerful tools with which the probability of exceedance or probability of occurrence of particular flood events can be estimated. This is achieved through a technique known as statistical inference. This technique includes a summarising of the flood data either through graphical and/or numerical methods, estimating certain characteristics, and the selection of an appropriate theoretical distribution with which probabilities can statistically be calculated.

The probability can either be expressed as percentage or in the recurrence interval form of 1 in N year flood for the data. A 1 in N year flood has a probability of exceedance of P % of occurrence with:

$$P\ \% = 1/N \times 100\% \qquad \textbf{Equation 3}$$

Data used in probability analyses can be graphically summarised which includes normal histogram, frequency distribution histogram and cumulative distribution. A histogram presents the flood peak record in the form of a graph, with the flood peak plotted on the ordinate and the years on the abscissa, illustrated in Figure 2.

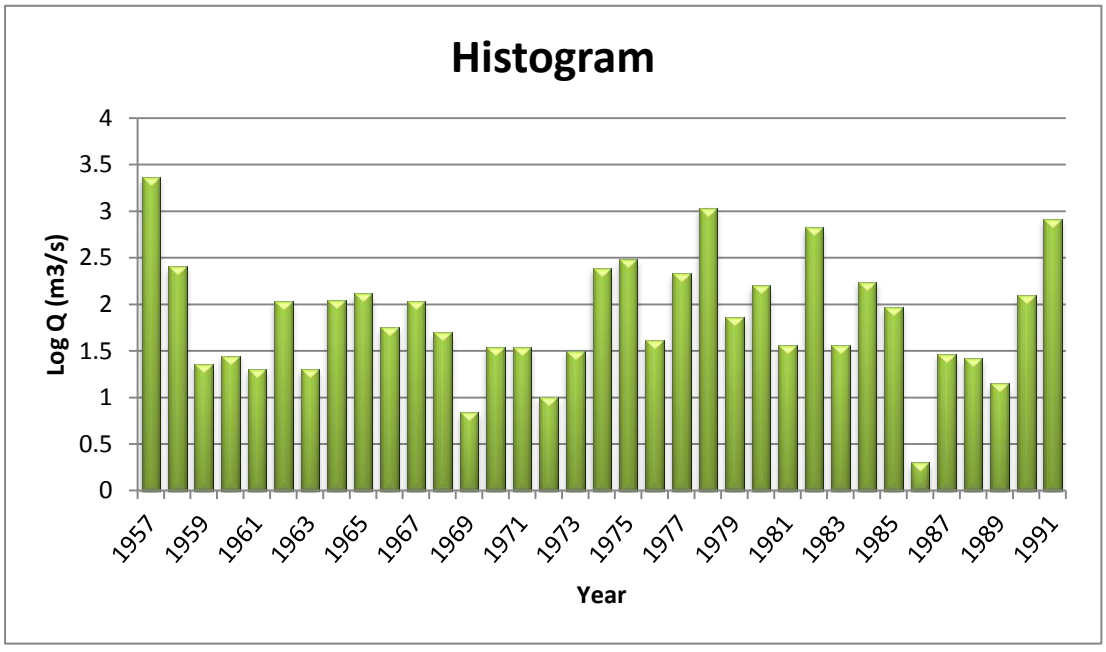

Figure 2: Histogram

The frequency distribution histogram presents the frequency distribution of predetermined ranges by plotting a particular flood peak on the ordinate and its corresponding relative frequency on the abscissa. This is obtained by grouping peak flows into clusters specified by certain intervals. The number of peak flows in each cluster is divided by the total number of peak flows to obtain the relative frequency of occurrence of each cluster. The relative frequency is a rough approximation of the probability of occurrence. An example is illustrated in Figure 3.

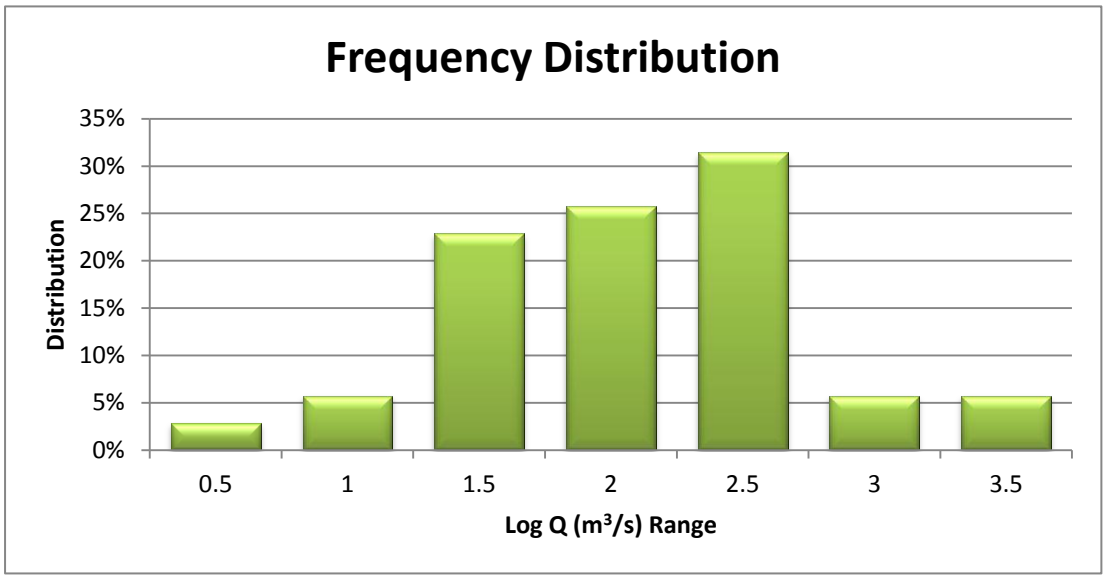

Figure 3: Frequency Distribution

The cumulative frequency diagram is obtained by summing the previously determined relative frequencies of the ranges and plotting it with the flood peak on the ordinate and the corresponding summed relative frequency on the abscissa, illustrated in Figure 4.

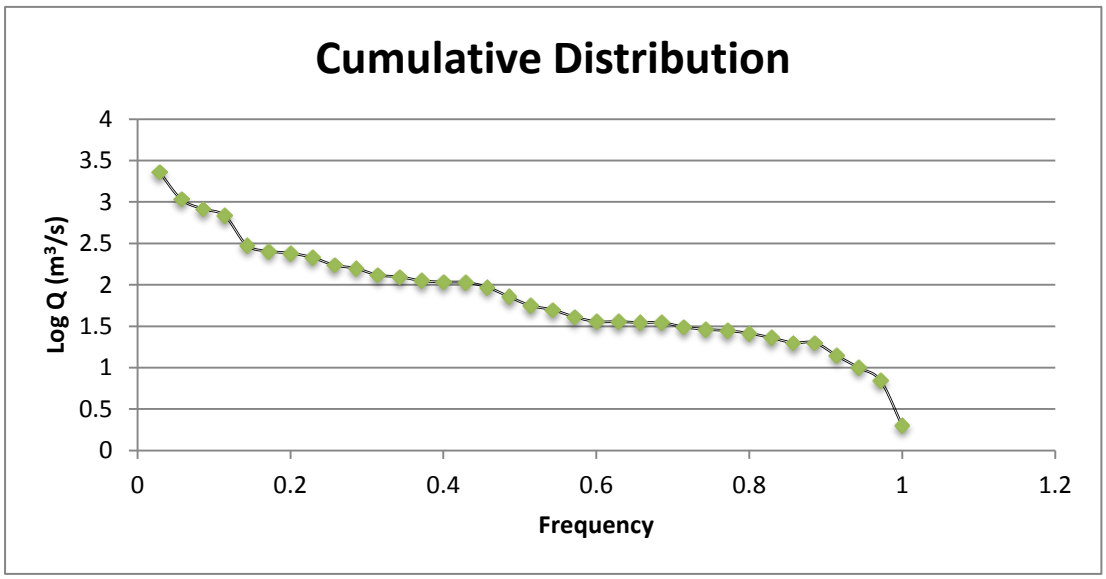

Figure 4: Cumulative Distribution

The parametric description of flood data is commonly used which includes parameters such as the arithmetic mean, mode, median, variance, standard deviation, coefficient of variation and skewness. These parameters (or results are used in formulae for statistical distributions to calculate probabilities of occurrence or exceedance for floods of certain magnitudes.

Figure 5 to Figure 7 illustrates the meaning of these statistical parameters by comparing two probability density function (PDFs) each with arbitrary Y and X values on the axes.

Figure 5 illustrates two PDFs with equal skewness and variance, however PDF 1 (or Dist. 1) has a smaller mean compared to PDF 2 (or Dist. 2).

Figure 6 illustrates two PDFs with equal skewness and means. PDF 1 (Dist. 1), however, has a smaller variance compared to PDF 2 (Dist. 2).

Figure 7 illustrates two PDFs with equal means and variance. PDF 2 (Dist. 2), however, has a smaller skewness compared to PDF1 (Dist. 1).

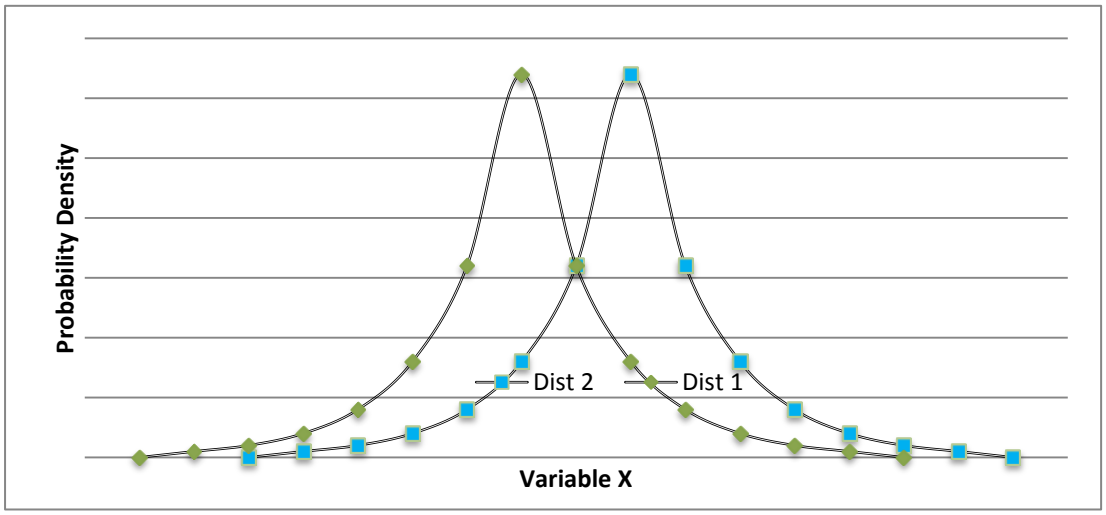

Figure 5: Different Means

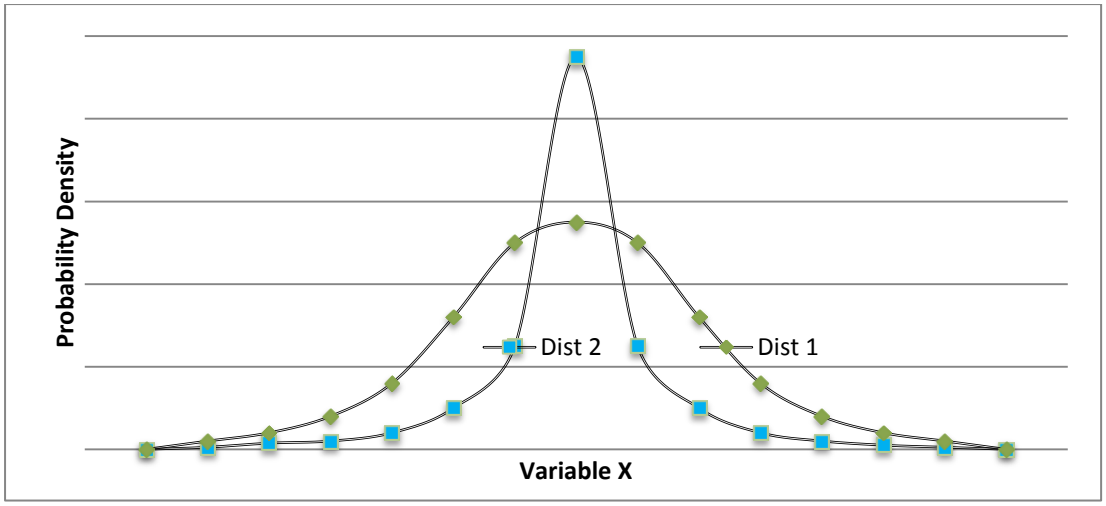

Figure 6: Different Variance

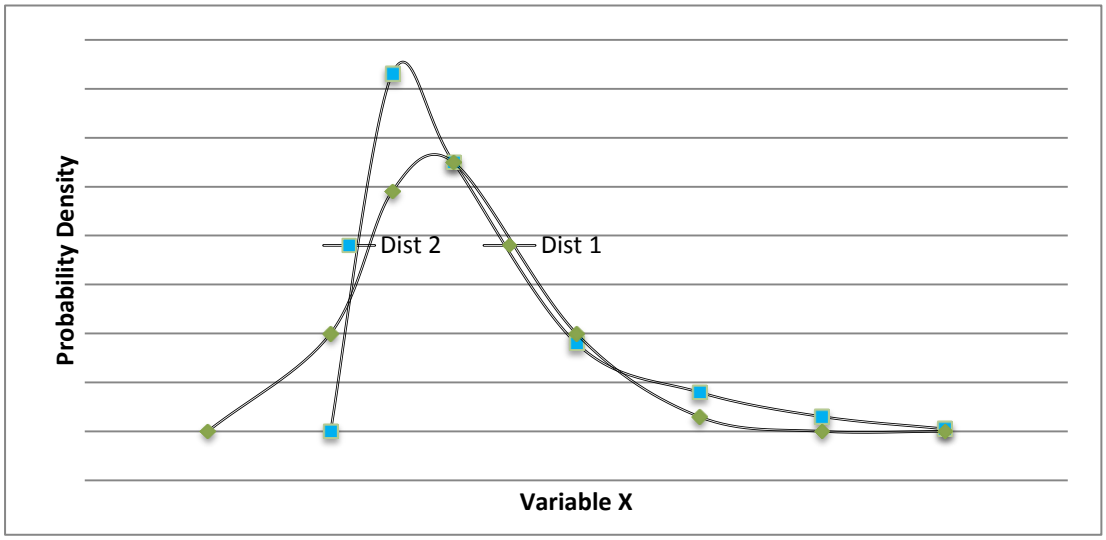

Figure 7: Different Skewness

Historical flood peaks observed at flow gauging stations are used in probability analyses. Because it is highly unlikely that historical flow sequences will be *'exactly'* repeated or duplicated the statistical properties of historical records can be examined and applied to make estimates of the likelihood of events of a given magnitude or *'severity'*. The most powerful *'toolbox'* or methodology that is available when determining or calculating design floods is that which is based on probabilistic analysis carried out using long periods of reliable annual peak flood records.

It should be noted that statistical analyses and the conclusions that are drawn from them, can only be as reliable as the data on which they are based. It is further recommended that no datasets of time periods shorter than thirty (30) years be used for design flood estimations (US, 2006). A thorough examination of all available data should also be carried out and any uncertainties investigated and rectified to obtain the most reliable dataset.

Probability analyses are done by applying probability distributions and their associated functionalities. If the top midpoints of the previously mentioned frequency distribution histogram were joined, the result would be a frequency distribution curve.

The equation which best fits the cumulative frequency distribution polygon is known as the cumulative distribution function or CDF which should have values for probability of exceedance probability that range between zero and one.

The most commonly used probability distribution functions include the normal, log normal, exponential, gamma, Pearson type III, Log Pearson type III, extreme value I (EV1), extreme value II (EV2), extreme value III (EV3), general extreme value (GEV), and Wakeby distributions.

The graphical method of *'statistical analysis or statistical representation of floods'* was the foundation of statistical and probabilistic flood hydrology and makes use of plotting positions such as those of Weibull, Blom, Grinorten or Cunane (US, 2006).

A plotting position represents an empirical estimate of the probability of exceedance or non-exceedance for a given flood peak. This enables the user to plot the corresponding annual exceedance probability on the abscissa on log-probability graphs against the associated flood peak.

A *'best fit'* line is then fitted through the points and enables the user to calculate the magnitude of specific probabilities by reading them from the graph. This graphical representation is not only limited to such use: There is *'built in added value'* when a visual comparison is made between all the data that has been plotted, the *'best fit line (or lines)'* and estimated probability distribution curve which is essential to effective statistical analysis.

The process of calculating plotting positions and then plotting them is relatively time consuming and odious to do. Distribution can be fitted through data using various methods such as the Method of moments (MM), Maximum Likelihood Procedure (MLP), Probability Weighted Moments (PWM), L-Moments (LM), Bayesian Inference and other parametric methods.

The most appropriate method to use is one which receives a great deal of attention in hydrological circles, for example, the L-moment method appears to have a very promising potential for application, research and development, although it has shortcomings. Statistical software has become the norm for fitting probability distribution given the computing power provided by computers.

Experience and research have identified that the distributions which best describe South African conditions are the log normal (LN), log Pearson type III (LP3) and the general extreme value (GEV) distribution.

The LN distribution is a normal distribution logarithm of the values, instead of the natural values. The normal distribution is symmetrical about the mean and is subsequently suitable for data with a skewness coefficient (g) of zero or close to zero. Although hydrological data are usually skewed the logarithms of the data have a near symmetrical distribution.

The LP3 is a Pearson type III distribution logarithm of the values. The Pearson type III distribution is, on the other hand, essentially a gamma distribution but with the mean displaced by a constant from the origin. The gamma distribution is strongly skewed with a lower bound of zero, and makes use of the factorial series 1/n! where n is an integer.

The general form for the probabilistic prediction equation for LP III is:

$$\log Q_p = \overline{\log Q} + S_{\log} \times W_P \qquad \textbf{Equation 4}$$

Where:

$\overline{\log Q}$	-	The mean of the log transformed sample.
$\log Q_p$	-	The log of the required value for exceedance probability.
P	-	Exceedance probability.
$S_{\log}$	-	standard deviation of the log transformed sample.
W_P		standardized variant (available in published tables) which is a function of the skewness of P.

Note: for the Log Normal distribution, determine W_P at skewness, g = 0.

The general extreme value (GEV) distribution is a three parameter distribution. It is generalised from the three extreme value distributions: EV1, EV2 and EV3.

The general form of the GEV equation is:

$$Q_P = \overline{Q} + f_g . S([k.WP + E(y) - 1] / [\sqrt{var(y)}]) \qquad \textbf{Equation 5}$$

Where:

$\overline{Q}$	-	The mean of the flood peak sample data.
Q_P	-	The required flood peak value for exceedance probability P.
f_g	-	$f_g = 1$ for $g < 1.13955$, otherwise $f_g = -1$.
S	-	The standard deviation of the sample data.
W_P	-	The standardised variant.
k	-	Shape characteristic (a function of g).
E(y), var(y)	-	Moments of y, as a function of k.
g	-	Skewness coefficient.

Where sufficient data is available at a drainage point probabilistic design flood estimation can be done on the data and the necessary conclusions drawn after having carried out a thorough statistical analysis. However, in most cases this is not possible because sufficient data is

seldom available for use at a particular drainage point, in which case data from nearby (or adjacent) locations have to be used.

Given the lack of availability of data at or around a drainage point, extensive studies have shown that the results from a regional approach to frequency analysis have proven to be more reliable (Smithers, 2003). Various hydrologists share this view and recommend that this is the best way of reliably estimating design floods (Alexander, 2007). This approach is known as regional frequency analysis and data is utilised from several sites to estimate the frequency distribution of observed data at each site.

A regional frequency analysis assumes that the standard variant has the same distribution at every site in the selected region. Data from a region can therefore be combined to produce a single regional flood or rainfall frequency curve. These would be applicable anywhere in the region with appropriate site-specific scaling and adjustments. Such regionalisation will enable the use of shorted datasets of annual peak floods by assisting with the identification of the shape of the parent distribution and leaving the measures of scale to be estimated from the at-site data (Smithers, 2003).

Regionalisation in the case of statistical inference refers to the identification of homogeneous flood response regions (not necessarily geographically defined) and the selection of an appropriate frequency distribution for the region. This approach can be used to estimate floods at sites where no data is available within the region.

Kkhandi et al. (Smithers, 2000) used the L-moment based procedure developed by Hosking and Wallis (Hosking, 1995) to identify both homogeneous flood producing regions and discordant gauging stations in South Africa. Thirteen homogeneous regions were delineated. The Pearson Type III distribution fitted by the PWM was found to be the most appropriate distribution to use in 12 of the regions. In the western coastal region of South Africa, the LP III distribution fitted by the MM was found to be the most appropriate distribution.

3.4 Empirical design flood estimation methods for South Africa

Empirical methods are mathematical models which are developed to fit available data and are therefore grouped under the Stream Discharge Analyses classifications of all possible flood estimation methods.

By definition empirical methods are not theoretically sound. Nevertheless they are relatively easy to use and have been in use for a very long time i.e. many decades. Early empirical methods were of the form:

$$Q = C.\ A^{k} \qquad \textbf{Equation 6}$$

Where:

Q	-	Design flood peak (m^3/s)
C	-	Independent catchment coefficient

A	-	Catchment area (km^2)
k	-	Constant

No commonly applicable method has been developed for South Africa. The flood studies component of DWAF (FS_DWAF) has made slight improvements to the methods over the years. The ultimate aim however is to combine all of the various methods into one method for the South Africa.

The three most commonly used methods in South Africa are the Midgley and Pitman (MIPI), Catchment Characteristic (CAPA) and the Regional Maximum Flood (RMF) method. Unfortunately there is still no absolute test against which these methods can be compared but experience over the years has shown that certain methods perform better compared to others in specific parts of the country and vice versa.

The focus of this study will be on the CAPA and MIPI methods. These two methods will be dealt with in detail in subsequent sections of this Thesis. The focus of this research falls outside the development of the RMF method which is an easy method to apply and especially helpful in estimating floods peaks for very large return periods.

3.5 MIPI method

The MIPI method can best be described as an Empirical-Probabilistic design flood estimation method which takes the form depicted by Equation 7, below.

$$Q_P = C.\ K_P.\ A^m \qquad \textbf{Equation 7}$$

Where:

Q_P	-	Design flood peak (m^3/s)
C	-	Catchment coefficient
K_P	-	Constant derived from an assumed probability distribution
A	-	Catchment area (km^2)
m	-	Constant (≈ 0.5)
P	-	Probability of exceedance.

The method is based on an earlier method called the Roberts Method (US, 2006). Roberts assumed a value of 0.5 for m and derived K_p from the Hazen frequency distribution. The major objection to this method is that the catchment coefficient (C) shows very wide variations from stream to stream. In addition, the method cannot be related to any region or measured variables. Another weakness is the assumption of the same variance and skewness for all South African rivers inherent to the Hazen distribution. Subsequently, the Roberts method gave way to other methods of design flood estimation, including the MIPI method.

Midgley and Pitman (US, 2006) retained the value of 0.5 for the m constant, but regionalized the catchment coefficient (C). They also made use of the log-Gumbel distribution to derive K_p. A weakness in the method was highlighted in later research carried out by FS_DWAF (US, 2006). This research showed that although the log-Gumbel distribution has a sound

theoretical basis it is less satisfactory than the Hazen, LN and LP III distributions. Another weakness of this method, as per the Roberts Method, is the assumption that the annual peak distributions for all South African rivers have the same variance and skewness.

The method is presented in graphical form in Figure 8. The three important characteristics (or parameters) for estimation are the recurrence interval, the catchment area, and the region which is determined from *'South African homogeneous flood regions'*.

The graph on the left of Figure 8 consists of the recurrence interval on the ordinate axis and seven diagonal regional lines. When applied, the corresponding recurrence interval is projected vertically upwards to a point where it intersects the regional line. The region is determined from the South African homogeneous flood regions diagram depicted in Figure 9. This point is then projected to the right hand side of the MIPI diagram (or Figure 8) to a point where it intersects the corresponding diagonal catchment area lines.

The graph on the right of the MIPI diagram consists of the flood peaks on the ordinate axis, diagonal area lines, and abscissa axis which corresponds to that of the graph on the left side of the diagram.

The intersection between projected line and catchment area intersect is projected vertically downwards to a point where it intersects the ordinate axis. The ordinate intersection represents the design flood peak for a given recurrence interval and area for the catchment.

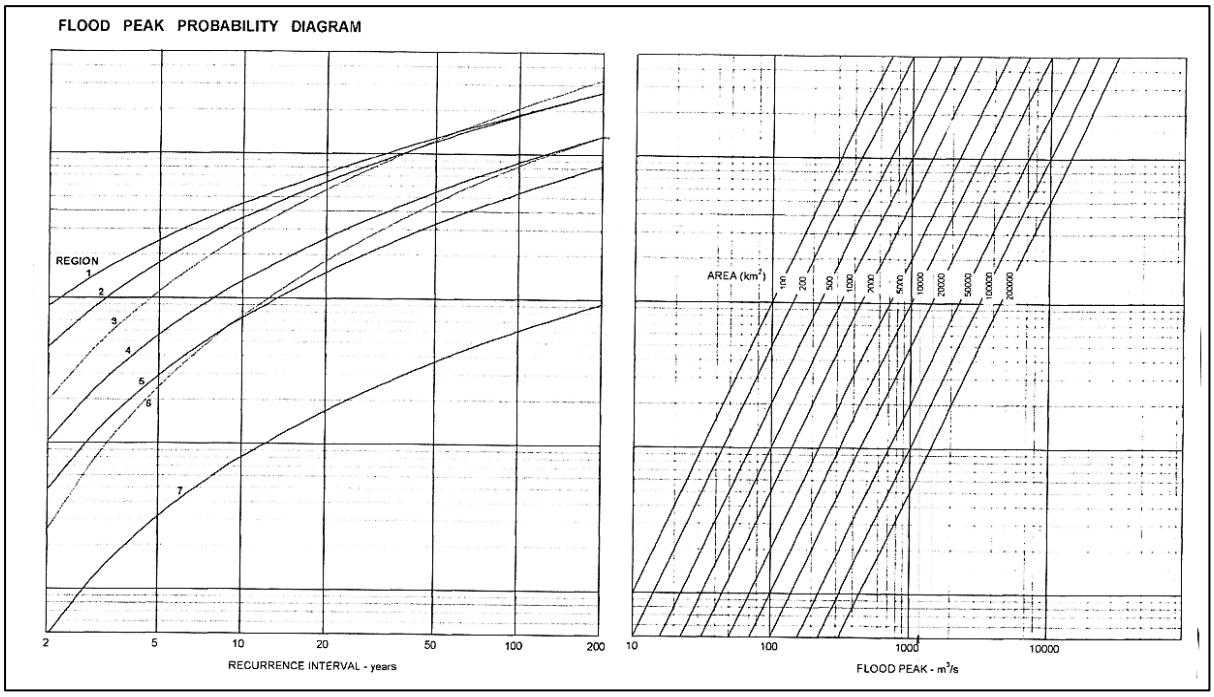

Figure 8: MIPI Diagram (US, 2006)

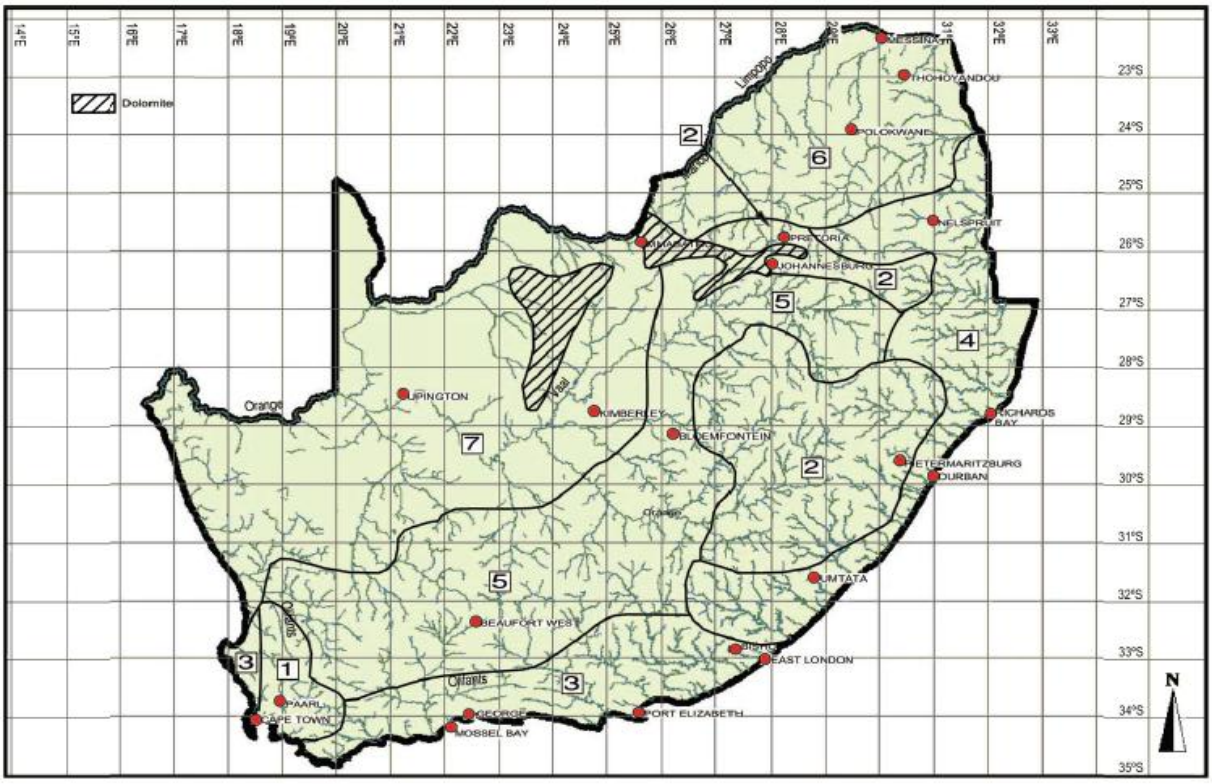

Figure 9: Homogenous Flood Regions (SANRAL, 2007)

3.6 Catchment Parameter (CAPA) method

The CAPA method was developed by McPherson (1983) and stems from an investigation done on methods for estimating the mean annual and 1:2 year floods for South Africa. McPherson (1983) stated that a rapid estimation of design flood peaks in an ungauged catchment requires the following steps:

- Estimation of the mean annual flood (Q_S) or the 1:2 year flood (Q_2).
- The development of a regional flood frequency growth curves by means of statistical analyses of annual maximum flood peak records.
- The restriction of the upper limits of frequency curves by a *'kind of'* maximum flood peak.

McPherson (1983) attempted to solve the first of the three mentioned steps by collecting and analysing hydro meteorological and physiographic data for more than 140 catchments in South Africa. Statistical analysis of the flood peaks revealed that it was preferable to use the mean annual flood, Q_S, instead of the 1:2 year flood, Q_2. The relationship between record length and error in the Q_S estimate was also investigated for various regions in the country (McPherson, 1983).

McPherson further investigated the correlation between Q_P and various catchment characteristics. A method followed this investigation to estimate Q_P, with has several easily obtainable characteristics. This gave rise to the basis of the CAPA method.

The method that was used to quantify the catchment slope in the initial research gave erroneous results (US, 2006). This was later rectified by Thobejane (2001) under the guidance of van der Spuy and Lindström.

The second step was researched to a degree by the Sub-directorate: Flood Studies of the Department of Water Affairs and Forestry (FS_DWAF) in order to be able to apply this methodology to estimate flood peaks for 1:5 to 1:100 year recurrence intervals. Unfortunately these findings have not been published. Research done by FS_DWAF showed that the method regularly produced acceptable estimations for flood peaks compared to other recognised methods (US, 2006).

In investigating the correlation between Q_S and various catchment characteristics, McPherson identified ten catchment characteristics which were likely to have an influence on Q_P. His preliminary analysis showed that four of the ten catchment characteristics were more influential than the other six. The four characteristics included:

- Area (A in km^2)
- Mean Annual Precipitation (MAP in mm)
- Mean Catchment Slope (S_A in m/m)
- Length of the longest watercourse (km) i.e. L (see use, below)
- Shape characteristic which is defined as L divided the square root of A

The area was found to be the most significant of the four characteristics. According to Smithers (2003) other research also concluded that a strong relationship exists between Q_S and the catchment area.

It was found by McPherson (1983) that a graphical plot of the characteristics could be simplified by plotting the mean annual flood (Q_S) on the ordinate axis and the catchment area (A) on the abscissa. The other three characteristics were combined to form a single, lumped characteristic M. M is defined as:

$$M = MAP\ [(S_A\ \sqrt{A})/(L)] \qquad \textbf{Equation 8}$$

Where:

MAP	-	Mean annual precipitation (mm)
S_A	-	Mean Catchment Slope (m/m)
A	-	Size of the catchment (km^2)
L	-	Longest watercourse length (km)

Clusters of lines of equal slope were drawn representing several values for M as illustrated in Figure 10.

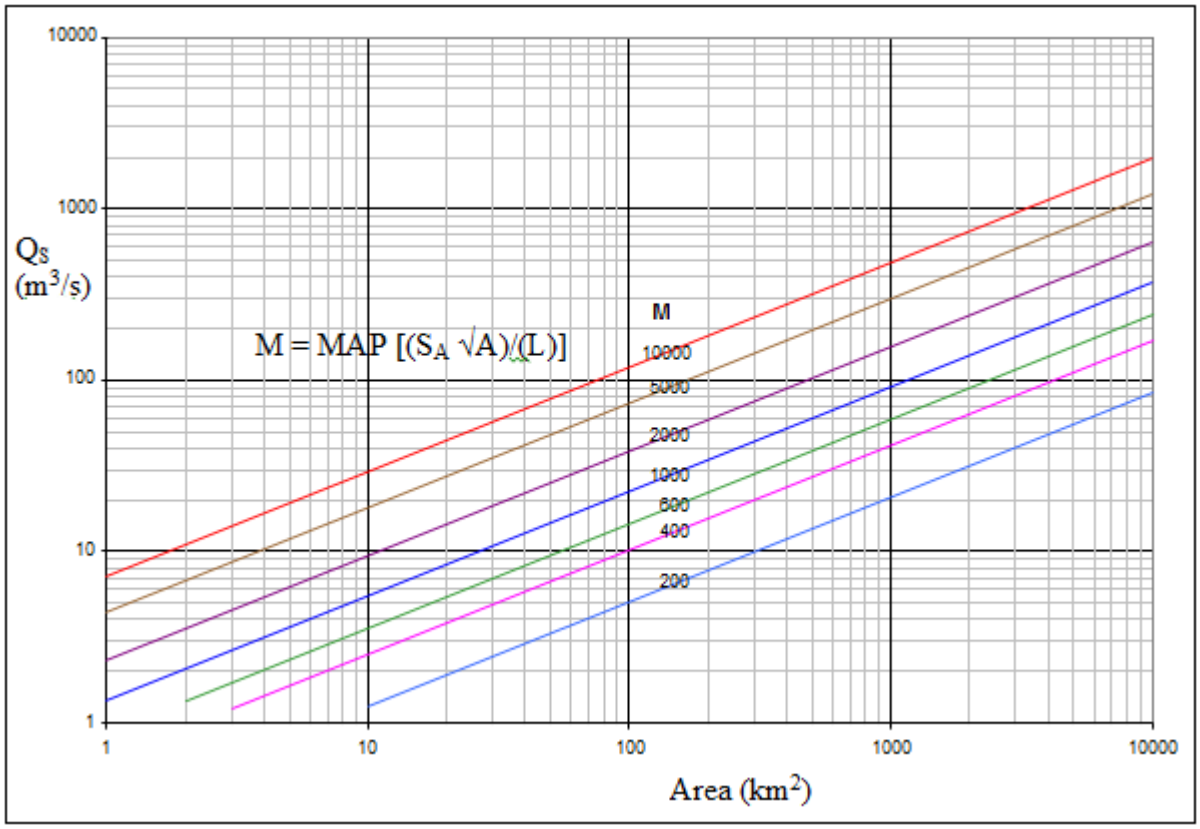

Figure 10: CAPA 'M' diagram to determine Mean Annual Flood

The use of the CAPA method firstly requires the estimation of the catchment area (A), mean annual precipitation (MAP), mean catchment slope (S_A) and longest watercourse (L). The A, MAP, S_A, L characteristics are used to calculate the lumped parameter, M. The lumped parameter and catchment area are then used to estimate the mean annual flood, Q_S.

The mean annual flood is then multiplied by the constant, K_P, to obtain Q_P. K_P is obtained from Table 3 by matching the MAP of the catchment and the probability of annual exceedance for which the design flood is estimated.

Table 3: Values of K_p for various probabilities of exceedance

MAP (mm)	Probability of annual exceedance (%)				
	20	10	5	2	1
100	4.49	9.49	16.97	31.41	45.36
200	3.27	5.96	9.65	16.26	22.15
400	2.47	3.97	5.89	9.13	11.81
600	2.13	3.2	4.52	6.72	8.45
800	1.93	2.76	3.79	5.46	6.75
1000	1.79	2.48	3.32	4.68	5.71
1500	1.57	2.05	2.64	3.58	4.26
2000	1.44	1.8	2.26	2.99	3.5

4 Quantification of catchment characteristics by means of GIS

Geographic information systems (GIS) are software systems used for capturing, storing, analysing and managing data and associated attributes which are spatially referenced. In essence GIS can be described as a tool that allows users to create interactive queries, perform spatial information quantification, store, view, and edit data and maps, and present the results of all these operations in either a graphical or text format.

Graphical representations together with the geographical computing capabilities for the calculation of characteristics such as area and mean catchment slope make GIS a very useful tool for the quantification of catchment characteristics. GIS can also be used to illustrate various data associated with flood hydrology which makes it very valuable to carry out research in this field. Given these advantages together with the very powerful versatility of GIS was the main reason why it was adopted in this research.

GIS is also extensively applied in many technical and scientific disciplines, numerous professions and fields of research: The applications and uses are *'virtually unbounded'*. This section only focussed on the processes and steps required to quantify four catchment characteristics which formed the basis of this research. These included the:

- Catchment Area
- Mean Catchment Slope
- Longest Watercourse
- Mean Annual Precipitation

Extensive use was made of the ESRI ArcView 9.1 *'GIS package'*: Various other versions of this package and other GIS software packages were readily available which could have been used.

4.1 Catchment Characteristics Quantification Process

The initial GIS input data used in the quantification of hydrological catchment characteristics consists of two key data sets. The first key dataset is relevant information required to quantify catchment characteristics such as Digital Elevation Models (DEM) of the area in and around the catchment, MAP, dolomite areas, soil cover, vegetation, and land use data covering the entire catchment.

The second important dataset required for *'quantification'* is the point coordinates of the drainage point (referred to the pore point in GIS) for which design flood estimation is required. Details (or particulars) of the drainage point are used in the DEM are initially used to define the catchment. Additional datasets are then generated and used with GIS tools to quantify the remaining catchment characteristics.

The following concepts described in sub-sections 4.1.1 to 4.1.9, inclusive, helped to provide a better understanding of the process required to quantify the catchment characteristics as well as the methodology used by the *'GIS software package'* to carry out the computations.

4.1.1 Drainage points

Drainage points are primarily represented in the GIS working pane by means of a point. The only relevant information required by GIS is the latitudinal and longitudinal coordinates to correctly orientate the drainage point within the GIS working pane as well as a name or description to label the drainage point. These coordinates and names are stored in table referred to as the attribute table.

GIS allows the user to add additional fields in the attribute table which can be populated with additional data, for example, catchment characteristics associated with single or multiple drainage points for single/multiple sub-catchment areas which form sub-sets of the main (or total) catchment area of interest.

4.1.2 Rasters

Raster datasets consist of a matrix of cells where each cell represents a measure of continuous variable. Rasters are normally presented by means of images (raster images) where each pixel (or cell) contains a colour. The colour normally represents a data range from a band of data ranges as illustrated in Figure 11.

These data ranges can either represent elevations, slopes, flow direction network values and flow accumulation network values, in the case of the different rasters used in the quantification of catchment characteristics. These rasters are generally generated from other rasters, point values or line value interpolations.

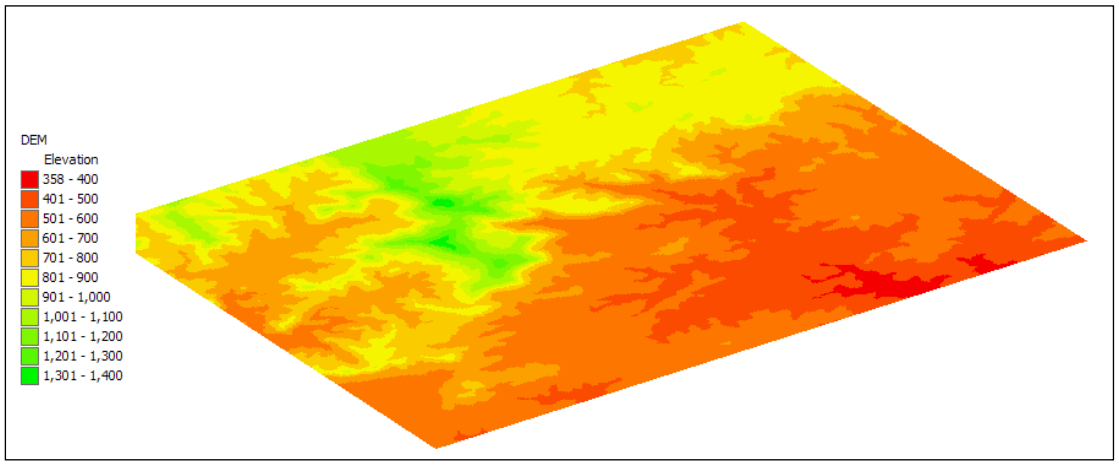

Figure 11: Elevation Raster (DEM) with 11 colour bands

4.1.3 Digital Estimation Model (DEM)

The raster used to generate additional rasters for the purpose of slope, flow lengths, and catchment delineation is a digital elevation model (DEM) where the cell values represent elevation. DEM sets are normally available but can also be generated.

Generation of a DEM makes use of either point elevations or contours, or both. The extension used in ArcGIS to generate such rasters is known as *Topo to Raster* found in the *Spatial Analyst Toolbox* under *Interpolation*.

The extension requires input features (predominately contours and point elevations in DEM generation) which will serve as the basis of DEM generation. Various other selections can and need to be made on the extensions popup interface. The most important of these selections for DEM generation are the input feature's Type and Field, the Output Surface Raster, Output Cell Size and Tolerance 1.

The type of input features needs to be identified for the input features *Type*. If the input features represent contours, *'contour'* needs to be selected, and the same applies for point elevation. The *Field* selection identifies the field in the dataset attribute table that contains the data values (elevation) which will be used in the interpolation process.

Output Surface Raster specifies the folder and name of the output raster. *Tolerance 1* needs to be set to a value equal to half the contour interval if contours are the primary feature used, and zero if point elevations are predominately used.

The most important, but also the most difficult, selection to be made is *Output Cell Size.* This selection specifies the output raster cell size. A smaller cell size increases the amount of cells in the raster matrix and the required computing time necessary. A trade-off, or optimisation, between time and a raster that is not too coarse is required.

If possible, a good method of selecting a *dataset area* which is sufficiently large so as to include (or embrace) the entire catchment area is to identify all quaternaries upstream as well as the quaternary just downstream of the drainage point. Any dataset area which includes the quaternaries that have been described above should therefore be large enough to include the catchment and to generate rasters.

4.1.4 Hydrologically Correct DEM

The next step in the quantification of catchment characteristics is to generate a *'hydrologically correct'* DEM (depressionless DEM). A DEM could possibly contain certain patches known as "*sinks*". A sink is an area in a DEM where all surrounding cells have higher elevations relative to the *'surrounded cell'*, as illustrated in Figure 12. Sinks are normally the result of the interpolation process but can also represent geographical features such as lakes.

The problem with a sink (or sinks) is that GIS generated runoff flows are collected at these points and there is no outflow. This results in a discontinuous rather than a continuous GIS flow direction raster which is used *'by default'* in the software for catchment delineation.

The ArcView extension that is used to *'fill'* (or correct) sinks is found in the *Spatial Analyst Toolbox* under *Hydrology* and referred to as *Fill*. This extension uses a raw DEM as input for which all sinks are identified and filled to generate a depressionless DEM. This output is then used to generate the flow direction raster for the DEM.

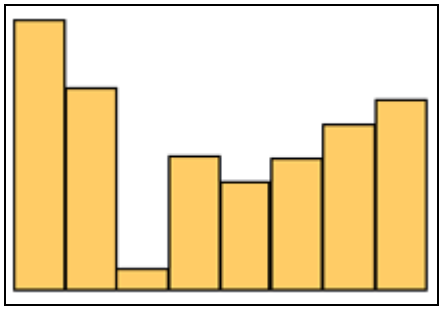

Figure 12: Cross section through a sink

4.1.5 Flow Direction Raster

The next step in the quantification of catchment characteristics includes the generation of a flow direction raster. A flow direction raster can be described as a matrix of cells containing the reference to the adjacent cell with the steepest descent signifying the flow direction. This raster is generated by the *Flow Direction* extension found in the *Hydrology* toolbox.

Cell referencing is done by means of the eight direction (or D8) flow model. Each cell has eight adjacent cells, each containing a specific value corresponding to the position of the adjacent cell in relation to the processed cell, known as direction coding, illustrated in Figure 13.

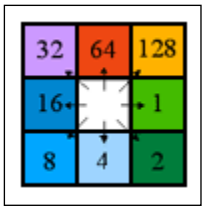

Figure 13: Direction Coding

The flow direction extension only uses a DEM as input and generates a flow directions raster as output. It is essential that a hydrologically correct DEM is used for this extension. The direction of flow is determined by the direction of steepest descent from each cell to one of its adjacent cells as illustrated Figure 14.

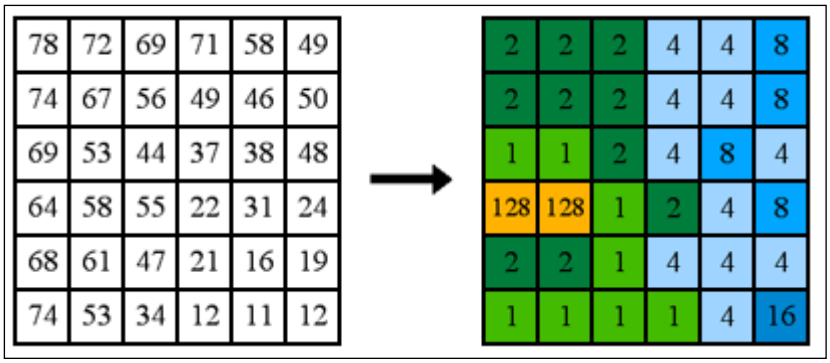

Figure 14: Elevation Raster Matrix and Corresponding Flow Direction Raster Matrix

The steepest descent is calculated by dividing the difference in elevation (Z-Value) by the distance between centres of the two cells and multiplying it by a 100. The direction of the cell that produces the highest value is then stored for the processed cell. If the descent to all adjacent cells is the same the neighbourhood is enlarged until a steepest descent is found.

Figure 15 illustrates a flow direction raster above the hydraulically corrected DEM that was shown in Figure 11. The eight colour bands correspond with the direction coding as illustrated in Figure 13.

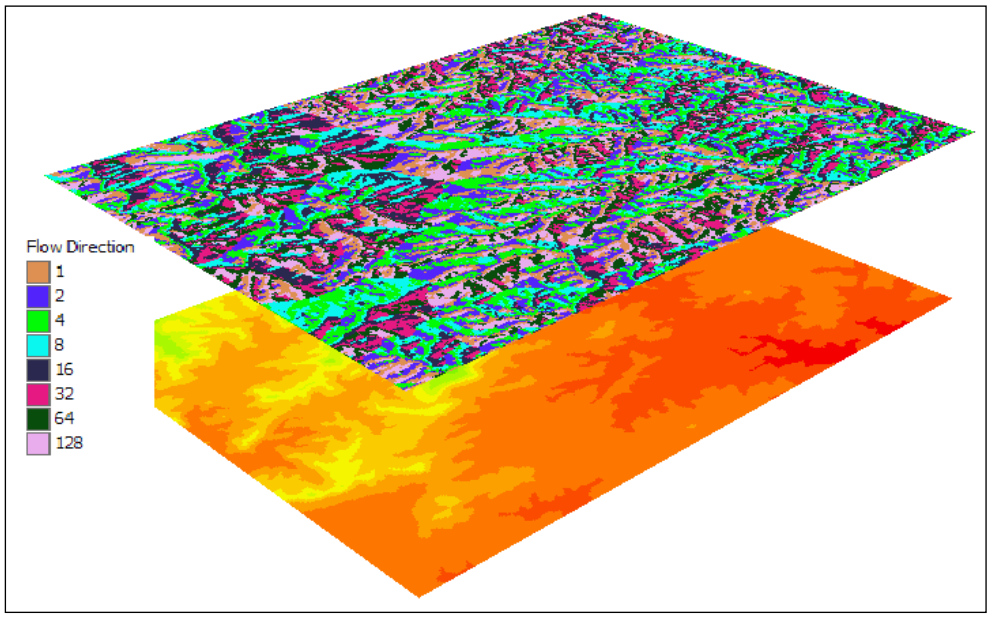

Figure 15: Flow Direction Raster and Corresponding Depressionless DEM

4.1.6 Flow Accumulation Raster

The flow direction raster is then used as the input raster to generate the flow accumulation raster using the *Flow Accumulation* extension found under the *Hydrology* toolbox. A flow accumulation raster is simply a representation of the stream network of a given DEM. Figure 16 illustrates the flow accumulation raster above the flow direction raster as illustrated in Figure 15.

A flow accumulation raster matrix consists of the accumulated flow for each cell which is based on the number of cells that drain through the processing cell without considering the cell currently being processed.

A flow accumulation raster mainly serves two purposes. Firstly, it is a very helpful tool for the identification of main streams and stream orders. Secondly, it is exclusively used in the software application for *Snap Drainage Point* extension as explained in section 4.1.8.

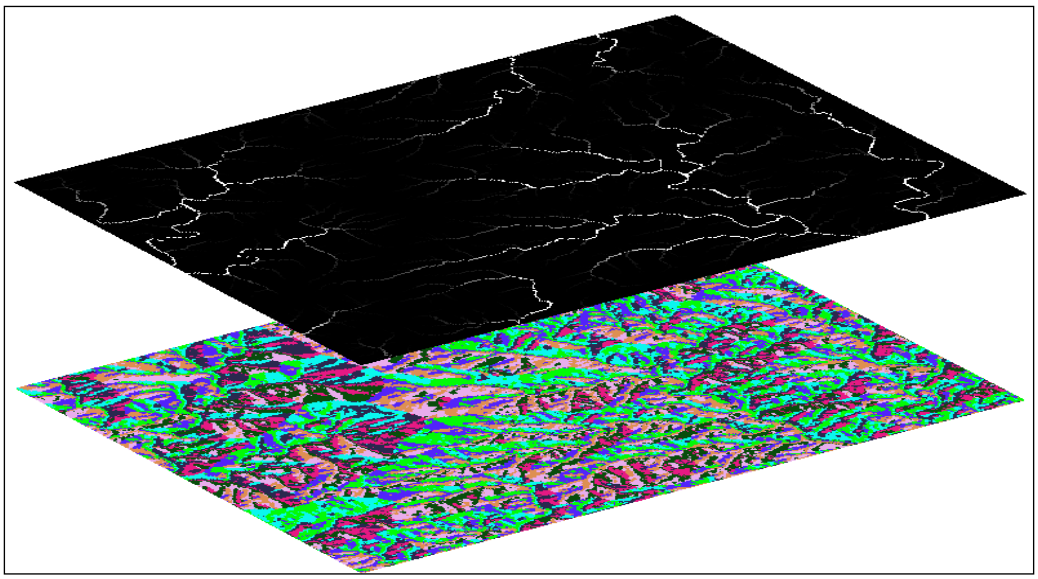

Figure 16: Flow Accumulation Raster and Corresponding Flow Direction Raster

4.1.7 Slope

The last raster which needs to be generated in order to complete the quantification of catchment characteristics is the slope raster. The slope raster is generated using the *Slope* extension found in the *Surface* toolbox under the *Spatial Analyst* extension.

The raster uses a raw DEM and generates a slope raster with a cell matrix which represents the maximum rate of change between each cell and its neighbours; for example, the steepest downhill descent for the cell (the maximum change in elevation over the distance between the cell and its eight neighbours). Figure 17 illustrates the slope raster above the corresponding DEM illustrated in Figure 11.

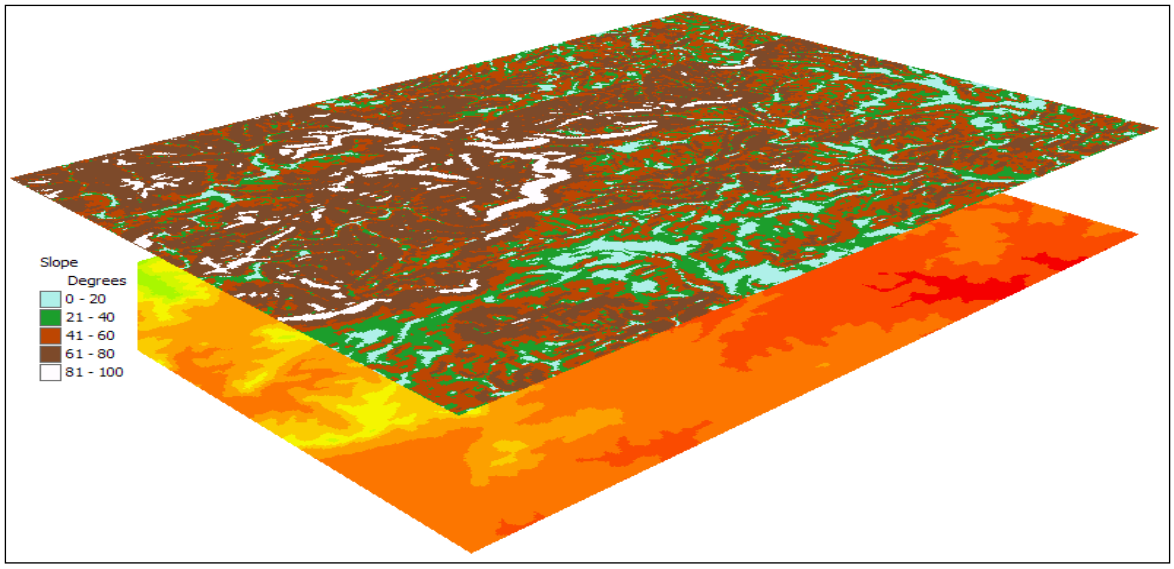

Figure 17: Slope Raster en Corresponding DEM

4.1.8 Snap Drainage Point

Stream networks generated from DEM do not always correspond to the natural stream networks in relation to the position as illustrated in Figure 18. Drainage points on the other hand are coordinate orientated and are correctly positioned for most cases. This results in drainage points that are normally situated next to main streams instead of in the main stream (or streams).

Figure 18 illustrates the correct positioning of a drainage point although the generated stream is offset to the left. The *Snap Drainage Point* is used to correct these errors.

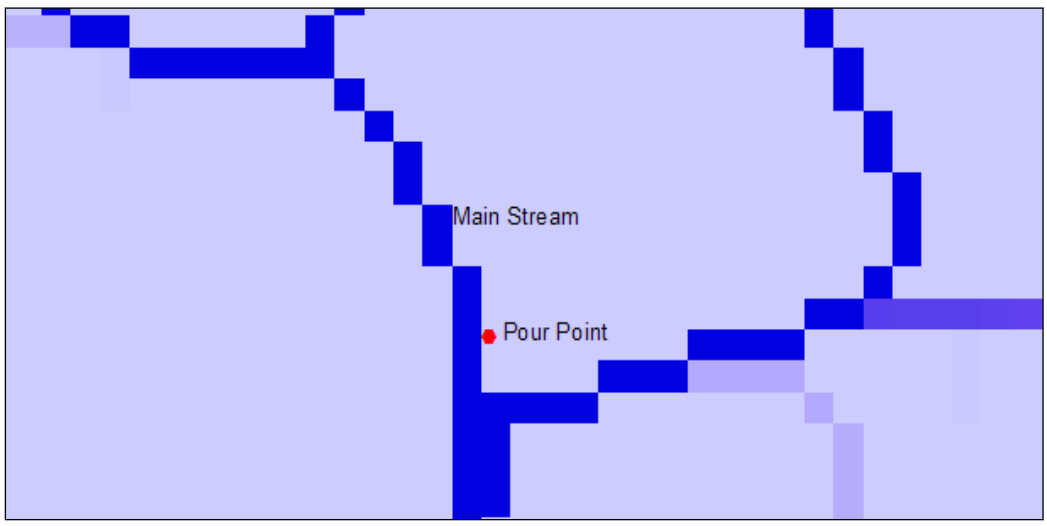

Figure 18: Incorrect Positioning of Drainage Point on Flow Accumulation Raster

This extension uses a flow accumulation raster, snap distance and drainage points as input characteristics to generate a drainage point that has been snapped onto a cell which has the

highest flow accumulation value within a specified radius, thus compensating for the errors of stream network miss-positioning.

Great care should be used when defining the snap distance. If a snap distance which is *'too large'* has been defined this can result in the assignment of the drainage point onto a neighbouring stream which would be incorrect, as illustrated in Figure 20. To prevent this from happening, the following procedure is adopted: Determine the distance between a drainage point and its allocated stream by using the *Measure* function found in the *Tools* toolbar as illustrated in Figure 19.

Figure 19: Measure Function

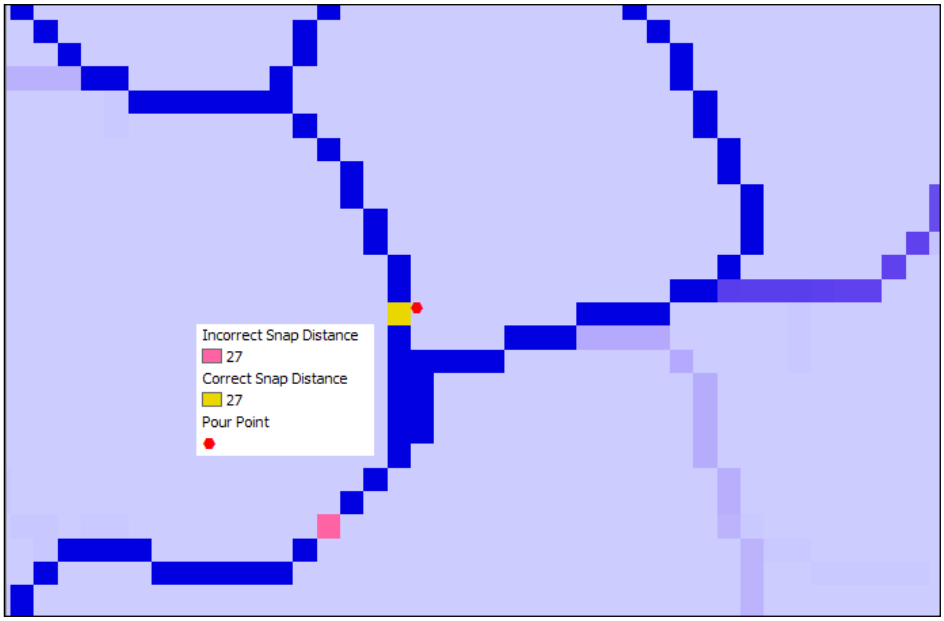

Figure 20: Correct and Incorrect Snap Distances on a Flow Accumulation Raster

4.1.9 Watershed

The *Watershed* extension found in the *Hydrology* toolbox is used for catchment identification for drainage points. This extension uses specified drainage points and a flow direction raster as input characteristics, and generates a watershed raster as output. This raster identifies the watersheds for the input drainage points which form the boundaries of the catchment.

The Snap Drainage Point output can be used in the instance where the drainage point positions are not located on the generated stream network (flow accumulation) as illustrated in Figure 18. Figure 21 illustrates the catchment for a drainage point.

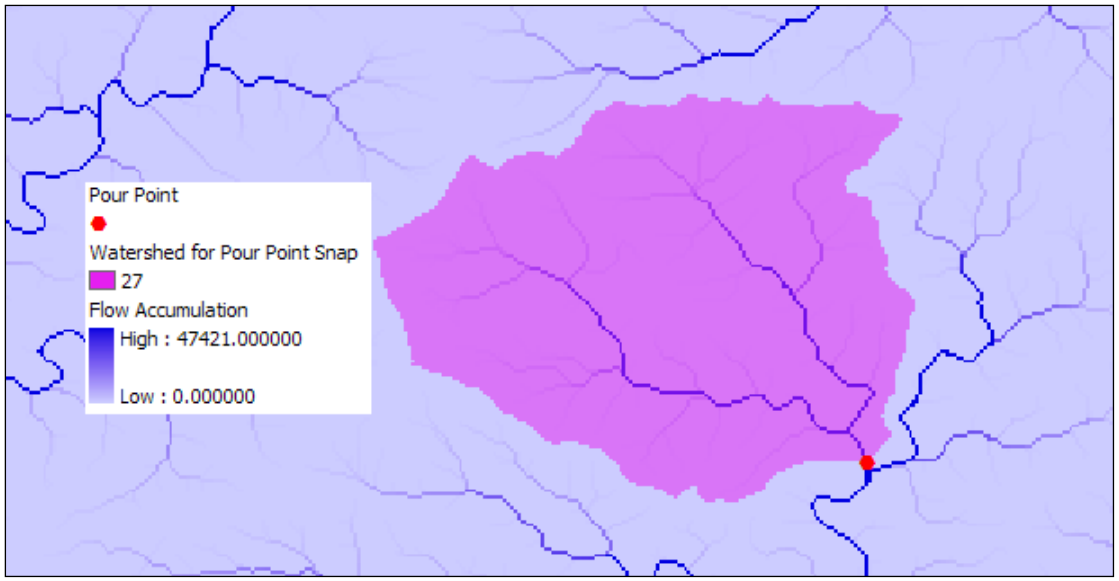

Figure 21: Watershed for a Snapped Drainage Point

4.2 Catchment Characteristics Calculations

The successful completion of the steps described above forms the basis needed for quantification of the four catchment characteristics which form part of the remainder of this research.

4.2.1 Projections

A very imported factor in the computation of catchment area and slope is the coordinate system or projection of the data used. Area computations can only be done in projected coordinate systems and not in geographic coordinate systems whilst slope computation is much easier if the x and y units are the same as the z units.

Data is normally presented in geographical coordinate systems and needs to be transformed to a projected coordinate system. The best method of transforming data to the correct projection is to transform the original drainage points and DEM to a projected coordinate system before data generation and quantification of catchment characteristics commences.

The GIS default coordinate system also needs to be converted to the same projected coordinate system because this is not automatically done when transforming data. If data is presented in projected coordinate system then projection transformation is not required, although the working environment projection must be converted to the same projection.

Raster projection is done with the *Project Raster* extension found in the *Raster* toolbox under *Projections and Transformation* extensions under *Data Management Tools*. This extension projects the input raster from the defined original coordinate system to the defined output coordinate system in order to form a new projected raster.

Working environment conversion is done by right clicking on *Layers* [Layers] and selecting properties. This opens the Data Frame Properties of the working environment from which the Coordinate System needs to be selected. *Import* is then selected and then the data which has already been projected is browsed and selected. This will import the projected coordinate system of the data and by selecting *OK*, convert the working environment projection to the same as the projected data.

A good projected coordinate system which can be used for South Africa is the *Africa Albers Equal Area* projection with modification. These modifications are carried out when selecting the output coordinate system by selecting the modify button. This coordinate system i.e. the output coordinate system can then be imported to be used as the coordinate system for the GIS working environment and for data projection.

Table 4: Africa Albers Equal Albers *Modifications*

Projection: Albers	**Projection: Modified Albers For RSA**
False_Easting: 0.000000	False_Easting: 0.000000
False_Northing: 0.000000	False_Northing: 0.000000
Central_Meridian: 25.000000	Central_Meridian: 24.000000
Standard_Parallel_1: 20.000000	Standard_Parallel_1: -18.000000
Standard_Parallel_2: -23.000000	Standard_Parallel_2: -32.000000
Latitude_Of_Origin: 0.00000	Latitude_Of_Origin: 0.00000
Linear Unit: Meter 1.000000	Linear Unit: Meter

4.2.2 Catchment Area

One more step needs to be completed in order to compute the catchment area. This consists of the generation of polygon shapes for the watershed as computed in section 4.1.9. This is done with the *Raster to Polygon* extension found in the *From Raster* Toolbox under the *Conversion* tools. The extension uses the generated catchment as input, and generates polygons from the cells which define the catchments and attribute table which can be used for catchment area computation.

Various methods exist in ArcGIS to calculate the area of catchments. The best suited method is done by making use of the attribute table. The attribute table is opened by right clicking on the created watershed polygon layer in the layer box and then selecting *Attribute Table*.

Area computation by means of the attribute table includes the addition of new field *Area*, and performing geometric calculations in the form of area for this field by right clicking on the field and selecting *Calculate Geometry*. This will calculate the area for the polygon catchment, and display it in the attribute table, which concludes area computation. This attribute table can then be exported into Microsoft Excel for further computations.

4.2.3 Longest Water Course

Computation of the longest watercourse in ArcView is carried out by means of the *Longest Flow Path* extension which forms part of the optional Arc Hydro extension which can be downloaded. This method is very cumbersome and inefficient because it requires extensive input of rasters and unnecessary long times for computations to be completed.

A much easier and less time consuming method of determining the longest flow path is to identify the longest flow path by inspection and then measure it by means of the *Measure* function found in the *Tools* toolbar.

The flow accumulation raster (see Figure 16) is a very useful method of identifying the longest flow path which is normally traced by following the most prominent stream from the drainage point. The longest length of the flow path can also be manually added to the catchment attribute table for each catchment.

4.2.4 Slope

Computation of the mean slope is done by means of applying the *Zonal Statistics as Table* extension which is found in the *Zonal* toolbox under *Spatial Analyst* extensions on the *Slope* raster. This extension generates a table which contains statistical information about the input data or raster for a defined zone. This table also contains mean values for zones which represent the mean slope for each catchment when a slope raster is used as input. This is illustrated in Figure 22.

A very important factor which must always be borne in mind is that a slope raster contains the maximum slope between a particular cell and any of its eight neighbours. The mean catchment slope must then be *'manually'* added to the catchment attribute table after computation of the mean slope has been completed.

4.2.5 MAP

Computation of the mean annual precipitation can be done by numerous methods in ArcGIS depending on the available MAP data such as isohyets, point MAP etc. The most common method of presenting MAP data is in the form of point MAP readings. Various methods exist

to transform MAP point data to area representation. The Thiessen Polygon is one of the most well-known transform methods.

This method can be applied in ArcInfo which is the most comprehensive ArcGIS package available. This method is not available in lower ArcGIS software packages such as ArcView.

An alternative method of MAP computation can be done in the same way as slope calculation with the exception of using a MAP raster generated for a region. The *Zonal Statistics as Table* extension is then applied in the same manner as described in section 4.2.4 to calculate the MAP. A MAP raster can be generated in the same way as described in section 4.1.3 with the exception of using MAP points as "heights". There is a good comparison between the Thiessen Polygon method and the newly proposed method.

The MAP for each catchment can then be added to the catchment attribute table which will contain all four of the characteristics at this stage if all steps have been successfully completed. Flood peaks for given probabilities can be calculated and imported into the catchment attribute table which will include all data to be used in this research.

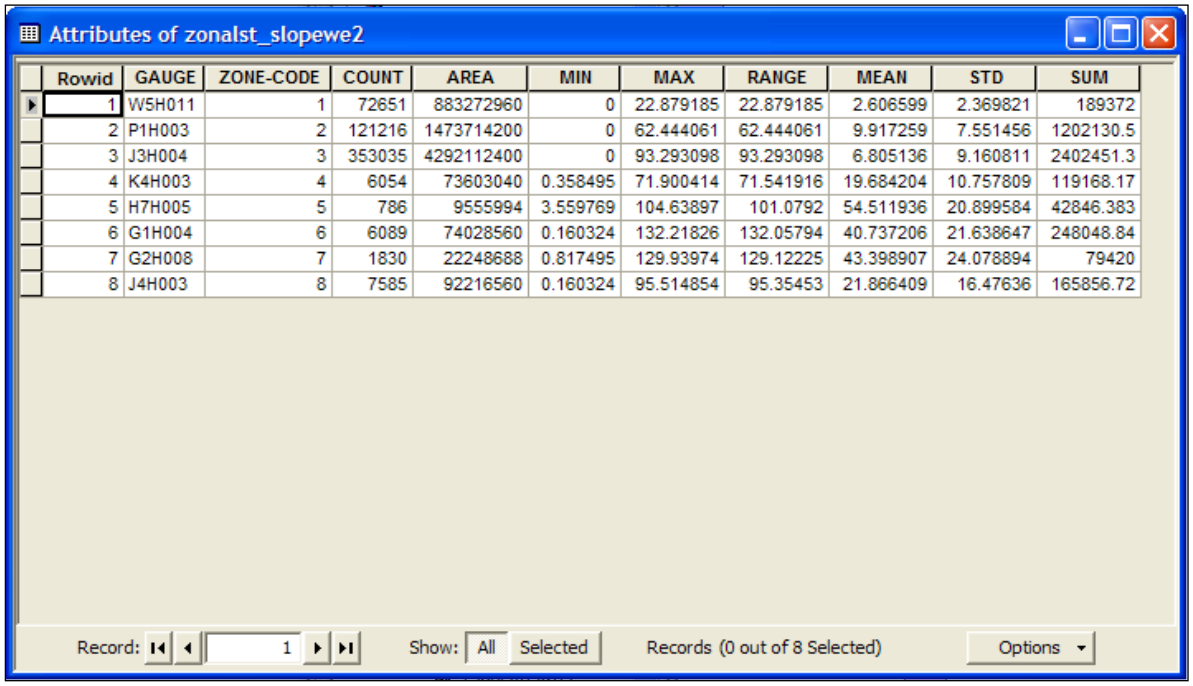

Rowid	GAUGE	ZONE-CODE	COUNT	AREA	MIN	MAX	RANGE	MEAN	STD	SUM
1	W5H011	1	72651	883272960	0	22.879185	22.879185	2.606599	2.369821	189372
2	P1H003	2	121216	1473714200	0	62.444061	62.444061	9.917259	7.551456	1202130.5
3	J3H004	3	353035	4292112400	0	93.293098	93.293098	6.805136	9.160811	2402451.3
4	K4H003	4	6054	73603040	0.358495	71.900414	71.541916	19.684204	10.757809	119168.17
5	H7H005	5	786	9555994	3.559769	104.63897	101.0792	54.511936	20.899584	42846.383
6	G1H004	6	6089	74028560	0.160324	132.21826	132.05794	40.737206	21.638647	248048.84
7	G2H008	7	1830	22248688	0.817495	129.93974	129.12225	43.398907	24.078894	79420
8	J4H003	8	7585	92216560	0.160324	95.514854	95.35453	21.866409	16.47636	165856.72

Figure 22: Zonal Statistics Table

5 Data Collection and Processing

The evaluation of the CAPA and MIPI design flood estimation methods was based on the comparison of two datasets. The first set of data was collected and statistically analysed annual flood peaks for a sample of flow gauging stations. The second set of data consisted of design floods estimated using the CAPA and MIPI method described in section 3.5 and section 3.6.

This section examines the methodology which was followed to obtain the two datasets.

5.1 Data Collection Process

The data collection process commenced with the identification of a sample of drainage points. The sample was selected from flow gauging stations as flow data and various catchment characteristics that was already available for these drainage points.

Flow gauging station information was obtained from DWAF in the form of GIS data. The attribute tables contained relevant information about each gauging station, excluding flood peak data. The data from DWAF was processed and yielded 2706 possible gauging stations from which a selection could be made. Figure 23 illustrates the 2706 gauging stations and their positions relative to the 22 primary drainage regions covering South Africa and Swaziland.

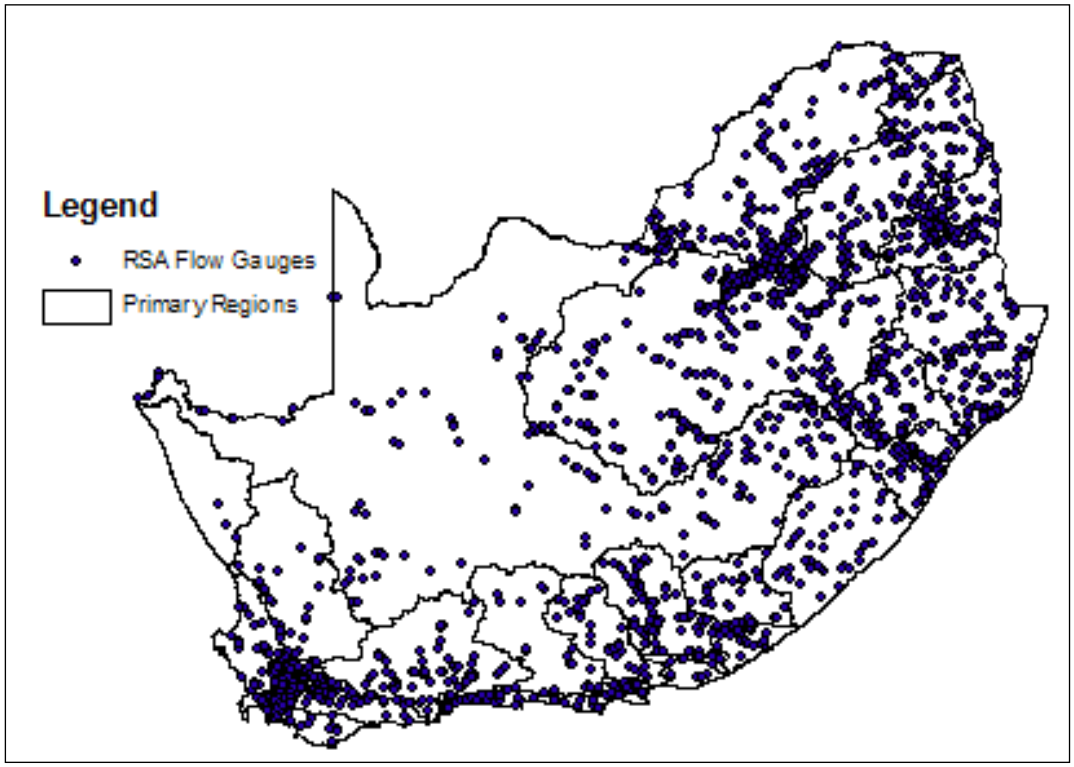

Figure 23: South African Flow Gauges

A selection criterion which was partly based on the flow data available for each gauging station was developed in order to identify those stations with the most reliable and suitable data. The first criteria focused on flows which were *'considered to be as natural as possible'* and applicable to surrounding areas, and secondly the length of data record available for each gauging station.

Uncertainty exists regarding the effect of dams and other structures which impede flow have on annual flood peaks. There are various opinions with regard to the use of flow records which have not been naturalised: They range from the use of *'raw data'* without adjustment to the naturalisation of flow records before they are used (DWAF, 2007).

The method used in this research to address the topic of natural flow, and hydrological data applicable to surrounding area, was to exclude gauging stations located downstream of a dam which had a storage capacity greater than 80% of the mean annual runoff (MAR) of the catchment area under consideration (Görgens, 2007).

The reasoning behind this is that any structure with a storage capacity less than 80% of the MAR will have an insignificant impact, or effect, on the annual maximum flood peaks and will closely represent natural flows.

Dams with a storage capacity greater than 80% the MAR of the upstream catchment area are seldom full and will attenuate floods passing through them most of the time. Watercourses and *'river reaches'* downstream of dams which satisfy this criteria will have their own flood characteristics and will not automatically produce naturalised flow records. These flood characteristics will also differ from those of tributaries joining the main stream downstream of dams or structures which impede, or attenuate, flow.

Dams with a storage capacity greater than 80% of the MAR of the catchment upstream will have little or no influence upstream. The flood characteristics of measurements upstream of these attenuation structures will closely resemble naturalised flow and share the same characteristics as tributaries entering the main stream.

On the basis of the *'80% MAR criterion'* it was decided to exclude all gauging stations downstream of any dams which have a storage capacity greater than 80% of the MAR of the catchment draining towards the dam. Flow records and other hydrological data were obtained from the DWAF for as many dams as possible – this data included the storage capacity and the MAR of the catchment area draining towards the dam. Data related to 235 dams was collected and only 69 dams had a storage capacity which was greater than 80 % of the MAR of the catchment area of the dam.

The 69 dams were plotted in ArcGIS and all rivers and streams downstream of them were selected for analysis. 870 of a possible 2706 gauging stations on selected streams and rivers were identified and excluded from the gauge selections. Figure 24 illustrates the 69 dams, the

rivers downstream of these dams and gauges on these rivers which had been excluded from selection.

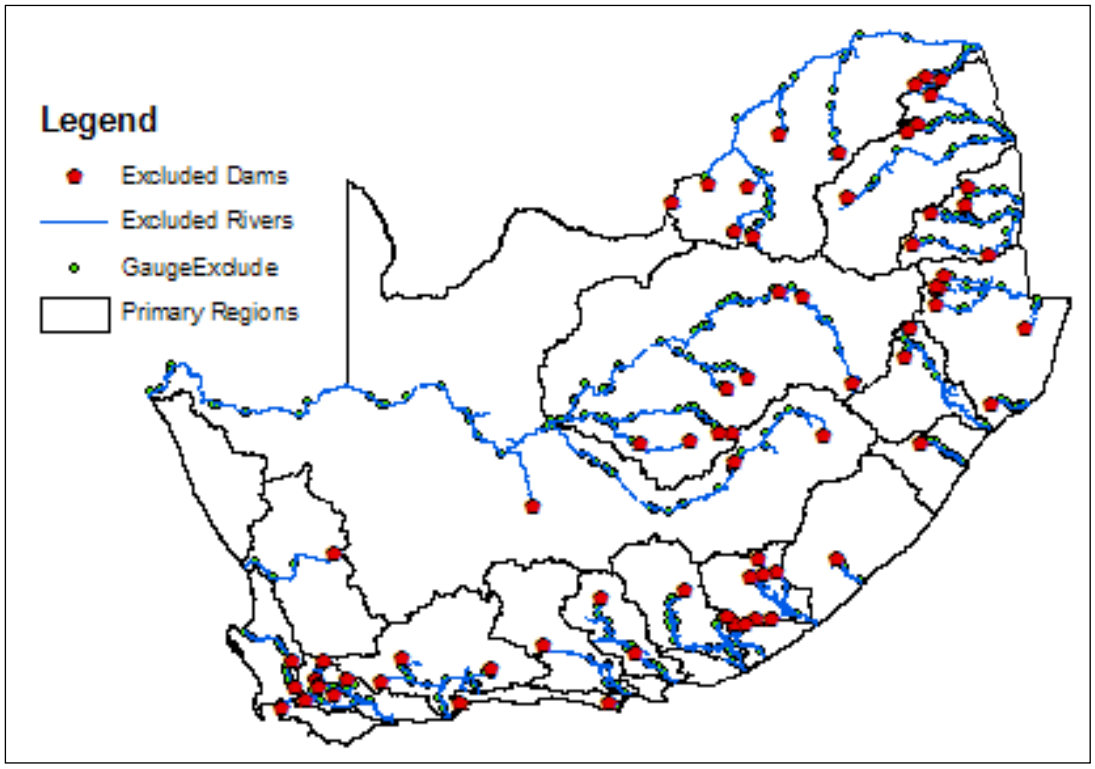

Figure 24: Excluded gauges based on the first selection criteria

The second selection criterion conducted involved both a good distribution of gauging stations over South Africa, and flow record lengths. Corrected DWAF flow records up to 1994 were utilised instead of the incomplete data set of DWAF flow records which could be obtained from the DWAF website at the time of this research. DWAF flow records exhibited too many discrepancies thus making the corrected data more reliable even though the *'corrected data set'* had a 12 year shorter record length.

It was decided not to use any data records shorter than 30 years with the exception that a record length of 20 years would suffice for areas where no other gauging stations existed to represent a specific area.

A subjective selection was then made on the basis of a good distribution of gauging stations over South Africa. This was done by selecting at least one gauging station for each of the 22 primary drainage regions in South Africa and with a maximum of five per primary drainage region. The criterion of record length was used as a check for *'suitability of analysis'* for each gauging station. If the selected gauging station did not meet the aforementioned criterion another station was selected within close proximity provided that the length of flow record was sufficient.

Certain areas did not have gauging stations with sufficient data or alternatives and could not be included for research and analysis. These areas where mostly in the dry north western regions of South Africa with no significant flood events expected, except for parts next to the Orange River. The surrounding regions share similar geographical, rainfall, vegetation, and flood characteristics. On the basis of these similarities it was decided that the exclusion of these stations would not have a significant effect on the analysis and updating of records and surrounding gauging stations could confidently be used to characterise these areas.

The final selection consisted of 53 gauging stations, with a combined record length of 2422 years averaging just less than 45 years per gauging station. The longest flow record had a length of 82 years and the shortest flow record was 23 years. The distribution of these 53 gauging stations over South Africa is illustrated in Figure 25.

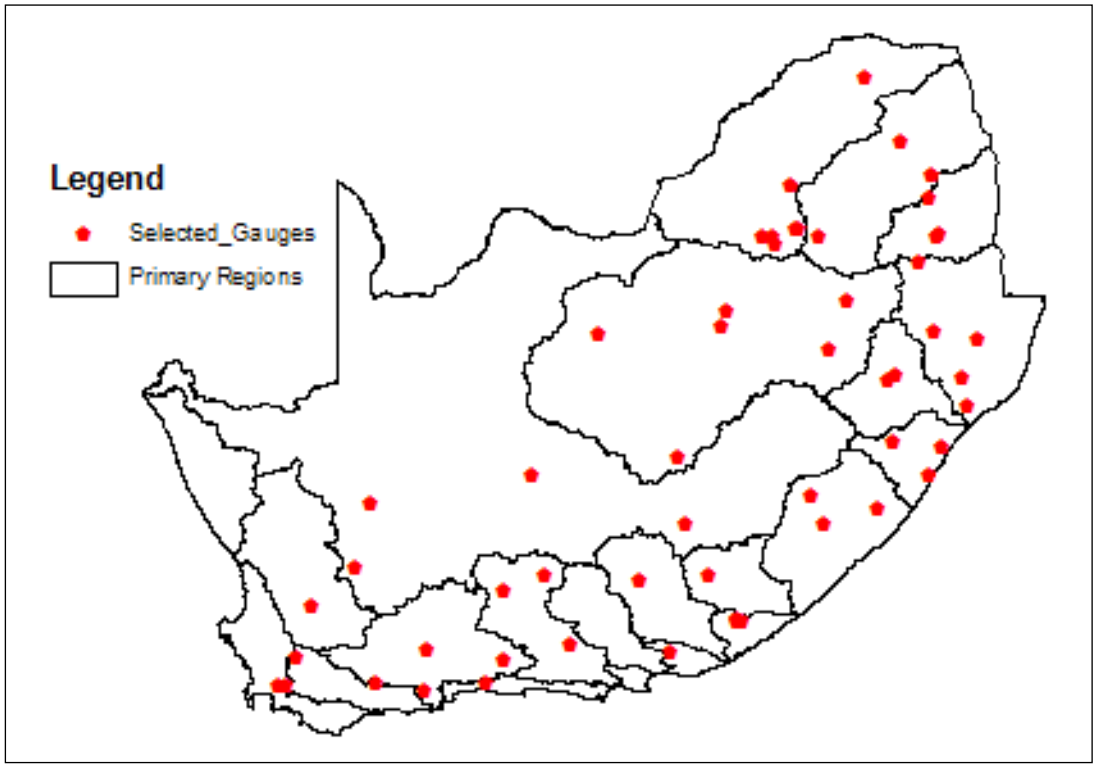

Figure 25: Selected Gauges

5.1.1 DEM generation

The next step required was to obtain a DEM which included the catchment areas for each of the 53 gauging stations. No accurate DEM was available and it was necessary to generate DEMs from contours available from the Chief Directorate of Surveys and Mapping. The generation of a DEM for the whole of South Africa was too time-consuming and it was decided to generate a DEM for each gauging station.

The first step was to identify all quaternary catchments upstream and one just downstream of each gauging station. These quaternaries are illustrated in Figure 26.

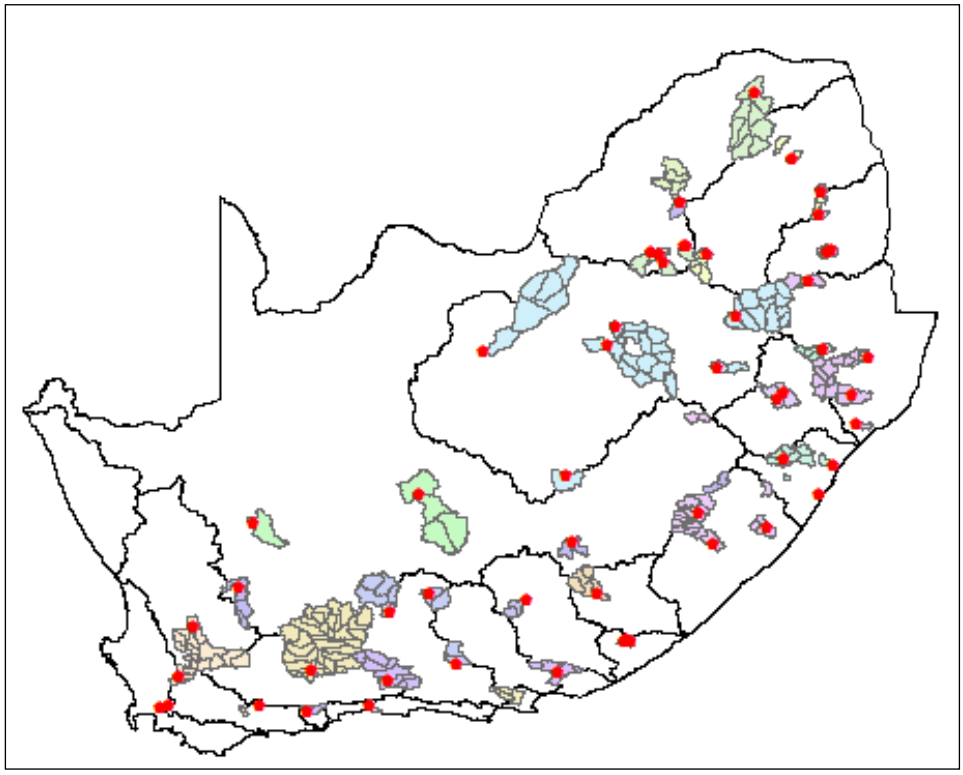

Figure 26: Upstream Quaternaries for selected gauges

The appropriate contours maps were then selected for each gauging station as illustrated Figure 27 for gauging station J3H004. These contour maps then formed the basis from which the DEM was generated as described in section 4.1.3.

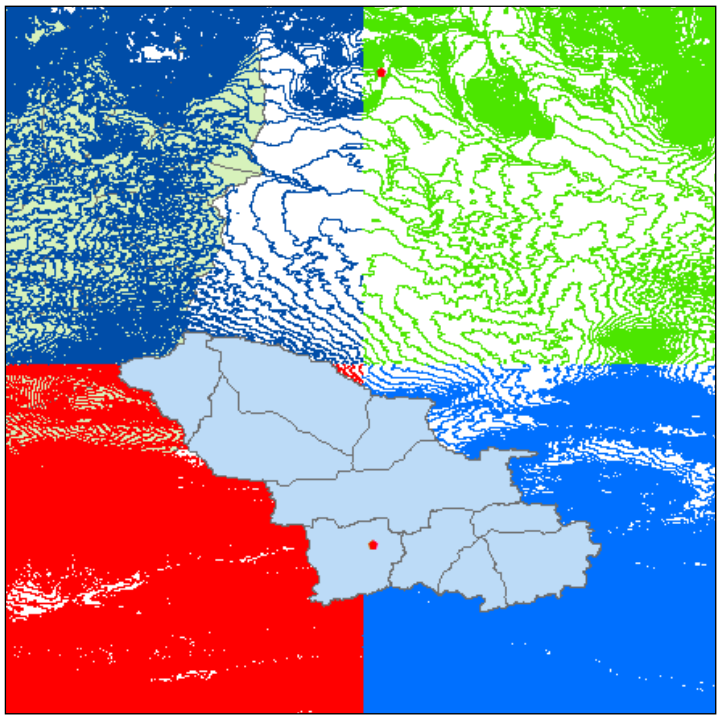

Figure 27: Quaternaries for J3H004 and the surrounding four contour maps

The quaternary boundaries helped to identify contour map clusters which were sufficiently large to ensure that the on DEMs that were generated completely included the catchment areas and aided with identification of possible discrepancies in the GIS catchment delineation process.

5.1.2 Quantification of Catchment Characteristics

The steps as set out in section 4 were followed to generate the necessary catchment characteristics by utilising the gauging stations as the allocated drainage points. The depressionless DEMs (Figure 28) were generated first: This was followed by the flow direction rasters and flow accumulation rasters (Figure 29). Lastly the flow accumulation rasters were used to define the catchments for the 53 gauging stations as illustrated in Figure 30.

The alignment of the gauging stations and GIS generated streams did not match for approximately 90% of the selected gauging stations. A process was followed in which the alignment of the gauging stations on top of rivers had to be assumed in order to successfully apply the *Snap Pour Point* tool. This assumed position was tested by comparing the GIS computed catchment areas with those calculated by the DWAF. In instances where there were large differences, the alignment of the gauge was re-examined, the position improved, the flow accumulation raster as well as the catchment delineation regenerated, the catchment sizes computed, and compared to the areas as calculated by the DWAF.

The catchment characteristics analyses for each of the 53 catchments were followed by the annual flood peak analysis for each of the stations. Flow records were extracted from corrected annual flood peak data files and imported into Microsoft Excel.

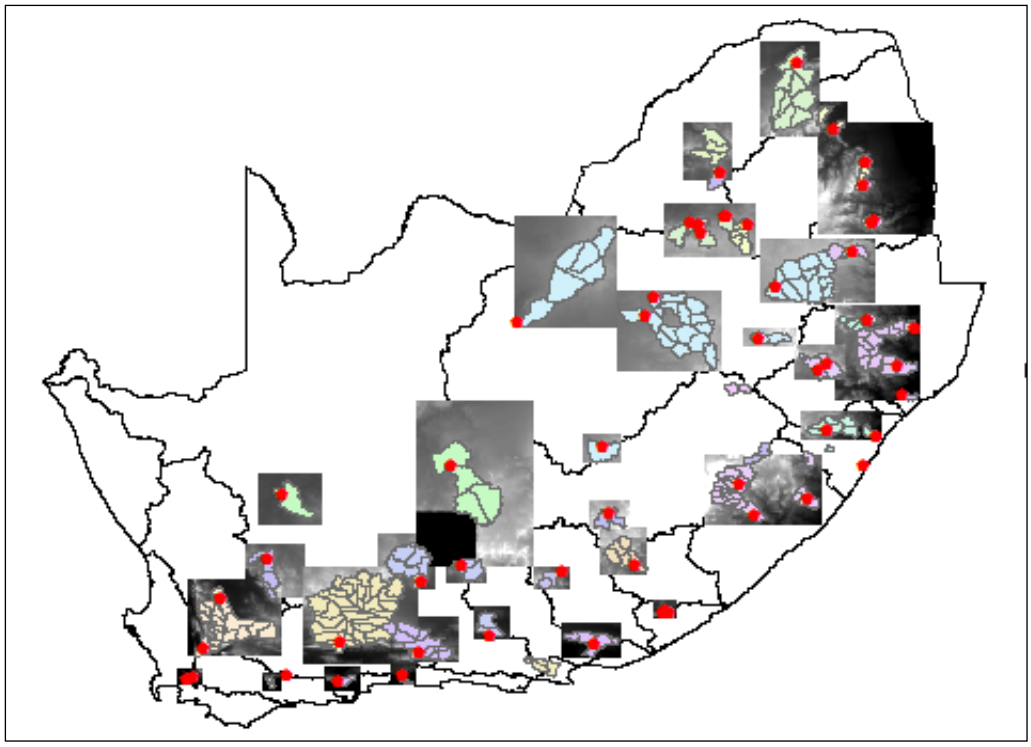

Figure 28: Depressionless DEMs

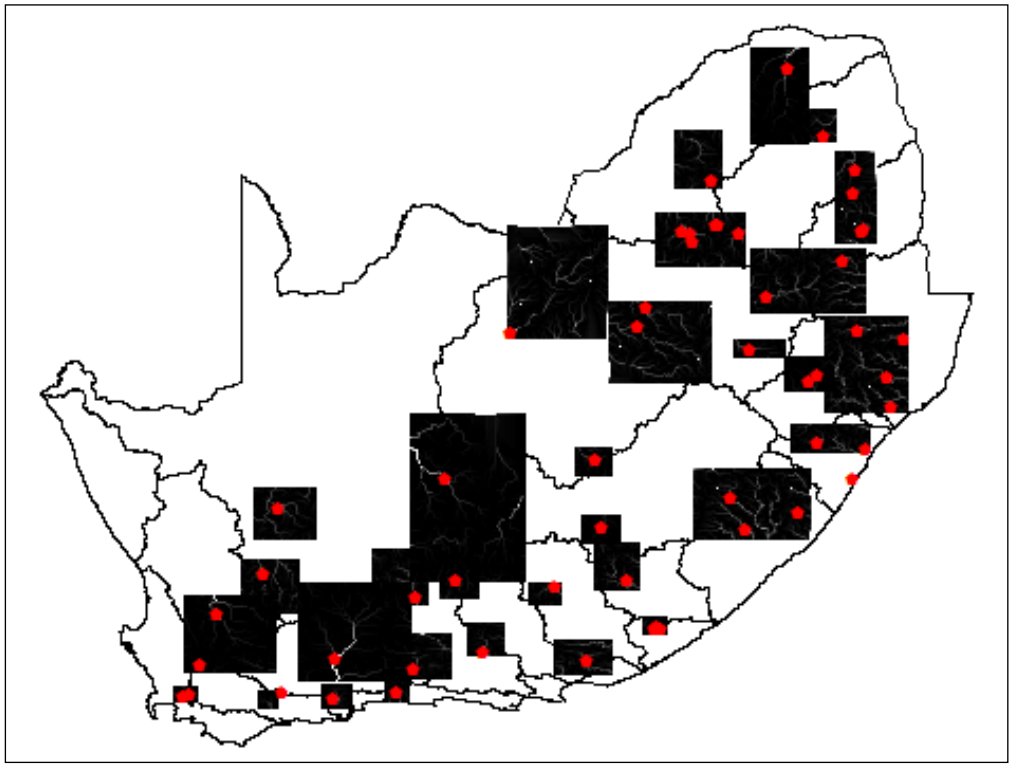

Figure 29: Flow Accumulation Rasters

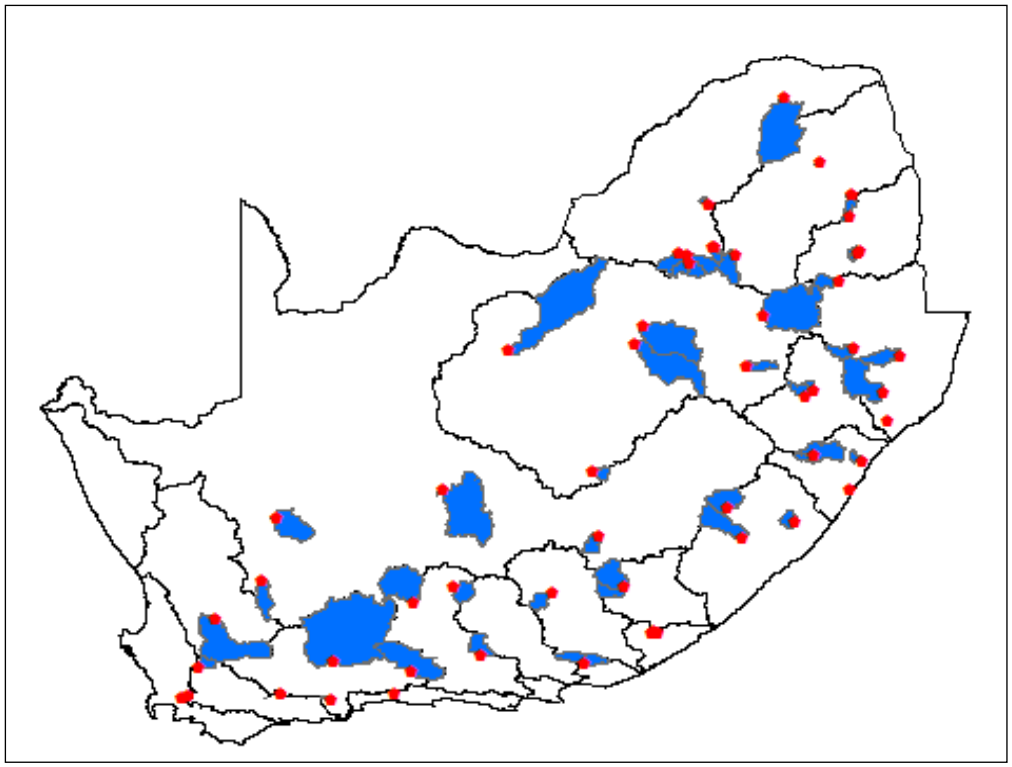

Figure 30: Catchments for Selected Gauges

5.1.3 Annual maximum flood peak analysis

This step involved the basic analysis of annual flood peak records. Annual flood peak records were ranked from high to low followed by determination of the plotting position for each annual flood peak record. The Cunane plotting position as recommended by the DWAF was used for this purpose.

After determination of the plotting positions probabilistic analyses were carried out on annual flood peaks using the LN and LP3 distributions. The design flood corresponding to the 50, 20, 10, 5, 2, 1 and 0.5 % probability of exceedance for each distribution was calculated as well as the statistical mean flood for each gauging station.

The plotted annual flood peaks were used to identify the peak floods that corresponded with the 50, 20, 10, 5, 2, 1 and 0.5 % probability of exceedance. The best fitted distribution was obtained for each gauging station by applying the chi-square test between both the LN and LP3 and annual peak floods identified from the plotting positions.

This analysis was carried out in order to determine which distribution yielded the *'best representation'* of the data for the 53 gauging stations. Of the 53 gauging stations analysed, 41 (or 76 %) were best represented by the LN distribution.

This concluded the data collection and statistical analysis of the 53 gauging stations. All the data was imported into Excel which was then used for computation purposes. The derived data is tabulated in Appendix A.

6 Reliability of Data

The reliability of a design flood estimation method is mainly dependent on two factors. These factors in order of significance are:

- The reliability of the data used to develop or update the design flood estimation method.
- The reliability of the input data into the design flood estimation method.

The primary objective when updating a design flood estimation method is to increase the reliability of the method to produce reliable design floods. It was very important to have a thorough understanding of the reliability of the data used during the research, as well the factors which could potentially influence the reliability of the data.

This level of understanding was achieved by means of a repetitative study and examination of the quality and reliability of the data that had been collected. This process also helped to identify and obtain a high degree of confidence of the limitations of the data and how it could potentially impact the reliability of the methods, as well as to identify possible problem areas which required consideration in the application of the data.

6.1 Data Quality and Good Practice

The quality and reliability of data used for any computation is a very important factor which required consideration and an understanding of their potential impact. One of the biggest limitations in the field of flood hydrology is the quality and correctness of flow data, and this is no exception in South Africa.

The three datasets which were examined for the purpose of this research included:

- Flood peaks of the gauging stations.
- Precipitation information.
- Catchment characteristics quantified by means of GIS.

Annual flood peaks of the gauging stations was the most significant of the three datasets as these served as the comparison measures used to evaluate the reliability of the two methods and to update the methods.

6.2 Flood peak data

A stumbling block in South African flood hydrology is the quality of available flood peak data and the availability of corrected flood data. Flood peak data is readily available for numerous agencies with the DWAF being the most prominent source: This data is mostly incomplete and contains numerous errors (US, 2007). Probably the biggest reason for this incompleteness of data is usually when flood events have exceeded the *'stage capacities'* of gauging stations (or measuring structures) as well as the lack of resources within the DWAF

to update the data. Data is then normally published without correction i.e. *'raw data'* when the stage capacity of a gauging station has been exceeded (US, 2007).

Correction is possible and will be of great value to the field of flood hydrology if this could be done and made available. Correction of the data may have been done by means of manually obtaining stage records, as was done with the flow data utilised for this research. The availability of such corrected data was also of great concern and very seldom available to public.

Another factor concerning flow gauging data is the ability of statistical distributions to accurately describe the natural distribution of a given dataset. One should always bear in mind that the statistical distribution used to describe a dataset is only a representation of the real dataset. The only way to achieve an acceptable degree (or level) of confidence when using a statistical distribution to describe a dataset is to test a multitude of distributions and use the best fitted distribution.

Section 5.1.3 pointed out that corrected DWAF annual flood peak records were used for the research. These records were corrected by means of obtaining stage data for relevant events, deriving flood peaks from the stage records, comparing them to currently available records, and improving the data if required (Odendaal, 2007).

Possible factors which could have influenced the reliability of the updated annual flood peaks include:

- The correctness of the stage discharge relationship which was used. Not all stage data was obtained at points with calibrated stage discharge relationships.
- The reliability of the stage measurements as some of the measurements were subject to eye witness accounts and their interpretation.

The only other factor which influenced the reliability of the data in the context of the research was the length of the annual flood peak records. The data used only included data up to 1994 and excluded major flood events between 1994 and 2007 which would have improved the reliability of the data. Numerous attempts were made to obtain corrected flow records for the *'13 year gap'* between 1994 and 2007 without success.

These factors were noted but it was assumed that the data could be considered reliable and no additional measures were introduced to verify this assumption or to improve the data.

6.3 Rainfall Data

The measurement of rainfall is a simple procedure provided that accuracy is not essential. An exact measurement of rainfall is impossible to obtain owing to the random and systematic errors that occur when measuring rainfall (Schultz, 1985). Boughton (1981) stated that deficiencies of 10%-20% could be expected in point measurement of rainfall due to numerous factors such as wind, obstructions and deficiencies, or shortcommings, in rain gauges or measuring instruments.

Probably the most influential factors which influence rainfall measurement are wind directions and speeds. When installed correctly rain gauges are normally perpendicular to the surface of the earth. Wind causes rain to fall at angles to the earth's surface and hence to the gauge.

During the examination of this phenomenon it was found that these angles can cause the effective catchment area of the rain gauge to shrink or expand which results in rainfall measurement over smaller or larger areas. For example, rain falling at an angle of 75 degrees to the earth's surface has a 10% decrease in effective area and 65 degrees produces a 20% decrease.

Boughton (1981) further stated that a further 10%-20% error is likely when extrapolating data from a point measurement to an aerial average. If this is true aerial measurement can have errors of up to 40%. This could be especially true for areas with very steep MAP gradients e.g. the Jonkershoek Valley near Stellenbosch in South Africa. Great care should always be taken when estimating aerial MAP, but one should always take into account the reliability and limitations of the data. Evaluation and careful scrutiny of the estimated aerial MAP is always a good idea.

For the purpose of this research evaluation of the collected MAP was conducted by comparing the MAP as calculated by the Thiessen Polygon method used in the GIS application, with the mean MAP as calculated by the MAP generated Raster and the Zonal Statistics extension in ArcGIS (section 4.2.5). The two methods were compared for the 53 catchments used for the research by comparing the percentage difference between the two methods.

A mean difference of 0.235% was found between the two methods with the maximum percentage difference being 18.2% and the minimum 0.006%, with a standard deviation of 4.177. The acceptable differences between the two methods were found to be satisfactory for the purpose of the research and it was opted to use the MAP generated Raster and the Zonal Statistics extension in ArcGIS method for MAP quantification.

6.4 GIS Generated Data

The three remaining catchment characteristics which required consideration were the catchment areas, mean catchment slopes and the longest watercourse.

The GIS generated catchments used in the research were improved by means of adjusting the drainage points until the generated catchments produced catchment areas similar to those of the DWAF data. During the improvement process catchments which showed a difference of more than 5% when compared to DWAF catchment areas were reexamined and recalculated if found to be incorrect.

During the iteration process it was found that 13 of the larger catchments could not be improved to have a difference of less than 5% when compared to the DWAF catchment areas. Adjusting the drainage point upstream increased the catchment area over 5% and vice versa. This illustrated the influence of DEM cell size and clearly showed that generated catchments could be improved by selecting smaller cell sizes that resulted in finer DEMs.

After the completion of all the necessary corrections the GIS generated and DWAF areas were compared. A good correlation was found between the two datasets with a maximum difference of 13.3%, a mean difference of -0.91% and standard deviation of 4.7%. Even though it was pointed out that problems have been found with DWAF catchments due to availability of data at the time of delineation, it was concluded that the reliability of the catchment data could not be improved.

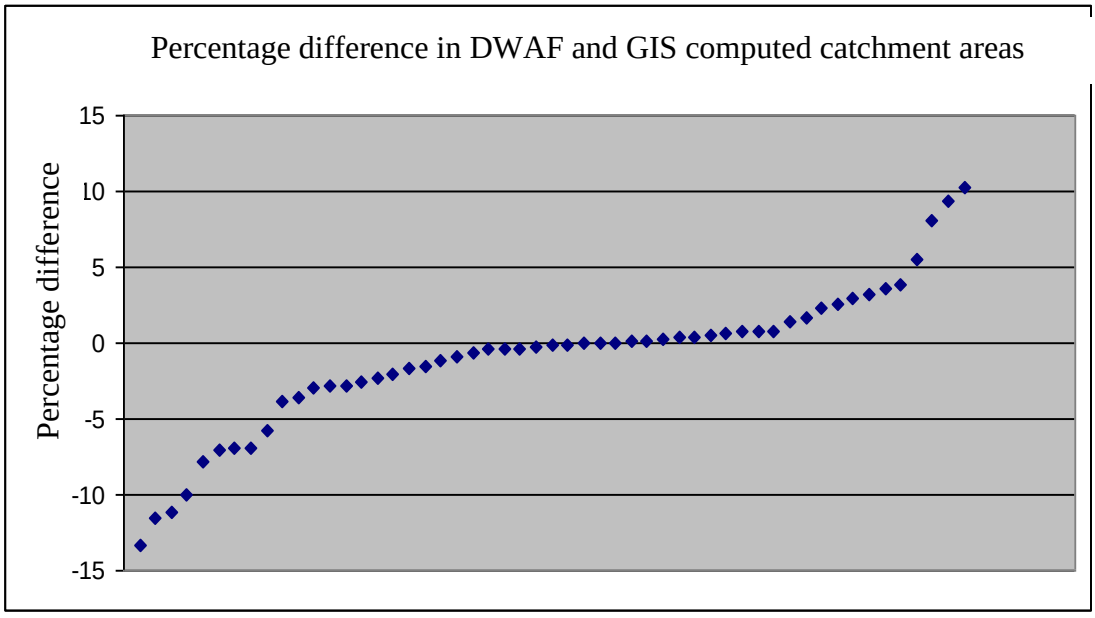

Figure 31: Percentage Difference in Catchment Areas

The possible differences which could exist between GIS quantified mean catchments slopes and other methods was briefly considered although no calculation was done on possible

differences which could exist. It was expected that GIS quantified mean catchment slopes would be more representative of the area compared to other methods.

The only potential problem which could be identified was the way in which ArcGIS estimates the slopes of cells. The slope of a cell was not the mean slope of all eight surrounding cells: Slope was selected by means of comparing the slopes with the eight surrounding cells and then selecting the maximum slope. This could potentially increase the mean catchment slope although the extent of influence could not be quantified.

The longest length of watercourse was quantified by means of GIS and compared with DWAF data. These lengths never differed by more than 2% and were found to be acceptable for the purposes of the study.

The next part of the research focused on the evaluation and potential updating of the two design flood estimation methods. This was done by means of delineating the methods, followed by the evaluation of each method against analysed annual flood records, and then the derivation of potential correction factors. The MIPI method was considered first.

7 MIPI Comparison

The MIPI method is based on two input characteristics namely, the catchment area and the hydrological region. No literature could be sourced on the development of the method which excluded the possibility of updating the method by means of repeating the steps used to develop the method. On the basis of this it was decided to evaluate the method *'as is'* and to suggest correction factors or changes which could be incorporated into the method.

The method was firstly analysed to see whether a pattern or formula could be found which could be used as a surrogate for the graphical approach of the MIPI method. This was done by considering the MIPI diagram as illustrated and explained in section 3.5.

7.1 Method Delineation

The analysis commenced with the evaluation of the right-hand part of the MIPI diagram (Figure 32). The flood peaks were used as the ordinate axis references with arbitrary values (referred to as abscissa Y-values in the research) on the abscissa (ranging from 5 to 50 000) to determine the positioning of the area lines.

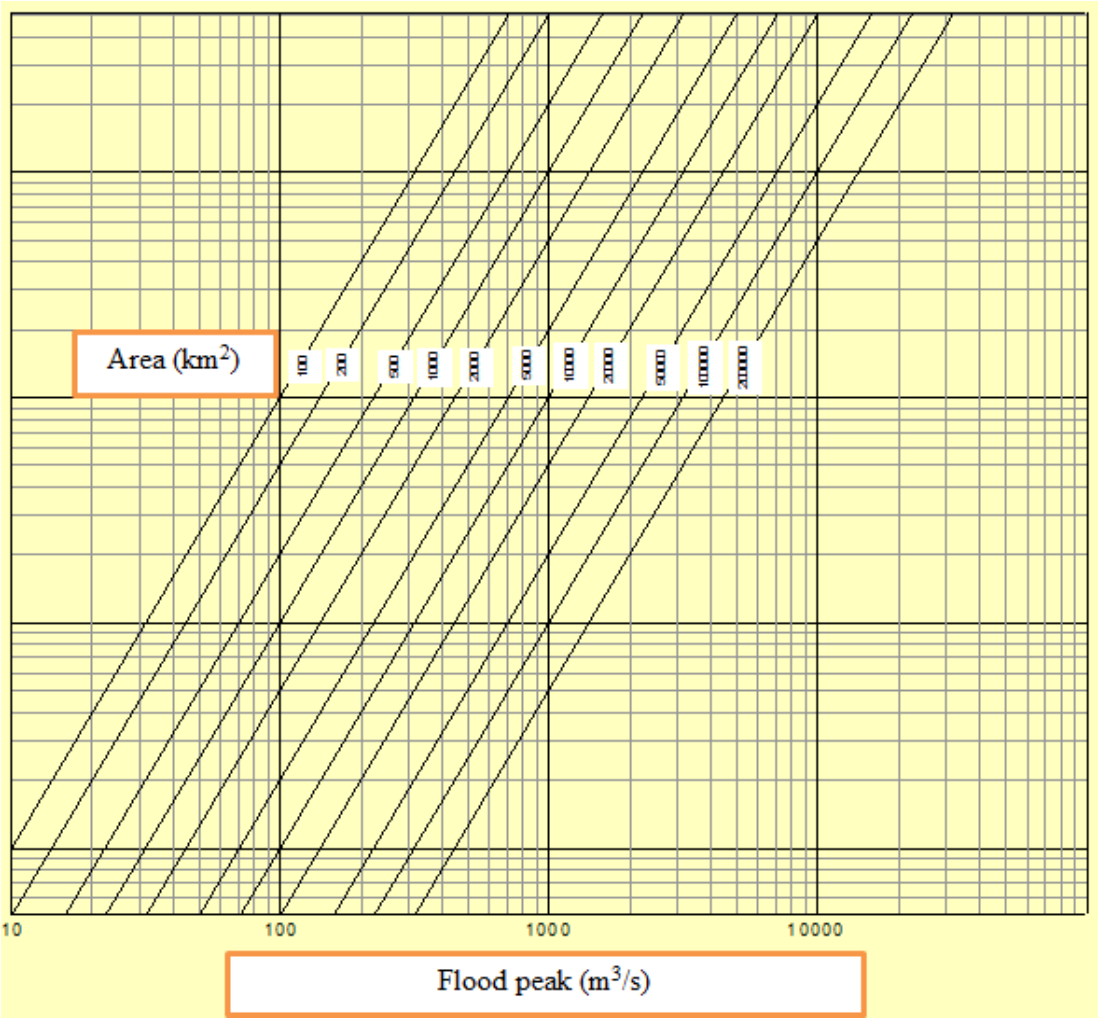

Figure 32: MIPI Diagram (Right-hand side of Figure 8)

The positioning of the diagonal area lines was determined by estimating the abscissa Y-values and corresponding ordinate flood peak values (Q) intersecting on the area lines. Ordinate intersection was determined for the first four area lines (100, 200, 500, 1 000) for an abscissa Y-value of 10 to 50 000. These four lines provided sufficient information which could be used to derive a formula with which to surrogate Figure 32

For the purpose of obtaining the relationship of Q with regard to the arbitrary abscissa Y-value the inverse of the right-hand section of the MIPI diagram was plotted in Excel. This was done by swapping the axes and plotting Q and Y on a logarithmic graph. A trendline which represented the inverse of the four area lines that had been evaluated was fitted to each of the four lines.. An equation was fitted to the trendlines which yielded an equation for each of the four lines in the form of:

$$Q = aY^{0.5} \qquad \textbf{Equation 9}$$

Where:

Y	=	Y-axis value.
a	=	Variable and a function of the catchment area i.e. a = f (A).
Q	=	The flood peaks on the X-axis.

Given the variability of “a” and “a” being a function of the catchment area i.e. a = f (A) a formula was required which represented “a” as a function of the catchment area. A trendline equation was fitted to the data (or plot) and yielded:

$$a = 0.326(\text{Area})^{0.5} \qquad \textbf{Equation 10}$$

The variable “a” in Equation 9 was substituted with Equation 10 which yielded Equation 11. In Equation 11 the design flood, Q is given as a function of the catchment area as well as the abscissa Y-value which is shared by both the right and left-hand side of the MIPI diagram.

$$Q = (0.326(\text{Area})^{0.5})\,(Y)^{0.5} \qquad \textbf{Equation 11}$$

In order to obtain a formula which could be used to surrogate for the MIPI diagram a formula was required which represented Y as a function of the regions and recurrence intervals. This formula was obtained by means of considering the left side of the MIPI diagram as illustrated in Figure 33.

Each regional line was considered separately and abscissa Y-value derived for each of the annual probabilities of exceedance (see Table 5).

Given the plot of the Flood Peak Recurrence Interval Diagram as well as the complexity of deriving formulae to represent the *‘regional lines’* as a function of recurrence intervals i.e. (say, for example) Y (or Y-value) = f (RI) or Y = f (T), it was decided to use the values in Table 5 to obtain the required Y-value directly for a given region and recurrence interval.

Table 5: Abscissa values (Y) for MIPI Recurrence Intervals and Region Intersections

	Recurrence Interval (years)						
Region	**2**	**5**	**10**	**20**	**50**	**100**	**200**
1	900	2600	4500	7350	13280	18000	26000
2	470	1700	3400	6250	13030	18000	26000
3	200	1070	2750	5800	12500	20100	32000
4	102	550	1300	2500	5350	8900	12500
5	50	295	760	1500	3150	5300	8050
6	27	235	750	1800	4600	8100	12500
7	4	32	80	170	370	600	910

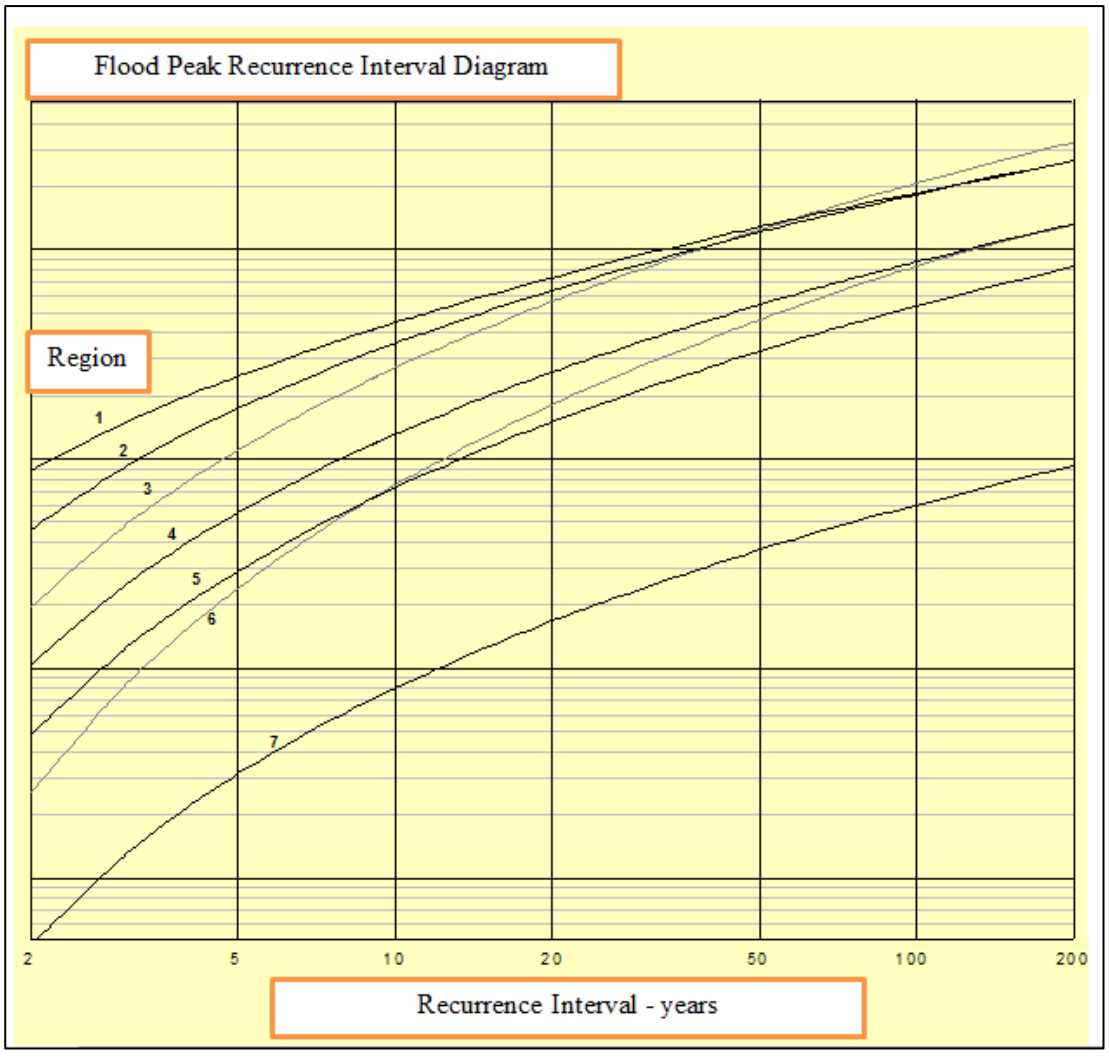

Figure 33: MIPI Diagram (Left-hand Side of Figure 8)

The MIPI diagram could thus be surrogated with the substation of the relevant Y-value for a given region and recurrence interval, out of Table 5 into Equation 11. The surrogate equation was particularly useful for this research in that the method could be applied to catchment areas smaller than a 100 km^2 whereas the MIPI diagram had no lines for catchment areas smaller than 100 km^2.

This improvement to the method meant that all 53 catchments that had been selected for *'research and analysis'* could be used instead of only those larger than 100 km^2. This could have resulted in a *'reduction in the sample/data set'* i.e. less than 53 for hydrological analysis with a negative effect on the outcome of the research. The design floods were estimated by means of applying the surrogate method for all 53 catchments. The results are listed in Appendix C.

7.2 Method Evaluation

The reliability of the MIPI method was evaluated by means of comparing the MIPI design floods against the assumed and more reliable probabilistic flood peaks. The comparison was based on the calculation of the percentage difference between the MIPI design flood and probabilistic floods, as a percentage of the probabilistic flood peaks. Negative or positive differences indicated an underestimation or overestimation of the MIPI design floods, respectively. For example, a 600 m^3/s MIPI design flood differed by a negative 25% compared to a 800 m^3/s probabilistic design flood i.e. Percentage difference = ([$^{600}/_{800}$ - 1] x 100).

No clear pattern was distinguishable during the comparisons and differences varied considerably between over estimations and under estimations. Table 6 illustrates the statistical characteristics calculated from the differences for all 53 gauging stations.

Table 6: Statistical Characteristics of the Flood Magnitude Differences in Percentage

	Recurrence Interval (years)						
	2	**5**	**10**	**20**	**50**	**100**	**200**
Max	1238%	798%	596%	492%	490%	487%	450%
Min	-73%	-70%	-70%	-71%	-73%	-74%	-76%
Mean	180%	111%	85%	67%	47%	44%	41%
Median	92%	49%	35%	29%	18%	18%	8%
St Dev.	306%	198%	160%	142%	137%	134%	126%

A pattern was identified for the estimated design floods when examined by Region, as can be seen when inspecting the standard deviation and trends for the *'differences in* percentage' for each Region (see Table 7, Table 9, Table 11, Table 13, Table 15, Table 17 and Table 18). Despite patterns having been identified it was virtually impossible to give any scientific meaning to them with such a small number of gauging stations, or to provide a better definition for these patterns (or tendencies). It was concluded that these patterns (or tendencies) could only be used as an aid for the identification of possible changes which could be used to improve the MIPI method.

7.3 Regional Evaluation and Updating

Given the above pattern it was decided to evaluate the regions separately and propose possible improvements per region. The only possible updating to the MIPI method which was considered was improvement of the MIPI diagram (Figure 8).

The number of gauging stations analysed per region made it impossible to redefine the regional boundaries with a high degree of accuracy. For the same reason only suggestions could be made as

to possible changes to improve the MIPI diagram, however it must be borne in mind that although only 83 gauging stations were used to derive the original regions.

The first step in the evaluation and updating of the MIPI regions focussed on grouping the gauging stations in the regions. This was followed by calculating the percentage difference between the design floods and probabilistic floods for each gauging station within a particular region. The corresponding data is tabulated in Appendix C. Equation 11 was then rearranged into Equation 12 to make Y a function of the design flow and the catchment area.

$$Y = (Q / (0.326(Area)^{0.5})^2 \qquad \textbf{Equation 12}$$

The design flood (Q) was substituted with the derived probabilistic floods and area with the known catchment areas of the 53 gauging stations. This substitution yielded the abscissa Y-values shared by the two parts of the MIPI diagram for each gauge. Plotting theses Y-values against the relevant recurrence intervals yielded a specific regional line for each gauging station.

The regional lines for gauging stations within the same region should more or less relate. As these regional lines were represented by the intersection of the recurrence interval and the abscissa Y-values, it would have been expected that the Y-values resulting from Equation 12 should have more or less corresponded per region and recurrence interval. This resemblance was not always evident and the gauging stations within a region formed bands instead of single regional lines.

The methodology followed in the potential updating of the method was to fit a line through the regional band in such a way that the minimum absolute difference, between the design floods and probabilistic floods, for each region and recurrence interval. The quartile rule along with the percentage differences for each gauging station were used to identify possible outlier gauging stations within the region and were excluded from the derivation of correction factors. Despite this *'exclusion'* these gauging stations were included in the evaluation of the improvement of the MIPI diagram.

Outlier gauging stations on regional boundaries were compared to surrounding regions and recommendations made on possible regional changes. These recommendations were not evaluated because they were considered to fall outside of the scope of this thesis and would form part of other, or future, research should the need arise. The presence of outliers on the boundaries and within regions suggests that the redefinition of regions and regional boundaries needs to be investigated.

The Y-values for the remaining gauging stations were averaged for each recurrence interval. The catchment area of each gauging station within the region and the derived average Y-value, instead of Table 5 Y-value, was substituted into Equation 11. This yielded design floods which were compared with the probabilistic floods and the average difference calculated for each recurrence interval.

An iterative process followed where the Y-value for each recurrence interval was adjusted upwards or downwards. The adjusted Y-value along with the catchments areas were again substituted into Equation 11 and the resulting design floods compared with the probabilistic floods. This process

continued for each recurrence interval until the smallest average difference was obtained between the design floods and the probabilistic floods.

The flowing results were obtained for each of the seven regions.

7.3.1 Region 1

Table 7: Region 1 differences

		Recurrence Interval (years)						
Gauge ID	**Area GIS**	**2**	**5**	**10**	**20**	**50**	**100**	**200**
G2H008	22	44	-20	-41	-53	-63	-70	-74
G1H004	74	-65	-58	-55	-51	-44	-42	-38
H1H006	734	-24	-16	-12	-7	1	2	8
E2H002	6784	197	148	125	112	102	87	82
	Mean	-15	-31	-36	-37	-35	-37	-35
	Std Dev	55	24	22	26	33	36	41

Gauge E2H002 was identified as a possible outlier and excluded from the calculations. It was suggested that this gauge form part of Region 5 although it was within the boundaries of Region 1. Even though the remaining sample of gauges was found to be too small for inferences evaluation of the method continued.

During the evaluation of each gauging station, it was found that G1H004 produced very large Y-values which were not excluded from the calculations even though this was not evident from the comparisons illustrated Table 7. By not excluding the large Y-values for G1H004 from the calculations yielded very high design floods for small catchment areas when compared to those from other gauging stations. The presence of this gauging station suggested that provision should be made for high rainfall areas situated in the mountains areas around Stellenbosch when redefining the regional boundaries of Region 1. The tendency for this gauging station to *'possibly influence'* and generally yield larger design floods for small catchment areas in Region 1 was considered but rejected. This is because the catchment area of gauging station G2H008 was smaller than that for G1H004 and it produced acceptable Y-values compared to station G1H004.

Considering the other three catchments and excluding outlier data, it was concluded that Region 1, on average, underestimated design floods as illustrated in Table 7. This meant that the regional line for Region 1 had to shift upwards on the MIPI diagram i.e. by increasing the Y-values in order to compensate for the underestimation of design floods.

The iterated Y-values confirmed underestimation of design floods for smaller recurrence intervals with the exception of the 1:50, 1:100 and 1:200 year design floods (see Table 8). The updated *'regional line'* was derived by means of plotting the Y-value and recurrence interval intersections and compared with the original regional line (see Figure 34).

Table 8: Original and iterated Y-values for Region 1

	Recurrence intervals (years)						
	2	5	10	20	50	100	200
Original Y-values	900	2600	4500	7350	13280	18000	26000
Iterated Y-values	1550	3700	5900	8500	13000	17200	22300

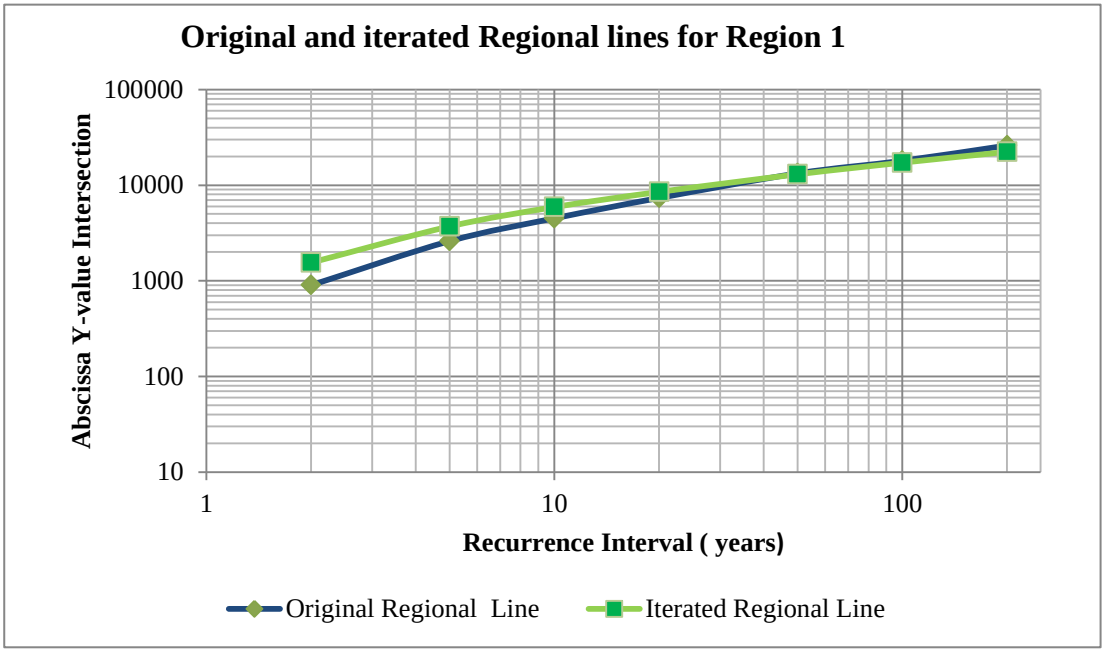

Figure 34: Original and iterated regional lines for Region 1

7.3.2 Region 2

Table 9: Region 2 differences

			Recurrence Interval (years)						
Gauge ID	Area GIS	Region	2	5	10	20	50	100	200
A2H029	124	2	1172	754	562	446	328	226	158
V6H003	295	2	23	31	37	43	54	49	49
U2H013	297	2	163	147	143	142	149	133	127
A2H027	367	2	213	121	88	67	49	28	15
V6H004	659	2	71	64	62	62	68	58	55
A2H023	688	2	59	64	68	75	87	80	80
A2H013	1062	2	224	99	56	30	8	-12	-24
B2H001	1582	2	187	69	30	7	-13	-30	-40
T3H002	2109	2	48	31	24	21	21	11	6
A2H012	2345	2	179	149	128	114	100	73	57
T3H005	2578	2	132	20	-14	-33	-49	-60	-68

Mean	130	79	62	53	47	33	26
Std Dev	74	47	48	51	58	58	59

Region 2 consisted of eleven gauging stations. A2H029 was identified as a possible outlier on the basis of applying the quartile rule on the percentage differences, and was excluded from any further

calculations. No factors could be identified which could have resulted in large differences between the MIPI design floods and probabilistic floods for A2H029.

Considering the remaining ten catchments and the differences as illustrate Table 9, it was demonstrated that the MIPI method overestimated the design floods for Region 2. Correcting this meant that the regional line would have to be shifted downwards resulting in a decrease of the Y-values.

The calculated Y-values supported this prediction (see Table 10). A proposed updated *'regional line'* was derived by means of plotting the Y-value and recurrence interval intersections and compared with the original regional line (Figure 35).

Table 10: Original and iterated Y-values for Region 2

	Recurrence intervals (years)						
	2	**5**	**10**	**20**	**50**	**100**	**200**
Original Y-interception	470	1700	3400	6250	13030	18000	26000
Iterated Y-interception	87	630	1900	3100	5800	12000	19800

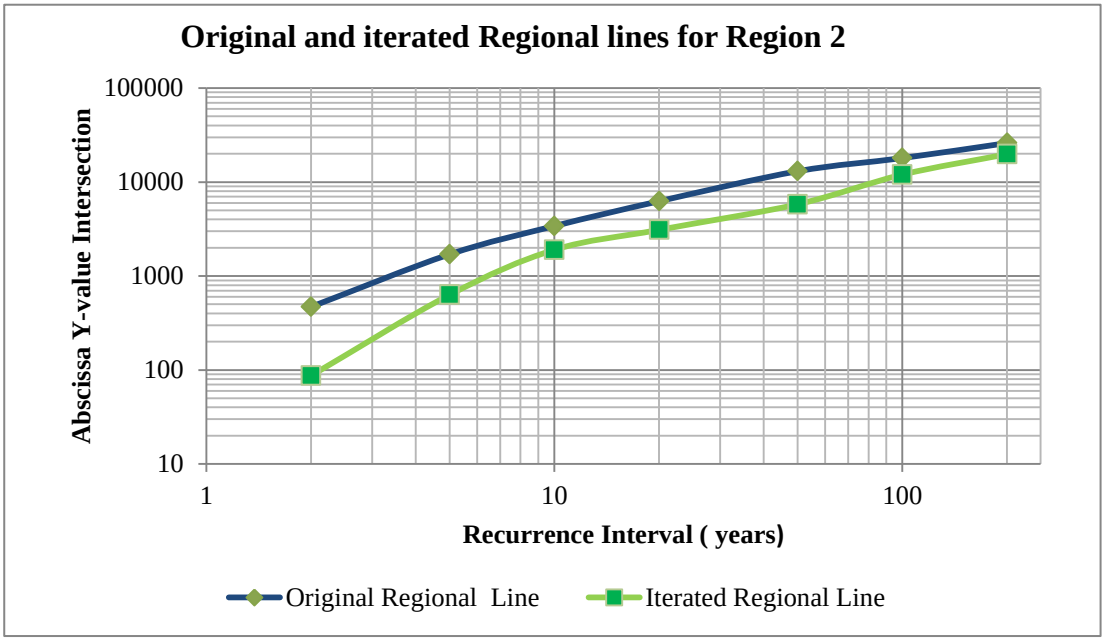

Figure 35: Original and iterated Regional Lines for Region 2

7.3.3 Region 3

Table 11: Region 3 differences

			Recurrence Interval (years)						
Gauge ID	**Area GIS**	**Region**	**2**	**5**	**10**	**20**	**50**	**100**	**200**
P1H003	1474	3	587	293	200	135	71	36	11
K4H003	74	3	250	134	90	56	17	-6	-22
J4H003	92	3	5	7	11	13	12	9	8
H7H004	10	3	29	26	25	21	11	1	-7
R2H012	17	3	105	42	16	-2	-22	-34	-43
R2H001	31	3	149	122	120	113	99	88	80
R2H008	68	3	94	-35	-61	-75	-86	-90	-93
Q3H004	873	3	154	78	52	32	8	-7	-18
L6H001	1287	3	101	9	-18	-36	-53	-63	-70
J3H004	4292	3	196	54	13	-14	-39	-52	-61
Mean			118	42	21	6	-12	-23	-30
Std Dev			54	50	56	59	59	58	57

Region 3 consisted of 10 gauging stations. P1H003, K4H003 were identified as possible outliers on the basis of applying the quartile rule on the percentage differences and were excluded from any further calculations. During the evaluation of the Y-values for these two gauging stations it was found that P1H003 shared the same Y-value characteristics as those found in Region 4, whilst K4H003 shared the same Y-value characteristics as those found in Region 5. It was concluded from these findings that a possible redefinition of Region 3 could improve the reliability of the method.

Considering the seven remaining gauging stations and the differences in (?) as illustrated in Table 11, it was concluded that the percentage in difference, between the design flood and the probabilistic flood, decreased as the recurrence interval increased. The method overestimated design floods for the 1:2, 1:5 and 1:10 year recurrence intervals and underestimated design floods for the remaining recurrence intervals.

Compensating for this meant that the updated regional line would have had to start a point lower and finish at a point higher compared to the original regional line, with an intersection between the 1:10 and 1:20 year recurrence interval line (?). The iterated Y-values supported this finding as illustrated in Table 12. This was also evident in Figure 35 which illustrated the original and iterated regional lines for Region 3.

Table 12: Original and iterated Y-values for Region 3

	Recurrence intervals (years)						
	2	**5**	**10**	**20**	**50**	**100**	**200**
Original Y-interception	200	1070	2750	5800	12500	20100	32000
Iterated Y-interception	60	460	2200	7800	33000	87000	211000

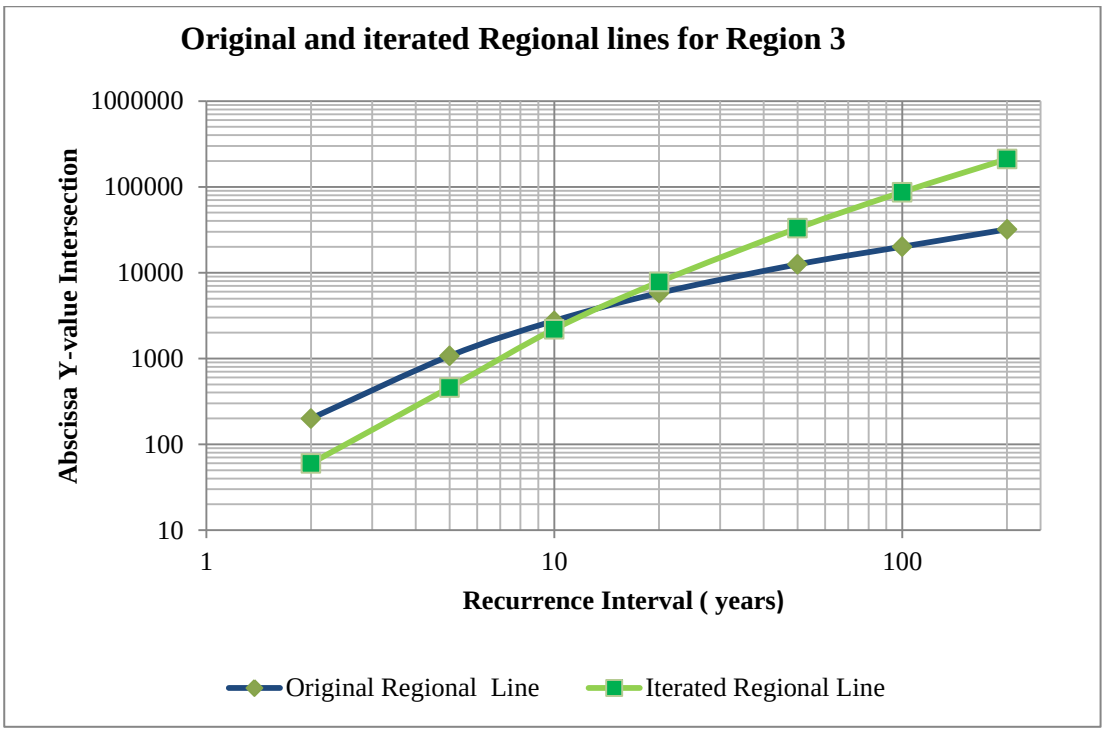

Figure 36: Original and iterated Regional Lines for Region 3

7.3.4 Region 4

Table 13: Region 4 differences

			Recurrence Interval (years)						
Gauge ID	**Area GIS**	**Region**	**2**	**5**	**10**	**20**	**50**	**100**	**200**
W5H011	883	4	458	465	474	466	463	461	425
W1H004	20	4	376	155	82	33	-5	-24	-42
X3H001	178	4	204	266	290	306	329	347	333
X2H008	187	4	46	41	36	27	21	16	6
X2H031	263	4	73	13	-10	-28	-43	-51	-60
U3H002	360	4	55	44	37	28	20	15	4
B6H001	514	4	15	25	29	29	30	31	23
W3H001	1466	4	36	-6	-23	-37	-49	-55	-63
T4H001	736	4	-11	-16	-19	-24	-28	-31	-37
S3H006	2207	4	159	129	113	95	79	70	51
U2H004	2261	4	20	39	49	53	61	66	60
W2H005	3952	4	-34	-35	-36	-38	-41	-42	-47

Mean	40	26	19	12	6	2	-7
Std Dev	55	47	47	46	48	49	47

Region 4 consisted of 12 gauging stations. W5H011 and X3H001were identified as possible outliers on the basis of applying the quartile rule on the percentage differences, and were excluded from any further calculations. During the evaluation of the Y-values of these two gauges it was found that both shared the same Y-value characteristics as those found in Region 7 which possibly pointed to the redefinition of Region 4.

Considering the remaining ten catchments and the differences as illustrated in Table 13, it was concluded that the MIPI method overestimated the 1:2 to 1:100 year design floods and underestimated the 1: 200 year design flood.

Compensating for this meant that the updated regional line would have had to start a point lower and finish at a point higher compared to the original regional line, with an intersection between the 1:100 and 1:200 year recurrence interval.

The iterated Y-values supported the findings described above for the 1:2 to 1:100 year design floods (see Table 12), however, the iterated Y-value for the 1:200 year design flood did not follow the predicted pattern. This was attributed to the distribution of the differences in percentage around zero for the 1:200 year design flood. Figure 37 illustrated the original and iterated regional lines for Region 4.

Table 14: Original and iterated Y-values for Region 4

	Recurrence intervals (years)						
	2	**5**	**10**	**20**	**50**	**100**	**200**
Original Y-interception	102	550	1300	2500	5350	8900	12500
Iterated Y-interception	54	290	740	1530	3700	6600	11600

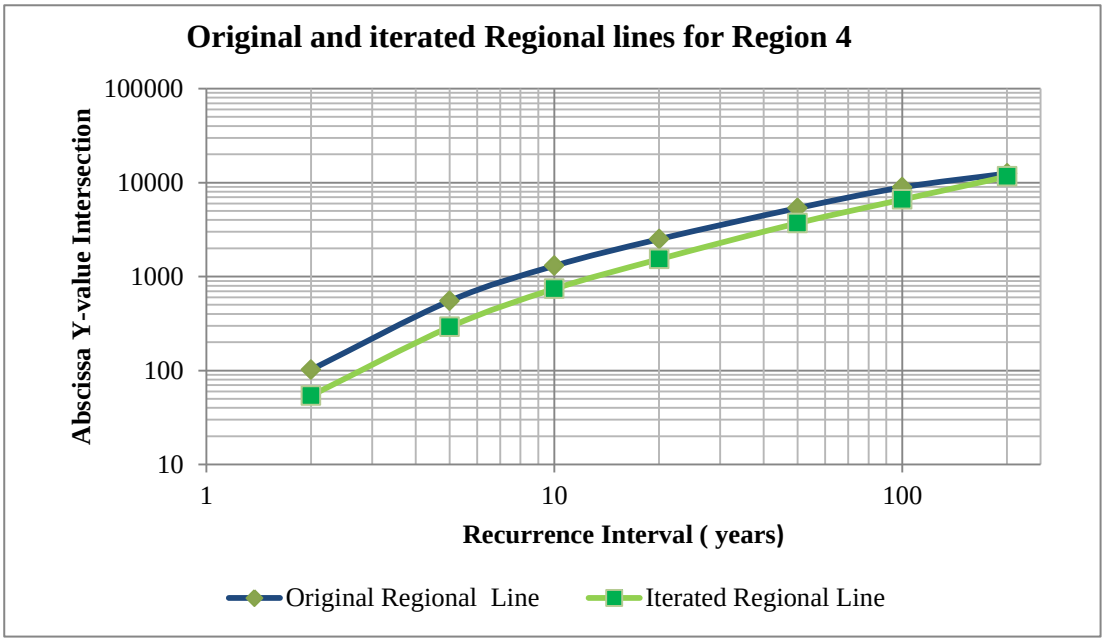

Figure 37: Original and iterated Regional Lines for Region 4

7.3.5 Region 5

Region 5 consisted of ten gauging stations. Gauging station J2H016 was identified as a possible outlier and was excluded. During evaluation of the Y-values for J2H016 it was found that the station shared the same Y-value characteristics as those found in Region 7, which possibly pointed to a need for the redefinition of Region 5.

Table 15: Region 5 Differences

			Recurrence Interval (years)						
Gauge ID	**Area GIS**	**Region**	**2**	**5**	**10**	**20**	**50**	**100**	**200**
J2H016	17085	5	813	336	198	107	35	4	-21
C7H005	5661	5	151	55	22	-5	-29	-41	-51
L2H003	1152	5	117	77	60	39	18	8	-4
C8H003	869	5	35	33	35	29	21	18	12
C5H008	608	5	13	-1	-6	-14	-24	-29	-35
D5H003	1487	5	44	31	25	15	3	-2	-10
D1H001	2387	5	10	-5	-8	-14	-19	-21	-23
L1H001	3934	5	-12	-13	-15	-21	-29	-34	-40
C6H001	5645	5	-58	-56	-54	-55	-56	-56	-58
C1H001	8009	5	-28	-21	-16	-16	-18	-17	-20
Mean			0	-4	-5	-11	-17	-20	-25
Std Dev			36	31	29	27	25	24	22

Considering the remaining nine catchments and the differences illustrated in Table 15, it was concluded that the MIPI method underestimated the flood peaks for the 1:5 to the 1:200 year design floods. The 1:2 year design flood was found to be a good representation of probabilistic flood. For this Region i.e. Region 5 it was also concluded that underestimation of flood peaks increased as the recurrence interval increased.

During the evaluation of the differences in (?) for Region 5 and subsequent identification of a definite trend of increased underestimation of floods with corresponding increase in recurrence intervals i.e. *'N, in years'*, it was predicted that the iterated regional line would shift downwards. This shift would also become more prominent as the recurrence interval increased. The iterated Y-values supported this prediction as is illustrated in Table 16. Figure 38 shows the original and the iterated regional lines for Region 4.

Table 16: Original and iterated Y-values Region 5

	Recurrence intervals (years)						
	2	**5**	**10**	**20**	**50**	**100**	**200**
Original Y-interception	102	550	1300	2500	5350	8900	12500
Iterated Y-interception	69	460	1000	2100	4600	7600	12200

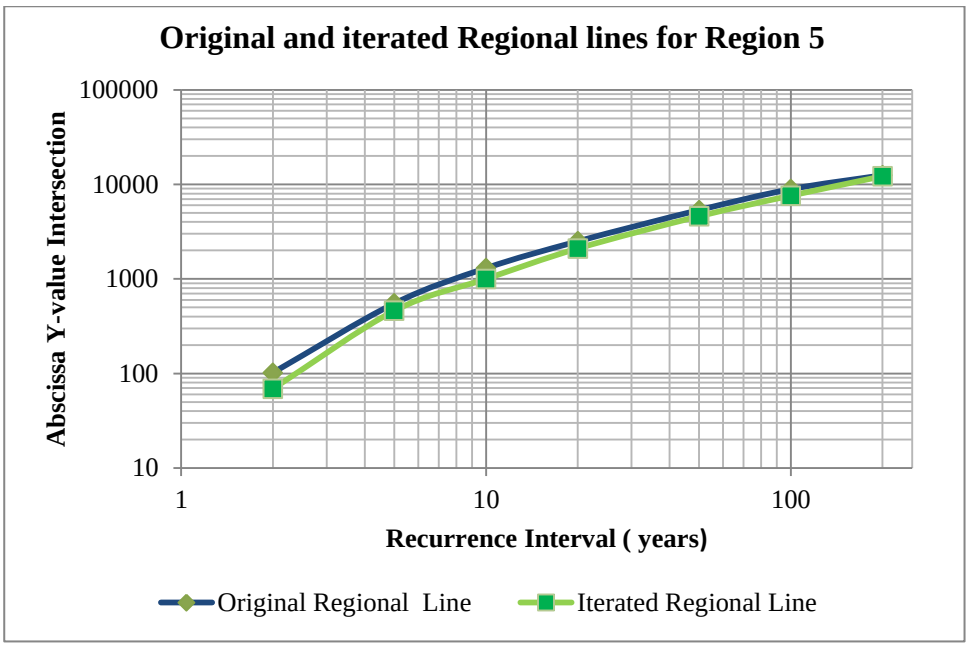

Figure 38: Original and iterated Regional Lines for Region 5

7.3.6 Region 6

Table 17: Region 6 Differences

			Recurrence Interval (years)						
Gauge ID	**Area GIS**	**Region**	**2**	**5**	**10**	**20**	**50**	**100**	**200**
A2H004	132	6	215	193	193	180	159	140	115
B7H002	62	6	44	-5	-31	-52	-71	-80	-87
A7H001	7704	6	125	86	65	42	15	-4	-23
Mean			85	41	17	-5	-28	-42	-55
Std Dev			58	64	68	66	60	54	45

Region 6 consisted of three gauging stations which were considered to be too small for inferences. The three gauging stations were evaluated and it was found that station A2H004 shared the same Y-values characterises as those of Region 7 which differed considerably from the remaining two gauging stations.

On the basis of these differences in Y-values it was decided to exclude A2H004 from further evaluation for Region 6. During the evaluation of the remaining two gauging stations it was found that the underestimation of the MIPI method increased as the recurrence interval increased.

No definitive conclusion could be drawn when the remaining gauging stations were analysed i.e. when gauging station A2H004 had been excluded from the dataset. The mean differences were then considered and it was assumed that the MIPI method overestimated the 1:2 to 1:10 year floods and underestimated the 1:20 to 1:200 year floods. New Y-values for Region 6 were not iterated and no recommendations were made for Region 6 due to a lack of data. There were no distinguishable trends or patterns in the small sample of data.

7.3.7 Region 7

Table 18: Region 7 Differences

			Recurrence Interval (years)						
Gauge ID	**Area GIS**	**Region**	**2**	**5**	**10**	**20**	**50**	**100**	**200**
D5H001	2165	7	-73	-70	-71	-71	-73	-75	-76
D6H002	6898	7	-65	-40	-26	-13	1	9	16
C3H003	11218	7	-43	-29	-29	-29	-32	-36	-41
		Mean	-60	-46	-42	-38	-35	-34	-34
		Std Dev	16	21	25	30	37	42	47

Region 7 consisted of three gauging stations and the data set was considered to be too small for inferences. However, despite this, the three stations were evaluated and it was found that all three shared the same Y-values characteristics.

During the evaluation of the three gauging stations it was evident that the MIPI method underestimated the flood peaks with the exception of the 1: 50 to 1:200 year floods for gauging station D6H002. The underestimation of the flood peaks also decreased as the recurrence intervals increased.

Keeping these patterns in mind the recommended (or proposed) correction would include upwards-shifting of the regional line. The iterated Y values have supported this prediction as illustrated in Table 19. The original and iterated regional lines are illustrated in Figure 39 for *'future reference and completeness of this research'* despite there being such a small sample of gauging stations in the region.

Table 19: Original and iterated Y-values for Region 7

	Recurrence Intervals (years)						
	2	**5**	**10**	**20**	**50**	**100**	**200**
Original Y-values	4	32	80	170	370	600	910
Iterated Y-values	32	87	157	340	810	1480	2600

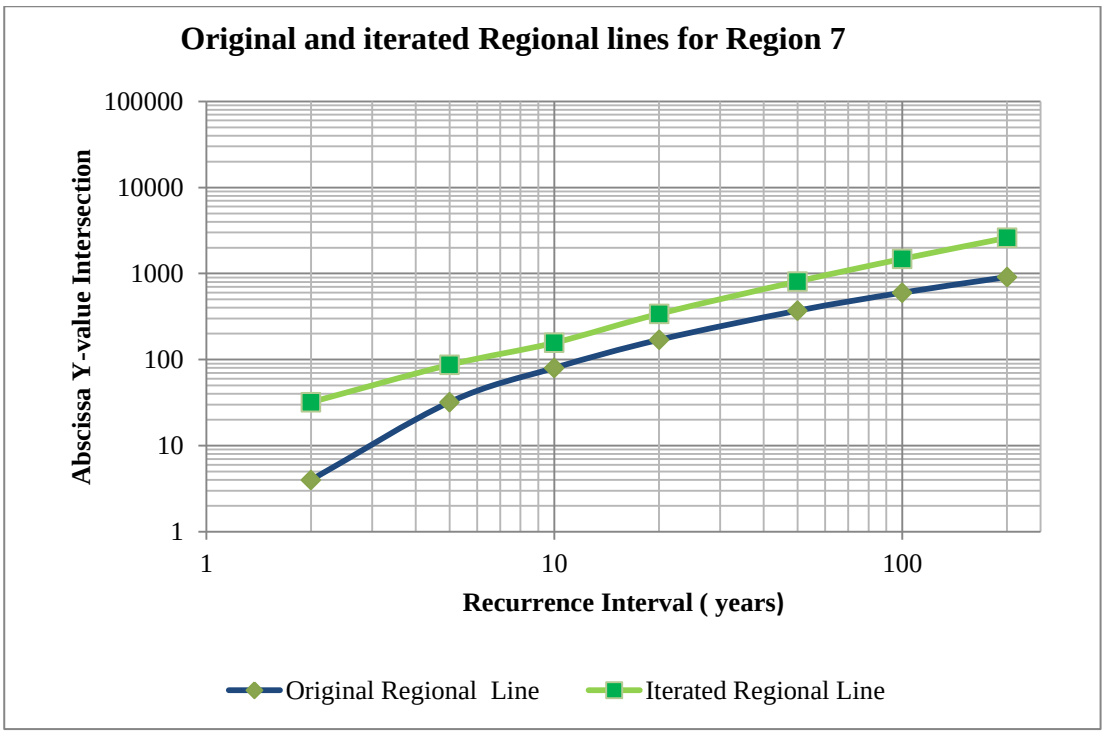

Figure 39: Old, Calculated and Proposed Regional Lines for Region 7

7.3.8 Proposed Update for the MIPI Method

The proposed process for updating the MIPI method has been illustrated and utilised to great effect in the research. This could, however, only be done and proven within the limits of the available data and methodology followed.

The iterated Y-values for each region which are listed in Table 20 together with Equation 11 have been presented as an update for the MIPI method to determine design floods for different recurrence intervals. The updated method could decrease errors associated with the use of the MIPI diagram as it currently stands with the advantage of making the method applicable to catchments areas smaller than 100 km^2. It is also recommended that the *'regional lines'* in the MIPI diagram be updated as shown in Figure 40.

Table 20: Proposed new Abscissa Y values for the MIPI Method

	Recurrence Intervals (years)						
	2	**5**	**10**	**20**	**50**	**100**	**200**
Region 1	1230	3388	5754	9120	15849	22909	27542
Region 2	105	692	1995	4365	9120	14791	22387
Region 3	31	460	2200	7800	33000	87000	211000
Region 4	69	460	1000	2100	4600	7600	12200
Region 5	41	329	906	2048	5030	8400	13840
Region 6	5	67	270	900	3500	8800	20900
Region 7	32	87	157	340	810	1480	2600

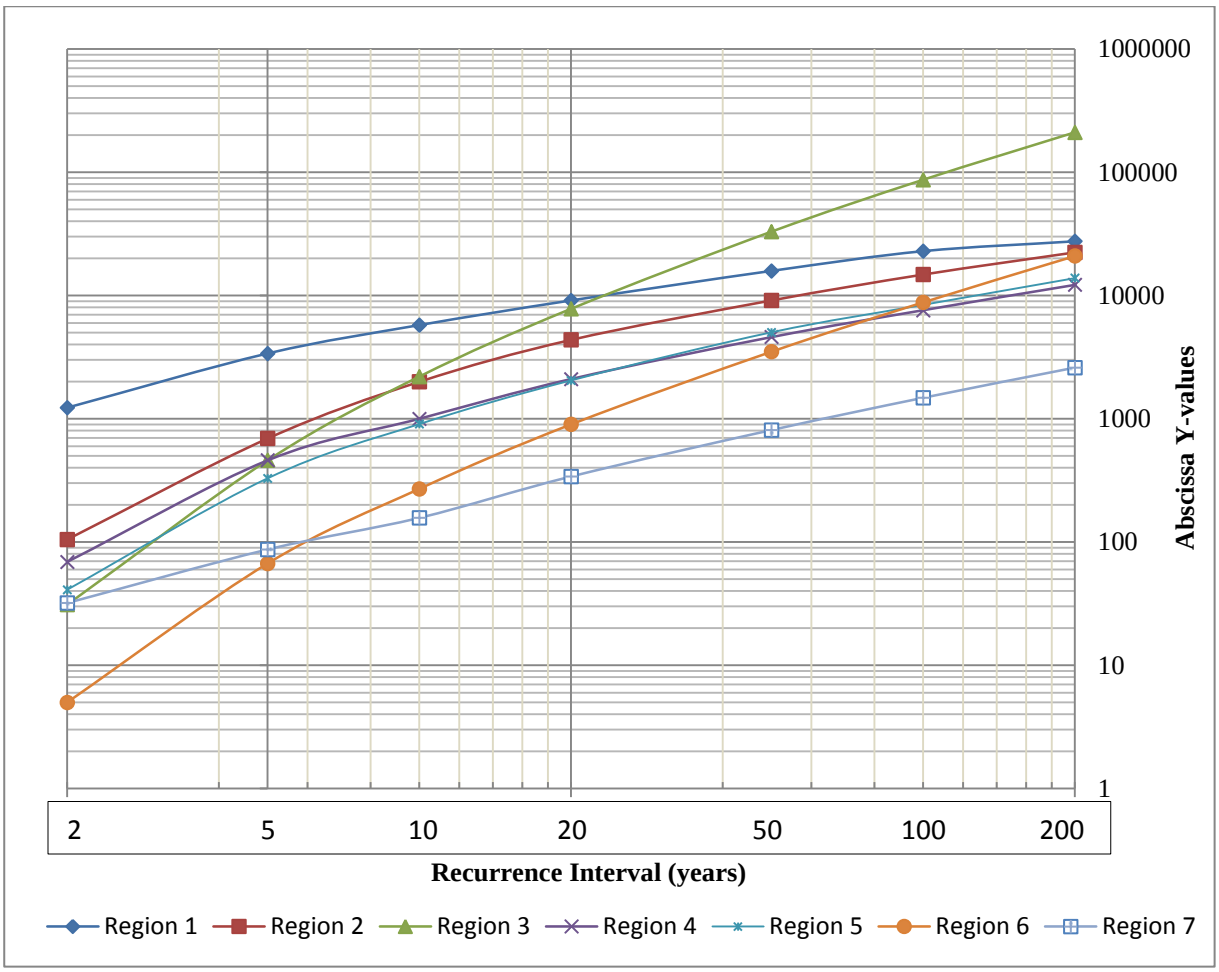

Figure 40: Proposed Update for the MIPI Diagram

7.3.9 Evaluation of the proposed updates

The proposed update was evaluated by means of plotting the differences between the original MIPI design floods and probabilistic floods as well as the differences between the updated MIPI design floods and probabilistic floods for all 53 catchments. Even though no distinction was made between the various recurrence intervals it could clearly be illustrated that *'updating'* decreased the differences through a visual inspection of a scatter diagram. The catchments were ranked according to regions and then design flood differences. The scatter diagram is illustrated in Figure 41. Statistical characteristics such as the maximum, minimum, mean and median for the *'Original'* and *'Updated'* Flood differences only showed a slight increase as a result of the inclusion of outliers (see Table 21).

Table 21: Statistical characteristics comparison between updated and original MIPI differences

	Original design flood differences							Updated design flood differences						
RI(yrs.)	**2**	**5**	**10**	**20**	**50**	**100**	**200**	**2**	**5**	**10**	**20**	**50**	**100**	**200**
Max	1238%	798%	596%	492%	490%	487%	450%	752%	473%	434%	443%	447%	443%	443%
Min	-73%	-70%	-70%	-71%	-73%	-74%	-76%	-69%	-52%	-59%	-59%	-60%	-63%	-61%
Mean	180%	111%	85%	67%	47%	44%	41%	89%	71%	63%	61%	45%	34%	23%
Median	92%	49%	35%	29%	18%	18%	8%	25%	25%	22%	20%	15%	7%	-2%

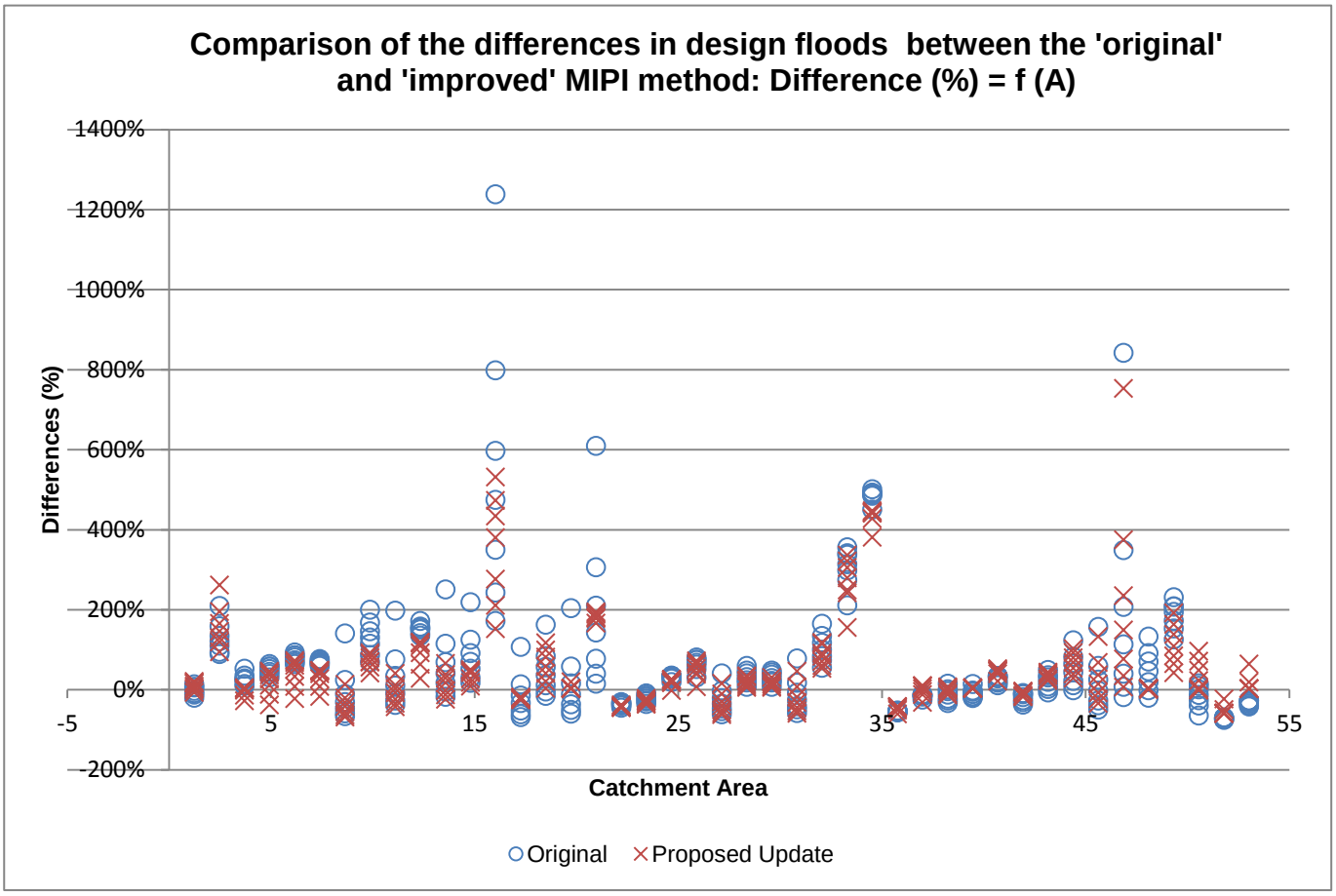

Figure 41: Proposed updates for the MIPI design floods compared to the original MIPI method differences.

8 CAPA Comparison

The CAPA method is based on four input characteristics namely, the catchment area, mean catchment slope, longest watercourse length and the MAP. No literature could be sourced on the development of this method thus excluding the opportunity of updating the method by means of following the steps that were originally used to develop the method. On the basis of this the author had no choice but to evaluate the method *'as is'* and to propose (or recommend) correction factors or changes which could be incorporated into the method.

The application of the CAPA Method was dealt with in section 3.6. The CAPA method uses more input characteristics compared to the MIPI method however it lacks the advantage of regionalisation or grouping which is the basis of the MIPI method. The CAPA method *'partially compensates'* for this by making use of the mean annual precipitation (MAP) as an input characteristic, or parameter.

It was hoped that the CAPA method might yield more reliable results as it made use of more input characteristics. Unfortunately this was found not to be the case and the most plausible explanation for this poorer reliability can be attributed to the large influence of the MAP.

The method was initially evaluated to see whether a pattern or formula could be found which could be used as a surrogate for the graphical approach of estimating the mean annual flood (Q_S). This was done by considering the CAPA diagram illustrated and explained in section 3.6. This was followed by an evaluation of the mean annual flood Q_S by means of comparing the CAPA quantified Q_S with the mean annual flood which was derived using statistical methods. The results from the comparison were then used to derive correction factors which had the potential to increase the reliability of the method used to estimate Q_S.

The second part of the CAPA evaluation focused on the reliability of the CAPA design floods. The design floods were compared to probabilistic floods by means of calculating the difference between the floods in the same manner that was used for the MIPI method comparison explained in section 7.2. The results were then used to derive correction factors which were evaluated by comparing the differences between the design and probabilistic floods using the *'original'* CAPA method, with the differences between the *'updated CAPA design floods'* and the more reliable probabilistic floods.

8.1 Delineation of the CAPA "M" diagram

The delineation of the M diagram focused on the relationship between the lumped diagonal parameter lines, the abscissa (Q_S) and ordinate axis (catchment area, A). The ordinate and abscissa values were plotted on a logarithmic graph and trendlines fitted to the lumped parameter lines. All seven lumped parameter lines were best described by an equation in the form of:

$$Q_S = C\ A^B \qquad \textbf{Equation 13}$$

Where:

Q_S = Mean Annual Flood (m^3/s)

C = Constant and a function of M
A = Catchment area (km^2)
B = Constant

From the equations fitted to the trendlines, it was found that both constant B and C differed for all seven lumped parameters i.e. M (see Table 22). The variation in the constant B was ascribed to small errors associated with the approximation of these values from CAPA diagrams. A mean value of 0.61 was assumed for constant B.

Table 22: Calculated Constant B and C

M	B	C
10000	0.6112	7
5000	0.6095	4.5
2000	0.64	2.384
1000	0.6125	1.344
600	0.616	0.871
400	0.6087	0.609
200	0.6114	0.299

Max	0.64
Min	0.6087
Mean	0.6156143
Std Dev.	0.0110072

C was plotted against the corresponding lumped parameter value (M) on a logarithmic scale (see Figure 42). A trendline was fitted to the points and an equation which best defined the line fitted to the graph (see Equation 14).

$$C = 0.0052\ M^{0.7983}$$ **Equation 14**

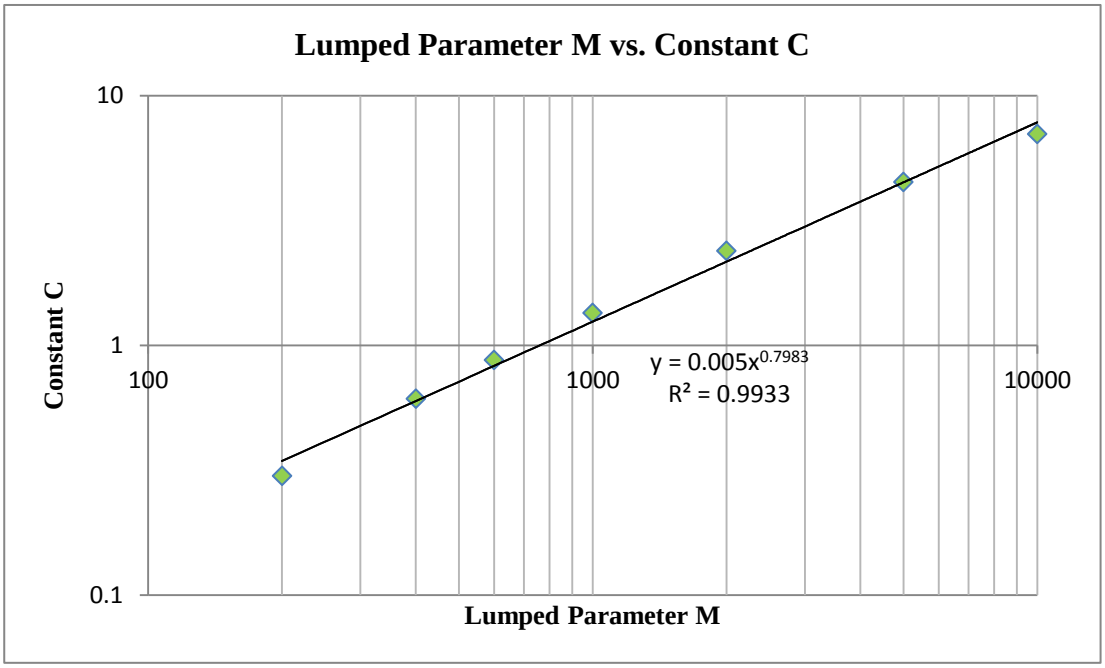

Figure 42: Lumped Parameter M vs. Constant C

Equation 15 was derived by substituting Equation 14 into Equation 13:

$$Q_S = 0.0052\ M^{0.7868}\ A^{0.61} \qquad \textbf{Equation 15}$$

Equation 15 was then used to determine Q_S (or the mean annual flood) for each of the 53 gauging station. The results are presented in Appendix E

8.2 Evaluation of CAPA Method quantified by Q_S

The annual mean floods that were derived were evaluated against the statistically determined annual mean floods (Qs) and the differences between the CAPA and the statistically determined annual mean floods in the same manner described in section 7.2.

No distinguishable patterns could be identified by evaluation of the differences on their own and results varied from a maximum underestimation of 75% to 366% between the mean annual floods. Further evaluation of the differences produced a mean underestimation of 6%, median underestimation of 28% and a standard deviation of 80%. The percentage differences ranked from low too high for all 53 gauging stations are illustrated in Figure 43.

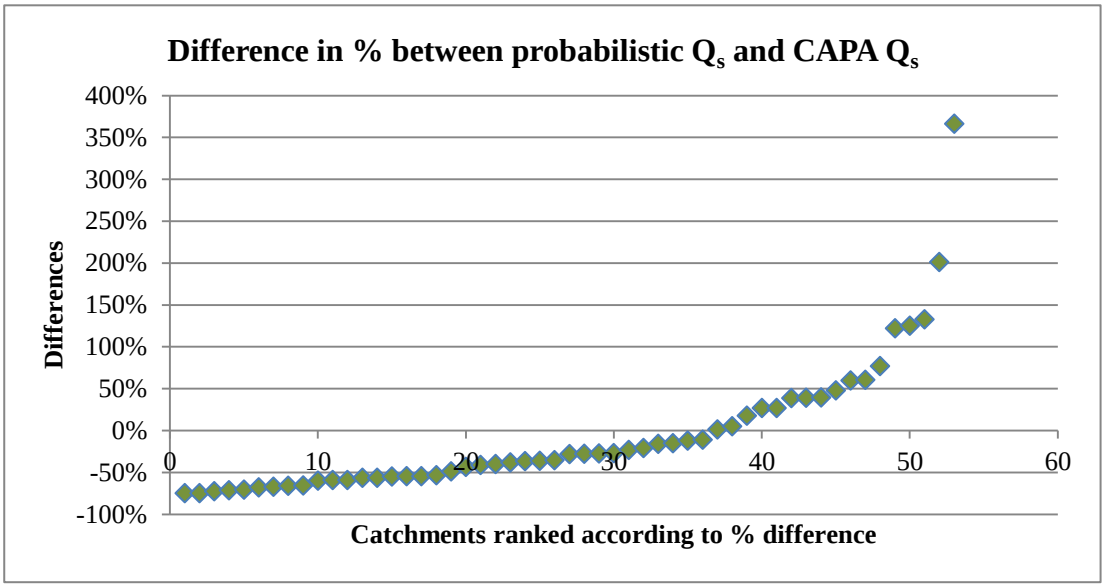

Figure 43: CAPA Percentage Differences

The differences were plotted against ranked characteristics in the attempt to identify patterns which could potentially be used to derive correction factors. Scatter diagram were used for the evaluation.

The differences in Q_S plotted against MAP of the gauging stations showed a tendency to increase as the MAP increased (see Figure 44). The band was distributed on both sides of the origin with the bulk of differences below the origin for values of MAP lower than 900 mm and vice versa. Apart from this trend no other trends could be identified.

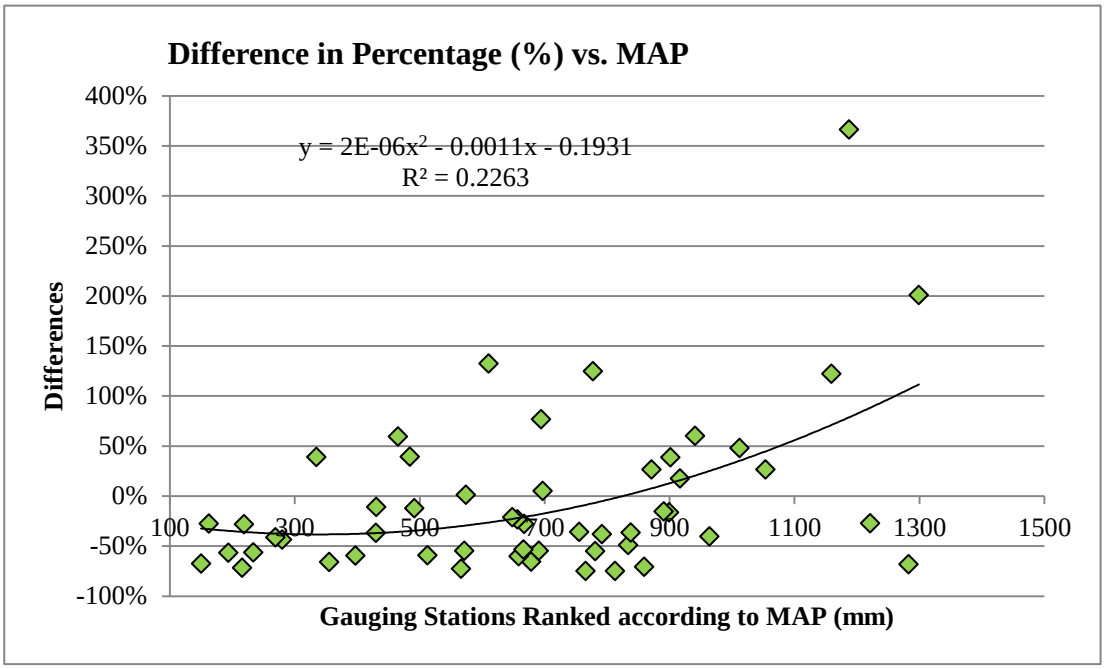

Figure 44: Difference in Q_S plotted against ranked MAP characteristics.

The differences in Q_S plotted against the catchment areas of the gauging stations are shown in Figure 45 which shows a tendency for the percentage (%) differences to decrease as the catchment area increases. The band was, however, distributed on both sides of the origin with the bulk of differences above the origin for catchment areas smaller than 600 km^2 and vice versa. Apart from this trend no other trends could be identified.

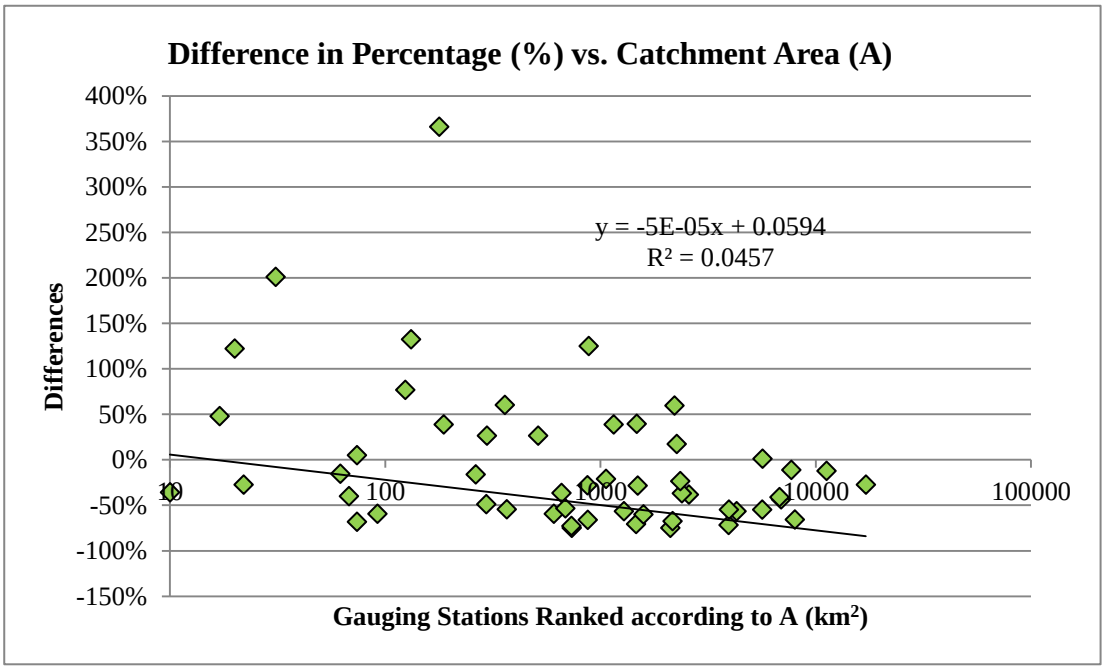

Figure 45: Difference in Q_S plotted against ranked catchment area characteristics.

The differences in Q_S plotted against the lengths of the longest watercourses for gauging stations showed a tendency to decrease with an increase in length (see Figure 46). The band was distributed on both sides of the origin with the bulk of differences below the origin for lengths longer than 36 km and vice versa. Apart from this trend no other trends could be identified.

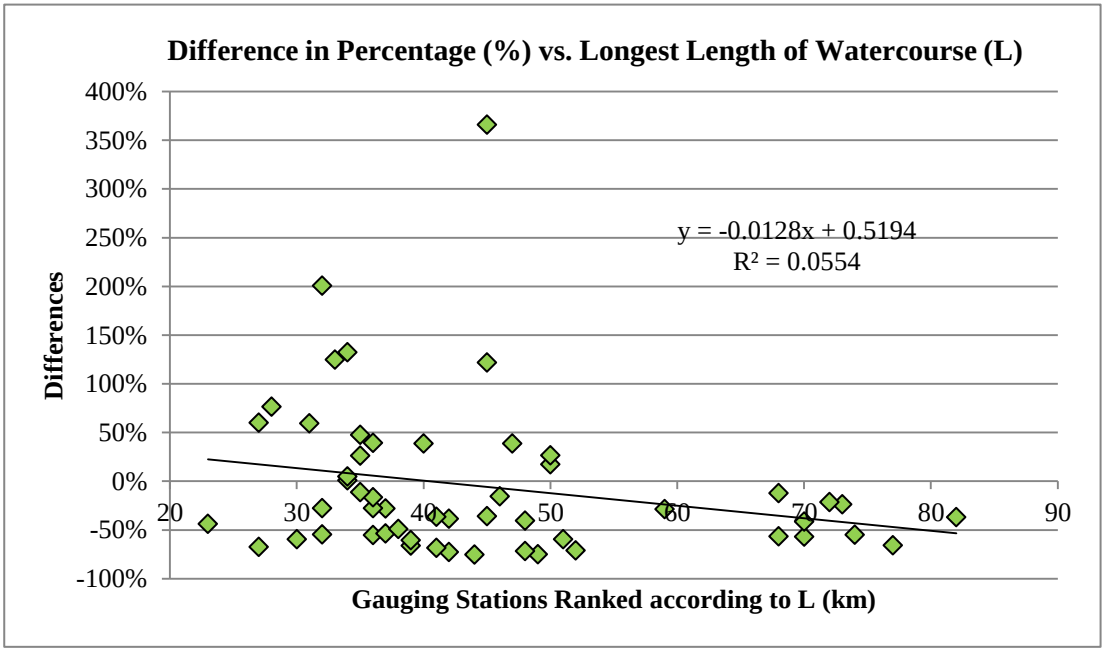

Figure 46: Difference in Q_S plotted against ranked longest watercourse characteristics.

The differences in Q_S plotted against the mean catchment slopes of the gauging stations exhibited three distinct clusters as illustrated in Figure 47.

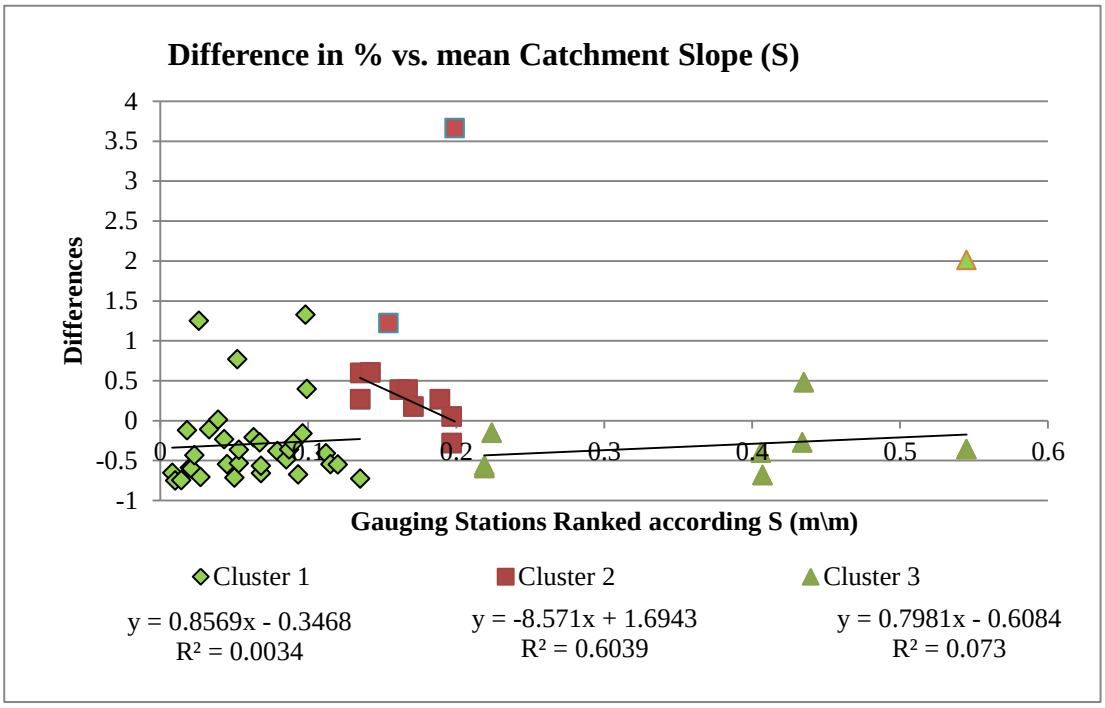

Figure 47: Difference in Q_S plotted against ranked mean catchment characteristics.

Cluster 1 was identified for slopes between 0 and 0.135 m/m where a clear underestimation of the mean annual flood was evident. Cluster 3, as illustrated in Figure 48, was not as prominent and was found between slopes of 0.197 and 0.55. Cluster 2 was found between 0.135 and 0.197. This cluster of points showed a clear overestimation of the mean flood with a linear decrease in difference as the slope increased. The presence of these three clusters, especially Cluster 2, could not be explained.

8.3 Updating of the quantified CAPA Q_S

The derived patterns between the differences and the ranked characteristics were evaluated in order to identify the best suited pattern which could be used to update the quantification of the mean annual flood (Qs) used in the CAPA Method. The pattern identified between the mean catchment slopes and differences showed the most promise and was selected for *'analysis'*.

The methodology that was adopted focussed on the derivation of correction factors for each of the three clusters. The clusters between 0 and 0.135 m/m (Cluster 1) and 0.197 and 0.55 m/m (Cluster 3) were analysed first. It was decided to derive a single correction value for each cluster after the fitted linear trendlines *'inherited'* flat gradients which could closely be approximated by a single value instead of *'arduous equations'*.

Apart from seven gauging stations in Cluster 1 and the two gauging stations in Cluster 3, all the other gauging stations showed an underestimation of Q_S. The possibility of minimising the influence of the gauging stations which overestimated Q_S by removing them from the *'dataset for analysis'* was considered. It was subsequently decided to derive 2 correction factors in an attempt to obtain a basis for more meaningful or scientific *'evaluation/analysis'*. One correction factor included data from those gauging stations which overestimated Q_S and one which excluded them. They were referred to as the *'complete gauge sample'* and the *'excluded gauge sample'*, respectively. The potential of these factors was evaluated and what was deemed to be the best correction factor selected.

The correction factor derivation process made use of the method of least squares and the correction factor was adjusted by means of iteration i.e. until the smallest absolute difference in summed Q_S was obtained for the gauging stations in the sample.

A correction factor of 1.70 and 1.68 was obtained for Cluster 1 and Cluster 3, respectively, when the *'complete gauge samples'* were analysed. In the case of analysis for the *'excluded gauge sample'* correction factors of 1.76 and 2.3 were obtained for Cluster 1 and Cluster 3, respectively. These results are summarised in Table 23 along with the absolute difference averages for each of the two clusters and gauge sample groups, compared to the original absolute difference.

Table 23: Absolute difference averages for Cluster 1 and 3 and the derived correction factors.

	Absolute difference average (m^3/s) (derived correction factor)		
	Original	**Complete gauge sample**	**Excluded gauge sample**
Cluster 1	107	73 (1.70)	72 (1.76)
Cluster 3	48	37 (1.68)	29 (2.3)

Substituting correction factors derived for the *'complete gauge sample'* into the *'excluded gauge sample'* showed a very slight increase in the averages for absolute differences i.e. 0.2 m^3/s and 3.7 m^3/s for Cluster 1 and Cluster 3, respectively. The correction factor derived for the *'complete gauge sample'* for Cluster 3 was substituted with 1.70 instead of the derived value of 1.68. This increased the absolute difference of the averages by 0.1 m^3/s for the Cluster 3 gauging stations (*'complete gauge sample'*).

Given these small increases in absolute difference averages it was decided to make use of the correction factors derived for the *'complete gauge samples'* for Cluster 1 and 3 it was decided to replace the correction factor derived for Cluster 3 with 1.7.

Instead of opting for a single correction value as per the previous two clusters it was decided to make use of the distinct linear pattern of Cluster 2 to derive a correction equation. The methodology made use of the method of least squares in which the intersection of the gradient and abscissa of a linear equation was subjectively altered through iteration.

Equation 16 resulted from the iteration process in which the absolute difference averages between statistically quantified values for Q_S and CAPA Q_S for Cluster 2 were reduced from 32 m^3/s to 17 m^3/s for the 11 gauging stations representing Cluster 2. The correction factor derived for Cluster 1 and Cluster 3 was also evaluated to see if it could be used to represent Cluster 2. This increased the absolute difference average between statistical quantified Q_S and CAPA Q_S to 109 $^3/s$.

$$\text{Updated } Q_S = 0.74\ Q_S \text{ original} - 1.26 \qquad \textbf{Equation 16}$$

Given the evaluation of the correction factor it was decided to propose a correction factor of 1.7 for catchments with slopes outside the ranges of 0.135 m/m to 0.197 m/m and Equation 16 for catchments slopes between 0.135 m/m and 0.197 m/m.

The correction factors were evaluated by means of comparing the original Q_S differences with the updated Q_S differences as illustrated in Figure 49. As expected, the correction factors decreased the percentage difference for the bulk of the gauging stations. This was however not the case for the overestimation of floods at gauging stations in Cluster 1 and Cluster 3. The linear correction equation for Cluster 2 showed very promising results.

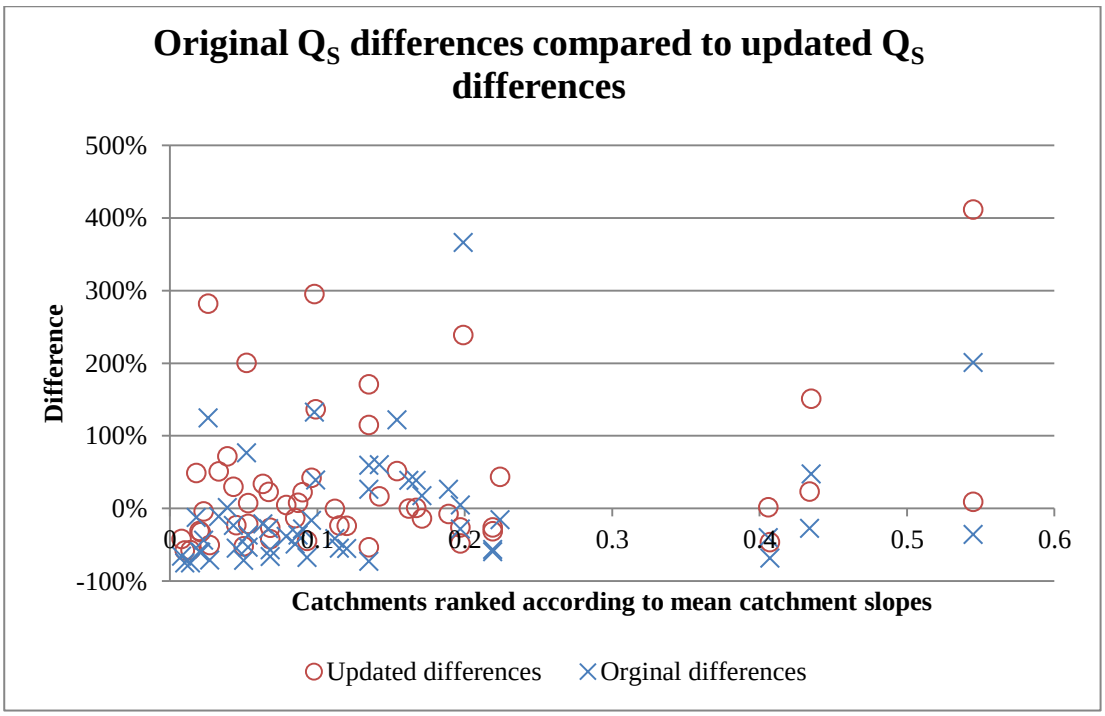

Figure 49: Original QS differences compared to updated QS differences

8.4 Delineation and Evaluation of the CAPA Method Design Floods

The next step focused on the evaluation of the CAPA design floods, calculated using the published factors (K_P) suggested by DWAF (US, 2006) illustrated in Table 24, and Q_S. The corrected Q_S from the previous phase of this research were used.

Table 24: Values of KP for various recurrence intervals (US, 2006)

	Recurrence intervals (years)				
MAP (mm)	**5**	**10**	**20**	**50**	**100**
100	4.49	9.49	16.97	31.41	45.36
200	3.27	5.96	9.65	16.26	22.15
400	2.47	3.97	5.89	9.13	11.81
600	2.13	3.2	4.52	6.72	8.45
800	1.93	2.76	3.79	5.46	6.75
1000	1.79	2.48	3.32	4.68	5.71
1500	1.57	2.05	2.64	3.58	4.26
2000	1.44	1.8	2.26	2.99	3.5

The delineation of the CAPA design flood estimation commenced with an evaluation of the K_P factors. An equation was derived which could be used to surrogate the process of interpolating a value from Table 24. This potentially decreased the errors associated with interpolation and increased the range of recurrence interval. This was done by plotting the factors in Table 24 for each recurrence interval against their corresponding values for MAP (see Figure 50).

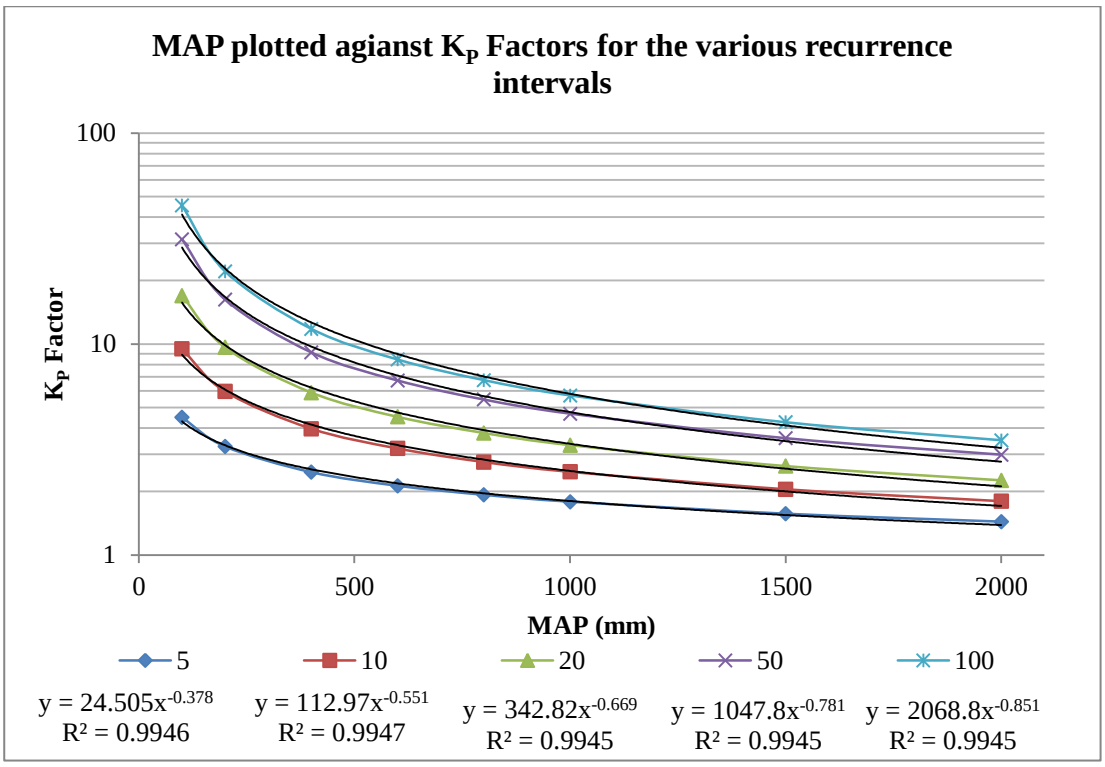

Figure 50: MAP vs. DWAF Factor

Trendlines and formulae were added to the graph. The equation that describes each of the K_P lines was found to be the form of:

$$K_P = C\,(MAP)^{B} \qquad \textbf{Equation 17}$$

The calculated constants C and B are illustrated in Table 25 for each of the recurrence intervals.

Table 25: Calculated Factors C and B for different Recurrence Intervals

Recurrence Interval (years)	100	50	20	10	5
B	-0.85	-0.781	-0.6693	-0.5514	-0.377
C	2068.8	1047.8	342.82	112.97	24.505

It was decided to use Equation 17 with the constants listed in Table 25 to derive design floods using the CAPA Method. The evaluation of the design floods was only based on the 1:5 year to 1:100 year recurrence intervals, the differences between the probabilistic floods and the CAPA derived floods. The differences were calculated in the same manner described in section 7.2.

Statistical characteristics were also computed, illustrated in Table 26. It was found that the CAPA method on average overestimated the design floods as is illustrated by the median and mean. It was further noted that the differences decreased with an increase in recurrence interval.

The large percentage difference of gauging station J2H016 was also noted. It was found that the catchment area (17085 km^2) of gauge J2H016 was the largest of the sample of gauges and also had the second smallest MAP (162 mm). This suggested that the CAPA method could potentially not be suited for larger catchments with smaller MAP.

Table 26: Statistical characteristics for the differences between the CAPA and probabilistic design floods

	Recurrence Interval (years)				
	5	**10**	**20**	**50**	**100**
Max	508%	391%	304%	376%	443%
Min	0%	-39%	-64%	-80%	-87%
Mean	72%	57%	50%	45%	39%
Median	58%	42%	40%	27%	19%

8.5 Updating of the CAPA Design Floods

No patterns could be identified by means of considering the design flood differences alone. The differences were then plotted against Q_S, M, K_P and the other four remaining catchment characteristics. The most distinct patterns resulted from plotting the differences between the CAPA design flood and the probabilistic floods, against the MAP and K_P. Figure 51 illustrates the pattern identified between the differences and K_P for the 10 year recurrence interval.

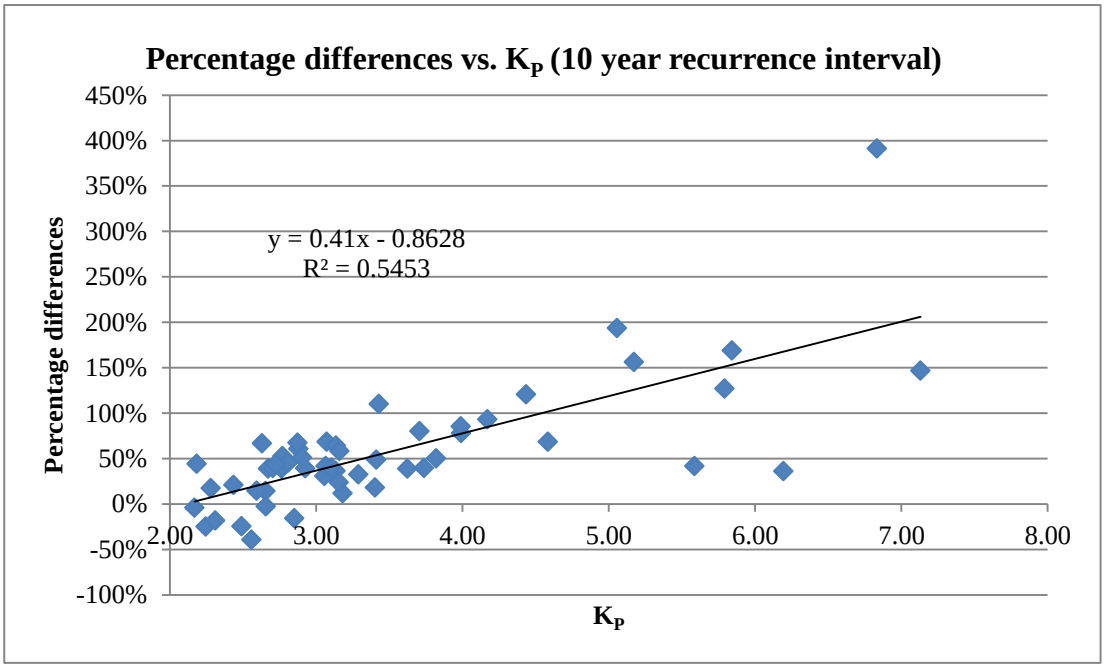

Figure 51: Pattern Identified between differences and K_P (10 year recurrence interval)

Given these patterns and the dependency of K_P on MAP, it was decided to evaluate and update the proposed values for K_P. The methodology proposed for the updating made use of the probabilistic floods to derive values for K_P values for all gauging stations and recurrence intervals under consideration. The range of recurrence intervals was increased to include the 1:200 year recurrence interval. The derived K_P values were then plotted on a scatter diagram against the MAP values for the sample of gauging stations and trend lines fitted to them. These plots for the 1:5 to 1:200 year

recurrence intervals are illustrated in

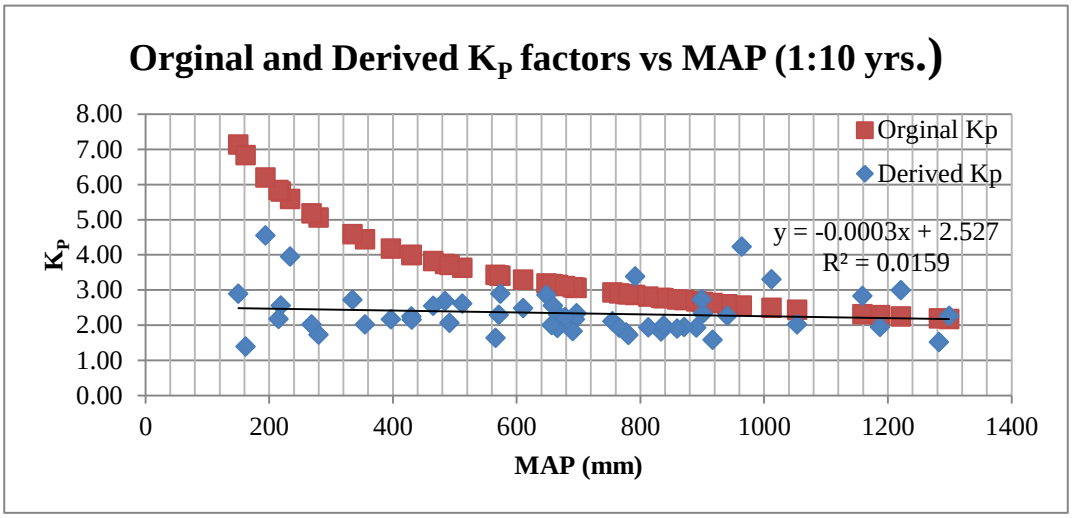

Figure 53 to **Error! Reference source not found.**.

During the evaluation of the scatter diagrams it was found the derived K_P had a linear tendency compared to the power tendency previously derived from the DWAF K_P values in Figure 50. These *'linear tendencies'* for all six recurrence intervals also inherited a small flat negative gradient. which pointed to the minute influence of the MAP on the value of K_P.

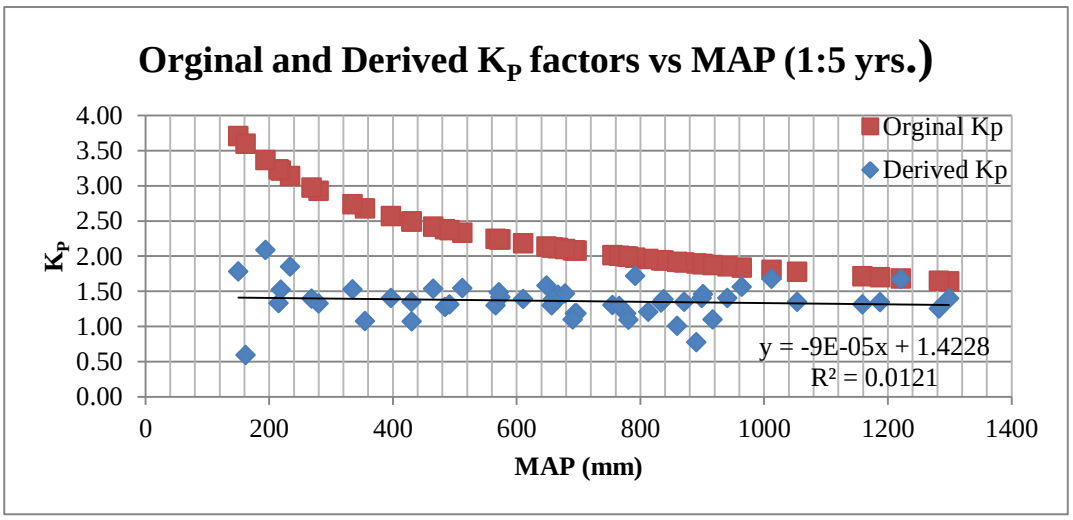

Figure 52: K_P values plotted against MAP for the 5 year recurrence interval.

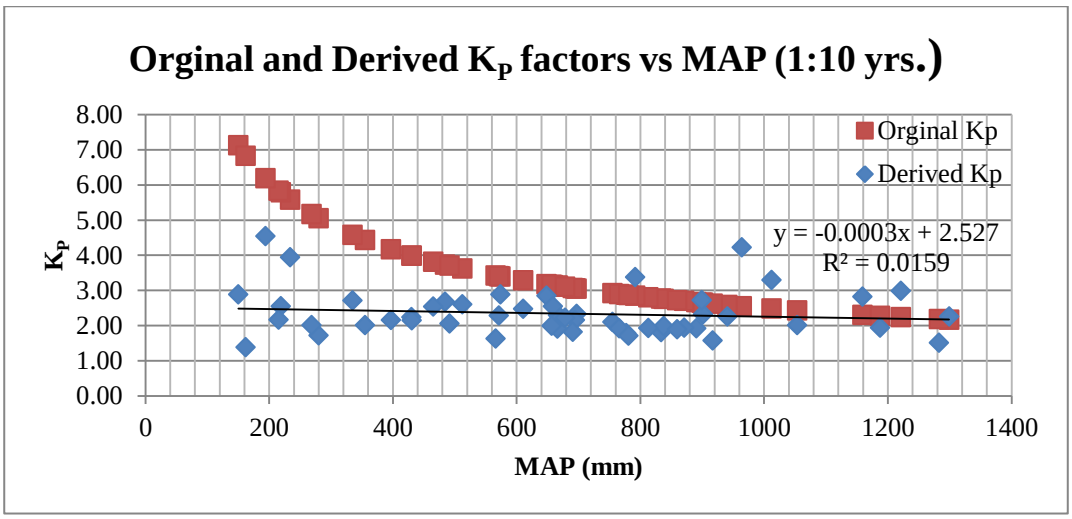

Figure 53: K_P values plotted against MAP for the 10 year recurrence interval.

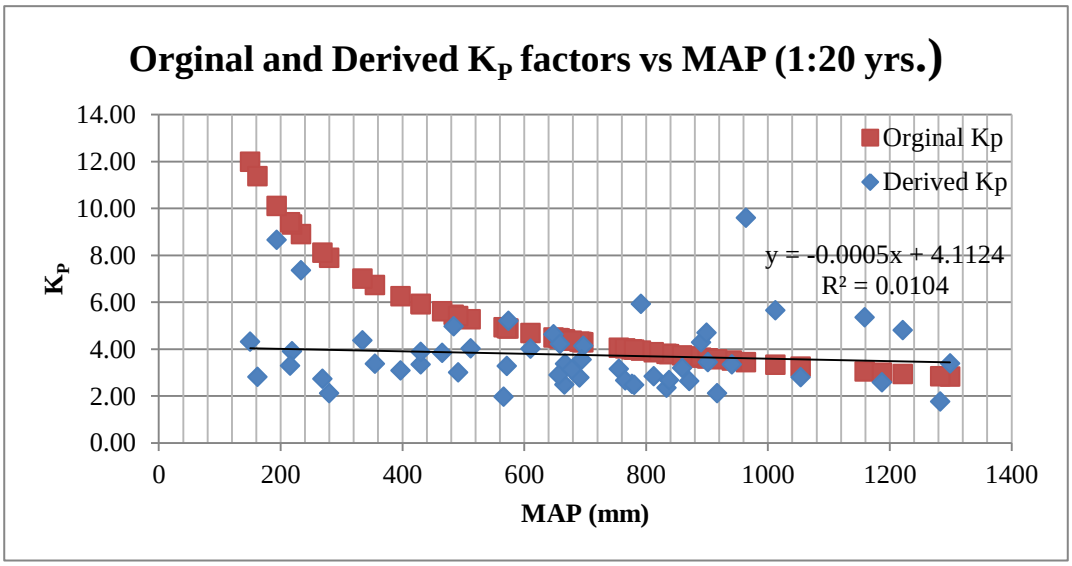

Figure 54: K_P values plotted against MAP for the 20 year recurrence interval.

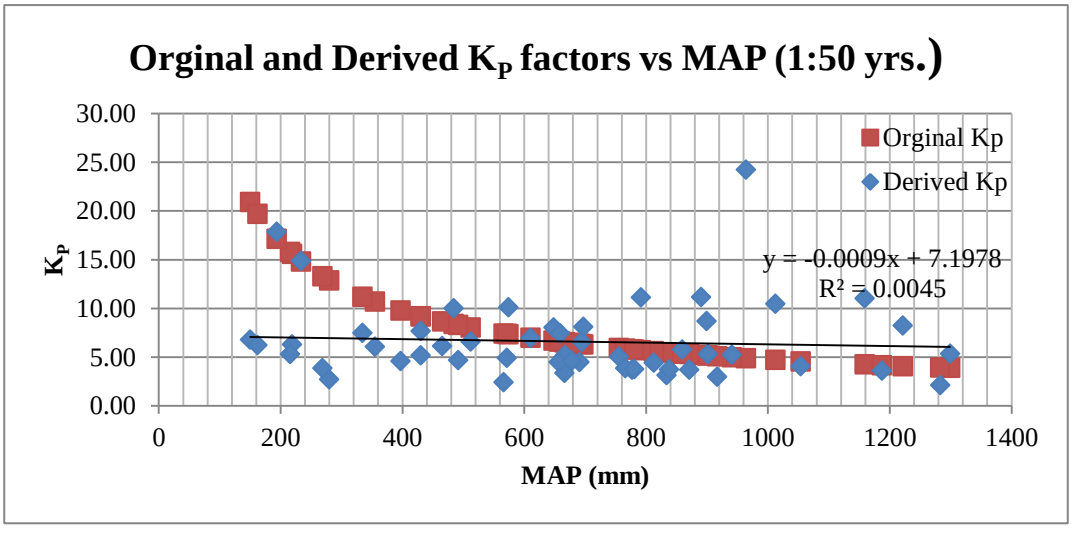

Figure 55: K_P values plotted against MAP for the 50 year recurrence interval.

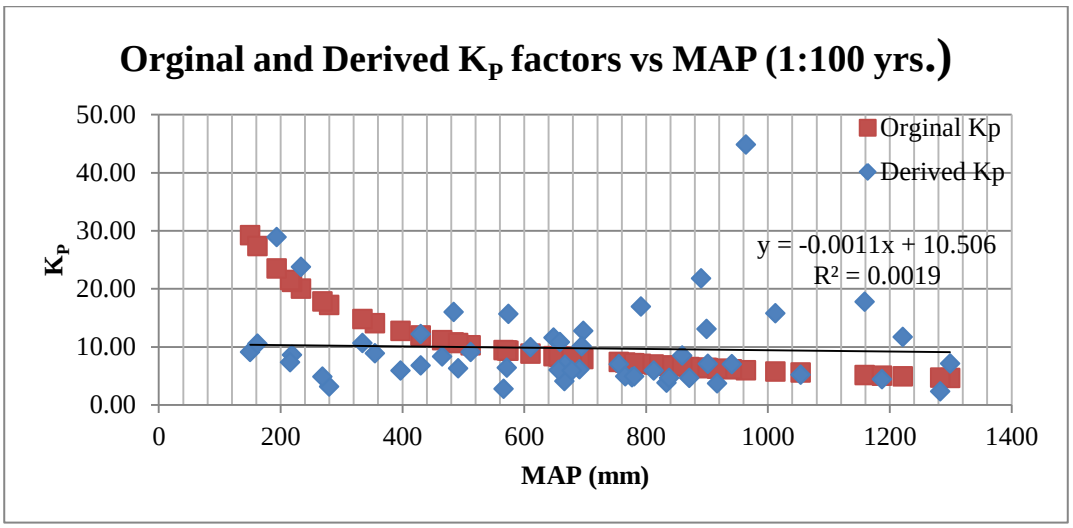

Figure 56: K_P values plotted against MAP for the 100 year recurrence interval.

Given the *'near common illustrative pattern'* that was exhibited by the MAP, it was concluded that a single K_P factor could possibly be derived to represent each recurrence interval. For this purpose, the method of least squares was used in which the value for K_P for each recurrence interval was derived by means of an iterative process. The K_P values were adjusted until the smallest summed difference was obtained for each recurrence interval. The derived K_P factors are illustrated in Table 27.

Table 27: Derived K_P Values

Recurrence interval (years)	5	10	20	50	100	200
Derived K_P Value	1.35	2.1	3.1	4.9	6.4	8.2

The correction factors were further evaluated by means of comparing the original difference statistics (illustrated in Table 26) with the statistical characteristics of the new differences illustrated in Table 28. The correction factors showed a clear improvement in both statistical characteristics and in the plots where the original and new difference were plotted against other, with differences referring to the difference between the probabilistic floods and the design floods, respectively. These plots are illustrated in Figure 57 to Figure 61.

Table 28: Comparison of statistical characteristics before and after updating

	Updated differences					Original Difference				
Recurrence interval (years)	5	10	20	50	100	5	10	20	50	100
MAX	128%	51%	75%	132%	170%	508%	391%	304%	376%	443%
MIN	-35%	-54%	-68%	-80%	-86%	0%	-39%	-64%	-80%	-87%
Mean	3%	-5%	-7%	-5%	-7%	73%	58%	51%	46%	40%
Median	0%	-3%	-8%	-8%	-11%	58%	42%	40%	27%	19%
Standard deviation	25%	22%	30%	44%	52%	70%	67%	73%	87%	97%

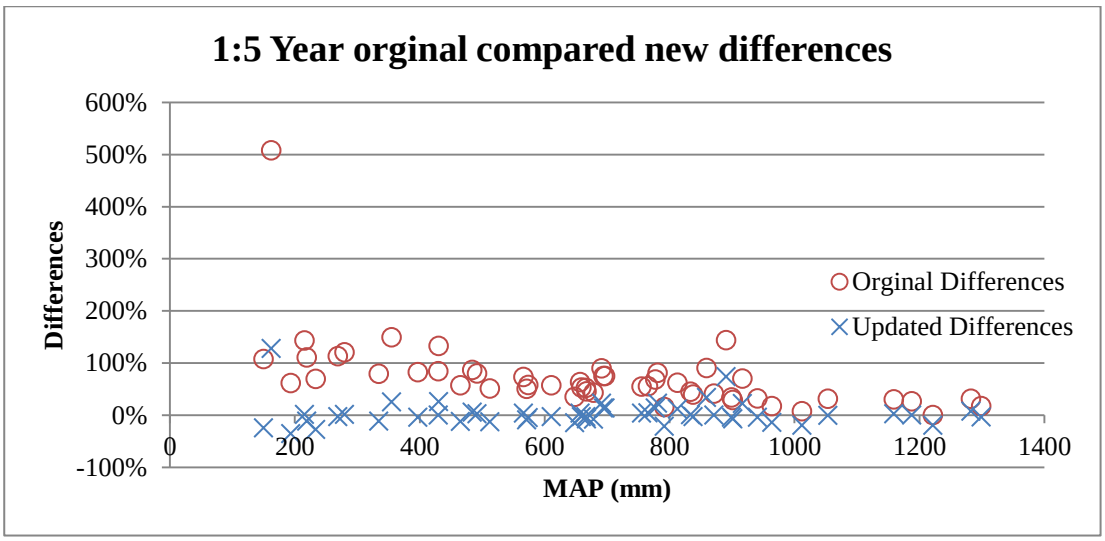

Figure 57: Comparison between the original and updated differences for the 1:5 year recurrence interval

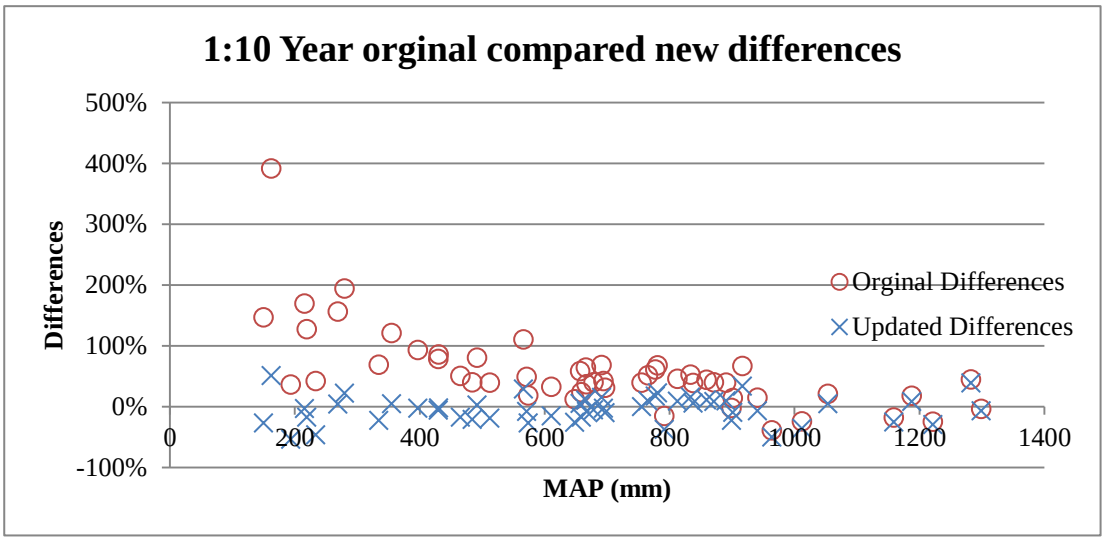

Figure 58: Comparison between the original and updated differences for the 1:10 year recurrence interval

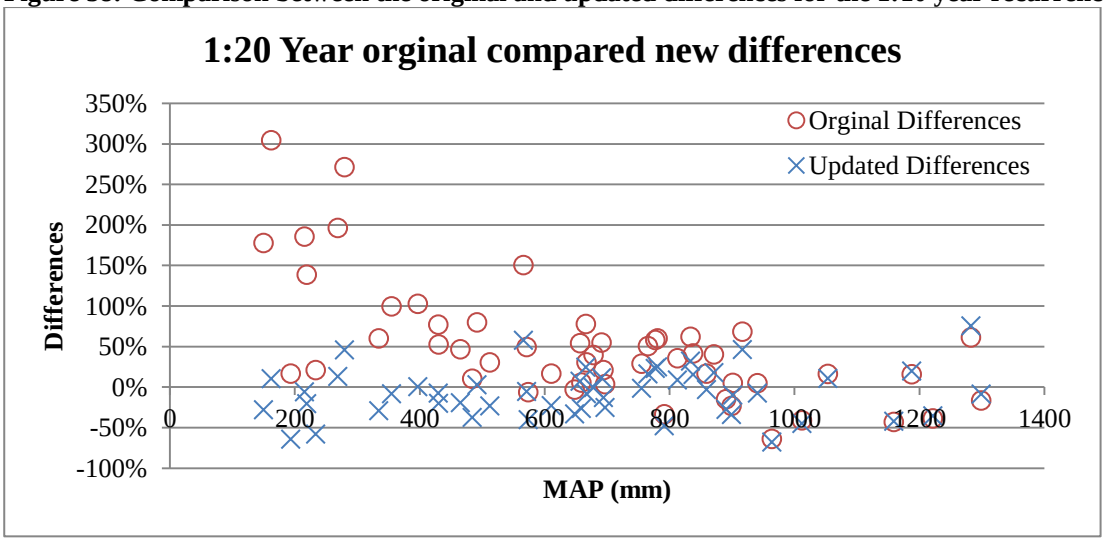

Figure 59: Comparison between the original and updated differences for the 1:20 year recurrence interval

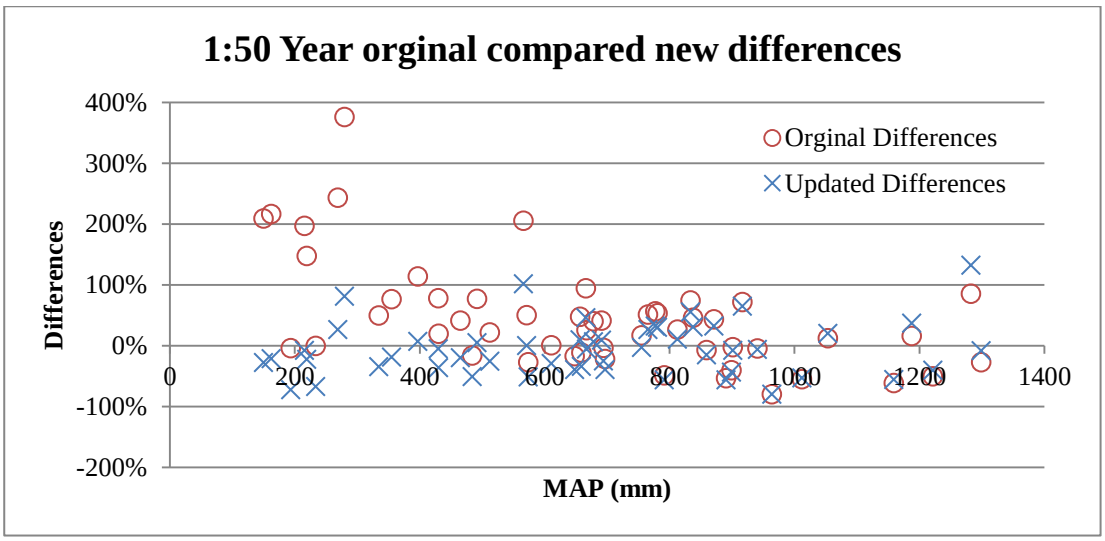

Figure 60: Comparison between the original and updated differences for the 1:50 year recurrence interval

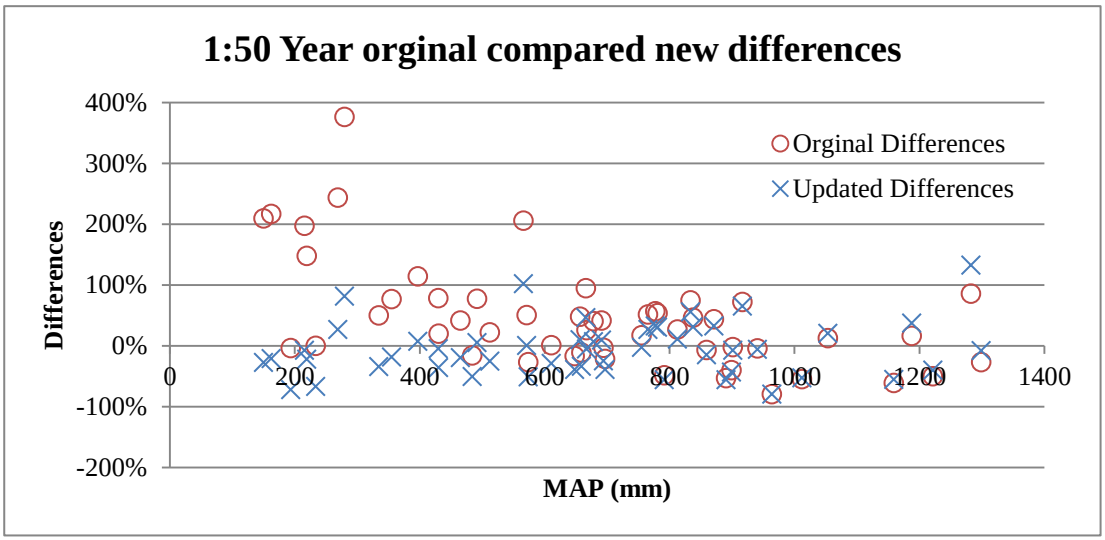

Figure 61: Comparison between the original and updated differences for the 1:100 year recurrence interval

This concluded the evaluation and potential updating of the CAPA method. In summary correction factors were derived for the mean flood (Q_S) (see Table 29) and new values for K_P (see Table 30).

Table 29: Correction Factor for Q_S

Range slope (m/m)	Correction factor
0 – 0.135	1.7
0.135 – 0.197	Updated Q_S = 0.74 (Q_S original) -1.26
0.197 – 0.55	1.7

Table 30: Derived K_P Values

Recurrence interval (years)	5	10	20	50	100	200
Derived K_P Value	1.35	2.1	3.1	4.9	6.4	8.2

The proposed process for updating the CAPA method was illustrated and utilised to great effect. This could, however, only be done and proven within the limits of the available data and methodology followed.

9 Considerations when Updating Methods Estimation of Design Floods

The following notes and conclusions were drawn from the methodology that was developed and followed to update the Catchment Parameter (CAPA) and Midgley and Pitman (MIPI) empirical design flood estimation methods. Although the updating was done for only two empirical methods it was concluded that the methodology and approaches that were adopted would be applicable to the updating of any method of design flood estimation.

The effectiveness of any updating would be the measure in which the reliability of a method could be increased. From the research it was concluded that the reliability of updated design flood estimation methods is function of the reliability of the data used in the process, methodology followed and intended use.

The proposed methodology can be subdivided into three phases i.e. (1) Data collection and evaluation; (2) Method of delineation and evaluation; and (3) Method of updating. Each of these three phases would require their own considerations and requirements.

9.1 Data Collection and Evaluation

The reliability of the results of any updated method of flood estimation will rarely exceed that of the data used in the updating, or the data used to calibrate against. The reliability of the data is thus of great importance. Evaluations and analyses should also quantify the limitations of data.

The processes used to update methods of design flood estimation make use of two basic datasets i.e. (1) Annual flood peak records; and (2) Catchment characteristics or other specific input data used in the method.

9.1.1 Annual flood peak records

Reliable records of annual flood peaks will always be one of the most important inputs in any updating process. The research highlighted the need to drastically improve the reliability of annual flood peak records in South Africa.

The suggested approach to address these deficiencies would be a combined (and dedicated) research project between specialists in flood hydrology and the DWAF which could be funded by research institutes such as the Water Research Commission (WRC). The advantages of this would be the publication of reliable flood records, the calibration of data and potentially very much improved methods of flood estimation that are highly dependent on this data.

It was further recommended that the influence of potential flood attenuation and the naturalisation of the records be research and quantified. The naturalised data could be used in

the calibration of methods which would be generically applicable to any river, stream or watercourse. The quantification of the effects of flood attenuation could be used to aid in the development of additional measures to increase the reliability of flow records (or recorded floods) in streams where attenuation plays a major role.

Research should also be furthered on the most suitable ways of fitting statistical distributions to peak flood data to help improve the reliability of probabilistic floods for streams.

9.1.2 Catchment characteristics or other input data

The reliability of input of any data used as input, whether catchment characteristic or not, is just as important. Measures should be developed to ensure that the reliability of data used in the updating of methods for estimating design floods is kept to as high a standard as possible.

During the research it was found that more than one method normally exists to quantify a specific catchment characteristic. The results of these methods usually differ as a result of the different approaches adopted or followed. In this regard it is recommended that all possible methods be evaluated which could potentially be used to derive an input characteristic, including GIS, for a given update or *'analysis'*. This outcome of this research has the potential to be done separately, used as input to refine and take the updating of the CAPA and MIPI Methods for estimation of design floods to higher levels i.e. PhD, and incorporated into other research or updates in the field of *'Flood Hydrology'*.

This evaluation can potentially be used to incorporate measures to increase the reliability of results if other methods were to be used to derive the specific characteristic. The most reliable and applicable method should further be selected for use during the updating and, hopefully, encourage other practioners (or users) to use the same method.

9.2 Method Delineation and Evaluation

The importance of updating methods from first principles i.e. by using the original methodology used for development of a particular method of *'design flood estimation'*, became apparent during the research. It is further recommended that all attempts to update methods of design flood estimation make use of first principles. This will improve the overall evaluation of the reliability of a particular method and also help with the evaluation of the methodology and methods used during the development of the method.

The results of this research could provide a high degree of *'added value'* to the discipline of *'Flood Hydrology'* where recommendations (or suggestions) based on the results of proposed alternatives to address deficiencies that were identified during development of the *'method of updating'* could also increase the reliability of method.

9.3 Updating of Methods of Estimation of Design Floods

Updating of methods should not be seen as a mere improvement of the reliability of the method through one or two changes to the original method. Instead it should be viewed as an overall improvement of a group of methods of estimation for design floods, for instance empirical methods for the estimation of design floods. The ultimate goal would be to combine all methods in a group into one reliable method which is flexible enough (and makes adequate provision) for the collection and analysis of a wide range of different hydrological characteristics.

The process of updating should include a careful and thorough evaluation of the input into the method and as well as an evaluation of the potential of substituting *'parts of the method'* with *'more suitable parts'* which would increase the reliability of the method of updating. A good example of this is to replace regions that have been used in a particular method with the *'MAP derived variable'* or vice versa. This would help to identify the best possible combination of inputs to combine into one reliable method.

The use of any updated method will be a function of its simplicity and range of application. All of the above should be incorporated into method which is as simplistic as possible with the potential to perhaps increasing the range of applicability to other countries and regions in Africa.

10 Conclusion

The knowledge gained this research into updating of the MIPI and CAPA design flood estimation methods was also used to great effect to develop methods, highlight essential requirements as well a certain considerations for subsequent research into updating of the methods used for the estimation of design floods. These requirements were also used to evaluate the proposed updates of the CAPA and MIPI method.

The methodology and scope of the flow data collection process and the statistical phase of the analyses was found to be adequate for the research. The reliability of the results from the probabilistic phase of analysis of peak floods at gauging stations could be significantly improved by following the additional steps which are listed below:

- The addition of the General Extreme Value (GEV) distribution instead of applying only one distribution i.e. Log Pearson Type III (LP III), given that the Log Normal (LN) distribution is a special case of the LP III distribution with a skewness (g) of zero. This could potentially result in the more reliable representation of some data.
- The use of longer flow records which include recent extreme flood events would further increase the reliability of the data. The addition of 16 years of data will also increase the sample size from which a selection could possibly be made.
- The assessment of flow data in order to try to determine the reliability of flow data and to amend the data where possible to improve the reliability.
- Possible naturalisation of flow records to maximise the sample size from which a selection can be made.

The use of GIS to define catchments and to quantify catchment characteristics would be relevant to similar types of studies. It has been adequately demonstrated that the results obtained and approach followed was found to be adequate for this research and can be very effectively used as guideline for subsequent research.

The methodology followed during the *'method delineation and updating phase'* was very simplistic in certain areas as a result of constraints which were identified and could not be avoided. The delineation of methods into formulas produced results which are consistent with manual applications of the methods and were found to be adequate for evaluation of the method results.

The improvement of the methods by means of correction factors were not the most appropriate approach and also border on the line of not being relevant. Even though the correction factors could be applicable, they are very simplistic in their derivation which could potentially reduce their reliability. Application of the correction factors is also cumbersome and would rarely if ever be applied in practise if not required or prescribed.

The more appropriate approach would be to attempt to update the methods by means of following the original methodology used to develop the methods for the estimation of design floods. The following advantages have been identified:

- This approach would yield a more in-depth understanding of the methods which could be used to improve the methodology that was originally used, thus increasing the reliability of the methods. A better understanding of the methods could also be used to identify *'parts (or portions) of the methods'* which could possibly be used to combine the methods into one method.
- The final deliverable would then yield methods similar in application to the original ones with amendments only to the graphs and/or formulas. This would have resulted in a less cumbersome application compared to one that requires correction factors.
- The approach would also yield more reliable results because the methods could be evaluated and updated based on the methods that were used for their original development instead of deriving formulae which approximate the original methods.

The proposed process for updating the CAPA and MIPI Methods for the estimation of design floods was well illustrated, validated and verified.. This could, however, only be done and proven within the limits of the available data and methodology followed.

These limits included the reliability of the probabilistic floods as a result was questionable reliability and length of the flow records. The reliability of the probabilistic floods could further be questioned by limiting the amount of distributions to basically only one, the Log Pearson Type III, given that Log Normal (LN) is a special case of the LP III.

Furthermore the formulas used to approximate the methods were based on best fit trend line formulas instead of the original method which could induce possible differences between the results of the original method and the approximated formulas.

The effectiveness of any updating would be the measure in which the reliability of a method could be increased. However no proof could be provided that updating of the method did indeed increase the reliability of design flood estimation using the MIPI and CAPA Methods.

11 Recommendations

The conclusions and recommendations in section 9 resulted from the updating of the MIPI and CAPA Methods for the estimation of design floods. Given the limitations of the methodology followed and the fact that there is a very limited amount of readily available and reliable data (also meaning *'high quality flow records'*), it must be realised (and accepted) that the research is not exhaustive. However, it is strongly recommended that the findings of this research be used as guide for subsequent research in this field of *'Flood Hydrology'*. It is also recommended that the findings in section 9 be improved if and when possible.

Although the proposed process for updating the methods were illustrated and utilised to great effect, it was done within the constraints of the data as pointed out in section 10. Given these findings it is recommended that the result of the updating merely serve an academic purpose, used to formulate the findings in section 6, until it can be proven through additional research that these suggestions do indeed increase the reliability of the two methods.

12 References

Alexander, W.J.R., 1990 (Alexander, 1990). Flood Hydrology for Southern Africa. SANCOLD, Pretoria, RSA.

Alexander, W.J.R., 2001 (Alexander, 2001). Flood Risk Reduction Measures. University of Pretoria, Pretoria, RSA.

Alexander, W.J.R., 2007 (Alexander, 2007). Personal correspondence.

Bouhgton, W.C. (Boughton, 1981). Effect of Rainfall data errors on the optimized values of model parameters. School of Australian Environmental Studies, Griffith University, Nathan, Queensland, Australia.

Campbell, G.V., Ward, A.D., Middleton, B.J., 1986 (Campbell, 1986). An evaluation of hydrological techniques for estimating floods from small ungauged catchments. Report No. 139/2/87, Water Research Commission, Pretoria, RSA.

Görgens, A.H.M., 2007 (Görgens, 2007). Personal correspondence.

Görgens, A.H.M., 2007. Joint Peak-Volume (JPV) Design Flood Hydrographs for South Africa. WRC Report 1420/3/07, Water Research Commission, Pretoria, South Africa.

Hosking, J.R.M., Wallis, J.R., 1995 (Hosking 1995). A comparison of unbiased and plotting-position estimators of L moments. Water Resources Research, 31(8): 2019-2025.

HRU, 1972. Design Flood Determination in South Africa. Report No. 1/72, Hydrological Research Unit, Department of Civil Engineering, University of Witwatersrand, RSA.

Kjeldsen, T.R., Smithers, J.C., Schulze, R.E., 2001(Kjeldsen, 2002a). Flood frequency analysis at ungauged sites in the KwaZulu-Natal province, South Africa. Water SA, 27(3): 315-324.

Kjeldsen, T.R., Smithers, J.C., Schulze, R.E., 2002 (Kjeldsen, 2002b). Regional flood frequency analysis in the KwaZulu-Natal province, South Africa, using the index-flood method. Journal of Hydrology, 255(1-4): 194-211.

Kovacs, Z.P., 1988 (Kovacs, 1988). Regional maximum flood peaks in South Africa. Technical Report TR137, Department of Water Affairs, Pretoria, RSA.

Pitman, W.V., Midgley, D.C., 1967 (Pitman, 1967). Flood studies in South Africa: Frequency analysis of peak discharges. Transactions of South African Institution of Civil Engineers, August 1967.

Roberts, D.F., 1963 (Roberts, 1963). Annual flood peak probabilities. Professional Paper 20, Department of Water Affairs, Pretoria, RSA.

Roberts, D.F., 1965 (Roberts, 1965). The empirical determination of flood peak probabilities. Technical Report No. 33, Division of Hydrology, Department of Water Affairs, Pretoria, RSA.

SANRAL, 2007. Drainage Manual (Fifth Edition) (SANRAL, 2007). South African National Roads Agency Ltd, Pretoria, South Africa.

Smithers, J.C., Schulze, R.E., 2000 (Smithers, 2000). Development and evaluation of techniques for estimating short duration design rainfall in South Africa. WRC Report No. 681/1/00, Water Research Commission, Pretoria, RSA.

Smithers, J.C., Schulze, R.E., 2003 (Smithers, 2003). Design rainfall and flood estimation in South Africa. WRC Report No. 1060/01/03, Water 17 Research Commission, Pretoria, RSA.

Smithers, J.C., 2007 (Smithers, 2007). Personal correspondence.

Van der Spuy, D., Rademeyer, P.F., 2010. Flood Frequency Estimation Methods as Applied in the Department of Water Affairs, Department of Water Affairs, Pretoria, South Africa.

Appendix A

Table 31: Gauge specific data in quaternaries A to D

Gauge ID	Record length (yrs.)	Best Fitted Dist.	Mean Flood (m^3/s)	Catchment Area (km^2)	MAP (mm)	Mean catchment slope (m/m)	Longest Watercourse (km)	Probabilistic floods (m^3/s)						
								Recurrence intervals (yrs.)						
								2	5	10	20	50	100	200
A2H004	34	LN	14	132	608	0.0977	20	6	19	34	55	95	136	189
A2H012	73	LP III	196	2345	664	0.0434	100	119	254	391	566	876	1186	1576
A2H013	72	LN	135	1062	650	0.0630	67	69	214	386	628	1089	1569	2196
A2H023	37	LN	151	688	674	0.0535	62	113	209	288	375	506	618	742
A2H027	32	LN	103	367	691	0.0452	41	42	113	188	287	463	636	851
A2H029	28	LP III	14	124	693	0.0525	27	6	17	31	51	94	145	220
A7H001	35	LP III	214	7704	423	0.0327	167	64	229	460	831	1641	2609	4016
B2H001	39	LN	221	1582	662	0.0214	74	95	306	564	933	1645	2399	3394
B6H001	50	LP III	99	514	991	0.1889	62	63	134	200	278	404	518	652
B7H002	46	LP III	52	62	878	0.2236	10	9	40	99	221	574	1124	2128
C1H001	77	LN	419	8009	676	0.0084	235	277	614	930	1310	1928	2492	3156
C3H003	68	LP III	204	11218	487	0.0176	292	118	268	420	615	954	1287	1702
C5H008	51	LN	87	608	505	0.0201	54	49	135	228	353	577	800	1079
C6H001	74	LN	618	5645	596	0.1152	238	401	919	1417	2025	3029	3959	5063
C7H005	34	LN	186	5661	572	0.0388	195	67	263	536	966	1875	2915	4372
C8H003	37	LN	83	869	668	0.0896	222	49	120	190	280	431	575	750
D1H001	82	LP III	207	2387	427	0.0526	65	99	280	465	695	1071	1415	1811
D5H001	27	LN	156	2165	147	0.0932	113	110	278	451	673	1056	1424	1875
D5H003	64	LN	97	1487	213	0.1969	94	60	160	268	410	662	910	1219
D6H002	23	LN	185	6898	279	0.0226	163	150	246	319	394	501	588	681

Table 32: Gauge specific data in quaternaries E to R

Gauge ID	Record length (yrs.)	Best Fitted Dist.	Mean Flood (m^3/s)	Catchment Area (km^2)	MAP (mm)	Mean catchment slope (m/m)	Longest Watercourse (km)	Probabilistic floods (m^3/s)						
								Recurrence intervals (yrs.)						
								2	5	10	20	50	100	200
E2H002	70	LN	384	6784	306	0.1118	154	263	535	775	1052	1486	1870	2309
G1H004	41	LN	267	74	1513	0.4074	15	233	334	404	472	563	633	706
G2H008	36	LN	56	22	1418	0.4340	7	31	94	168	270	462	659	915
H1H006	42	LN	402	734	579	0.1354	45	337	521	655	790	976	1123	1278
H7H004	45	LP III	20	10	755	0.5451	9	11	26	42	63	101	141	192
J2H016	32	LN	275	17085	160	0.0667	217	32	163	383	775	1713	2903	4714
J3H004	70	LN	212	4292	189	0.0681	130	99	441	962	1830	3780	6123	9539
J4H003	30	LN	66	92	423	0.2187	20	41	93	143	204	303	394	503
K4H003	34	LP III	32	74	696	0.1968	16	11	38	75	133	260	410	626
L1H001	48	LP III	296	3934	214	0.0503	130	159	393	642	974	1571	2176	2945
L2H003	40	LN	68	1152	321	0.1669	59	35	104	185	298	509	726	1007
L6H001	68	LN	183	1287	232	0.2186	79	80	339	722	1349	2726	4353	6692
P1H003	36	LP III	79	1474	475	0.0992	87	25	101	212	393	792	1269	1957
Q3H004	39	LN	160	873	353	0.0681	67	52	172	322	540	968	1428	2039
R2H001	32	LN	19	31	1299	0.5445	7	10	26	42	63	99	133	175
R2H008	48	LN	84	68	951	0.4065	17	19	131	354	805	2032	3760	6620
R2H012	35	LN	18	17	1012	0.4352	6	9	30	59	101	187	282	410

Table 33: Gauge specific data in quaternaries S to X

Gauge ID	Record length (yrs.)	Best Fitted Dist.	Mean Flood (m^3/s)	Catchment Area (km^2)	MAP (mm)	Mean catchment slope (m/m)	Longest Watercourse (km)	Probabilistic floods (m^3/s)						
								Recurrence intervals (yrs.)						
								2	5	10	20	50	100	200
S3H006	31	LN	99	2207	440	0.1348	91	58	152	252	380	606	826	1097
T3H002	44	LN	354	2109	776	0.0098	84	213	457	681	947	1372	1756	2203
T3H005	42	LN	322	2578	786	0.0794	136	150	552	1088	1906	3583	5453	8021
T4H001	49	LN	198	736	825	0.0143	64	97	239	382	564	874	1169	1528
U2H004	50	LN	231	2261	919	0.1714	165	127	254	364	490	685	856	1051
U2H013	35	LN	68	297	864	0.1352	29	45	91	131	178	250	314	387
U3H002	27	LN	70	360	932	0.1419	26	39	98	158	234	365	491	645
V6H003	38	LP III	128	295	826	0.0851	35	96	171	232	300	402	490	589
V6H004	41	LN	147	659	840	0.0872	70	103	204	293	395	551	689	846
W1H004	45	LN	10	20	1125	0.1541	7	3	13	28	53	109	176	273
W2H005	36	LN	650	3952	776	0.1201	180	302	712	1114	1612	2444	3223	4157
W3H001	52	LN	300	1466	824	0.0267	126	90	302	569	959	1729	2559	3668
W5H011	33	LN	33	883	777	0.0261	61	17	39	59	83	122	158	200
X2H008	47	LN	49	187	956	0.1618	27	30	72	115	170	262	351	457
X2H031	36	LN	75	292	905	0.0956	37	30	106	206	355	656	987	1437
X3H001	45	LN	20	198	1112	0.1993	19	14	27	39	52	72	89	109

Appendix B

Table 34: Distribution specific probabilistic floods in quaternaries A to D

Gauge ID	Record length (yrs.)	Best Fitted Dist.	Mean Flood (m^3/s)	LN Probabilistic floods (m^3/s)							LP III Probabilistic floods (m^3/s)						
				Recurrence intervals (yrs.)							Recurrence intervals (yrs.)						
				2	5	10	20	50	100	200	2	5	10	20	50	100	200
A2H004	34	LN	14	6	19	34	55	95	136	189	6	19	34	54	91	128	174
A2H012	73	LP III	196	125	259	380	520	740	936	1162	119	254	391	566	876	1186	1576
A2H013	72	LN	135	69	214	386	628	1089	1569	2196	82	218	332	451	609	726	840
A2H023	37	LN	151	113	209	288	375	506	618	742	116	210	281	354	455	535	618
A2H027	32	LN	103	42	113	188	287	463	636	851	36	105	200	357	724	1197	1939
A2H029	28	LP III	14	7	18	29	43	67	90	118	6	17	31	51	94	145	220
A7H001	35	LP III	214	67	233	447	766	1405	2102	3045	64	229	460	831	1641	2609	4016
B2H001	39	LN	221	95	306	564	933	1645	2399	3394	98	308	552	888	1500	2115	2892
B6H001	50	LP III	99	63	134	199	277	400	512	641	63	134	200	278	404	518	652
B7H002	46	LP III	52	10	43	92	172	346	552	848	9	40	99	221	574	1124	2128
C1H001	77	LN	419	277	614	930	1310	1928	2492	3156	313	622	834	1032	1269	1433	1583
C3H003	68	LP III	204	122	271	412	581	858	1110	1408	118	268	420	615	954	1287	1702
C5H008	51	LN	87	49	135	228	353	577	800	1079	59	137	193	245	307	348	385
C6H001	74	LN	618	401	919	1417	2025	3029	3959	5063	446	932	1296	1656	2121	2462	2793
C7H005	34	LN	186	67	263	536	966	1875	2915	4372	76	269	486	768	1240	1672	2169
C8H003	37	LN	83	49	120	190	280	431	575	750	51	121	184	257	368	465	572
D1H001	82	LP III	207	93	276	487	778	1319	1874	2587	99	280	465	695	1071	1415	1811
D5H001	27	LN	156	110	278	451	673	1056	1424	1875	133	280	375	457	547	603	649
D5H003	64	LN	97	60	160	268	410	662	910	1219	69	163	235	307	399	465	527
D6H002	23	LN	185	150	246	319	394	501	588	681	155	248	311	371	448	506	563

Table 35: Distribution specific probabilistic floods in quaternaries E to R

Gauge ID	Record length (yrs.)	Best Fitted Dist.	Mean Flood (m^3/s)	LN Probabilistic floods (m^3/s)							LP III Probabilistic floods (m^3/s)						
				Recurrence intervals (yrs.)							Recurrence intervals (yrs.)						
				2	5	10	20	50	100	200	2	5	10	20	50	100	200
E2H002	70	LN	384	263	535	775	1052	1486	1870	2309	267	537	765	1020	1403	1729	2090
G1H004	41	LN	267	233	334	404	472	563	633	706	238	336	397	452	520	568	614
G2H008	36	LN	56	31	94	168	270	462	659	915	38	96	142	186	240	278	312
H1H006	42	LN	402	337	521	655	790	976	1123	1278	348	525	640	748	884	983	1080
H7H004	45	LP III	20	12	27	40	57	84	109	138	11	26	42	63	101	141	192
J2H016	32	LN	275	32	163	383	775	1713	2903	4714	24	141	428	1182	4136	10173	24299
J3H004	70	LN	212	99	441	962	1830	3780	6123	9539	120	453	817	1266	1968	2567	3212
J4H003	30	LN	66	41	93	143	204	303	394	503	42	94	142	199	290	371	466
K4H003	34	LP III	32	12	39	73	122	220	325	465	11	38	75	133	260	410	626
L1H001	48	LP III	296	164	397	630	922	1415	1882	2445	159	393	642	974	1571	2176	2945
L2H003	40	LN	68	35	104	185	298	509	726	1007	40	106	165	230	321	393	466
L6H001	68	LN	183	80	339	722	1349	2726	4353	6692	106	344	548	751	1005	1178	1332
P1H003	36	LP III	79	25	101	210	382	752	1178	1782	25	101	212	393	792	1269	1957
Q3H004	39	LN	160	52	172	322	540	968	1428	2039	51	171	325	553	1012	1518	2205
R2H001	32	LN	19	10	26	42	63	99	133	175	10	26	42	62	95	126	163
R2H008	48	LN	84	19	131	354	805	2032	3760	6620	29	133	242	363	524	639	744
R2H012	35	LN	18	9	30	59	101	187	282	410	12	30	42	51	60	65	69

Table 36: Distribution specific probabilistic floods in quaternaries S to X

Gauge ID	Record length (yrs.)	Best Fitted Dist.	Mean Flood (m^3/s)	LN Probabilistic floods (m^3/s)							LP III Probabilistic floods (m^3/s)						
				Recurrence intervals (yrs.)							Recurrence intervals (yrs.)						
				2	5	10	20	50	100	200	2	5	10	20	50	100	200
S3H006	31	LN	99	58	152	252	380	606	826	1097	69	155	216	274	344	392	435
T3H002	44	LN	354	213	457	681	947	1372	1756	2203	237	464	623	775	963	1097	1224
T3H005	42	LN	322	150	552	1088	1906	3583	5453	8021	175	565	959	1428	2140	2740	3380
T4H001	49	LN	198	97	239	382	564	874	1169	1528	86	227	403	671	1242	1918	2905
U2H004	50	LN	231	127	254	364	490	685	856	1051	106	227	381	621	1160	1836	2884
U2H013	35	LN	68	45	91	131	178	250	314	387	44	91	133	182	262	335	421
U3H002	27	LN	70	39	98	158	234	365	491	645	41	99	153	219	323	416	522
V6H003	38	LP III	128	97	171	230	294	387	465	550	96	171	232	300	402	490	589
V6H004	41	LN	147	103	204	293	395	551	689	846	103	205	292	390	539	668	812
W1H004	45	LN	10	3	13	28	53	109	176	273	3	13	25	42	73	103	139
W2H005	36	LN	650	302	712	1114	1612	2444	3223	4157	250	642	1183	2090	4265	7168	11893
W3H001	52	LN	300	90	302	569	959	1729	2559	3668	76	281	611	1224	2833	5134	9061
W4H004	42	LP III	177	115	244	363	503	726	927	1161	125	247	339	429	547	636	722
W5H011	33	LN	33	17	39	59	83	122	158	200	16	37	61	95	161	234	333
X2H008	47	LN	49	30	72	115	170	262	351	457	32	73	109	149	207	255	305
X2H031	36	LN	75	30	106	206	355	656	987	1437	32	108	194	308	507	699	927

Appendix C

Table 37: MIPI design flood evaluation for region 1 to 3

Gauge ID	Region	Original MIPI design floods (m^3/s)							Probabilistic floods (m^3/s)							Difference in %						
		Recurrence intervals (yrs.)							Recurrence intervals (yrs.)							Recurrence intervals (yrs.)						
		2	5	10	20	50	100	200	2	5	10	20	50	100	200	2	5	10	20	50	100	200
E2H002	1	813	1381	1817	2322	3121	3634	4367	263	535	775	1052	1486	1870	2309	209%	158%	134%	121%	110%	94%	89%
H1H006	1	268	456	600	767	1031	1200	1442	337	521	655	790	976	1123	1278	-20%	-12%	-8%	-3%	6%	7%	13%
A2H012	2	357	679	960	1302	1880	2209	2655	119	254	391	566	876	1186	1576	200%	167%	146%	130%	115%	86%	68%
A2H013	2	242	460	650	882	1273	1497	1799	69	214	386	628	1089	1569	2196	251%	115%	69%	40%	17%	-5%	-18%
A2H023	2	185	352	498	675	975	1146	1377	113	209	288	375	506	618	742	64%	68%	73%	80%	93%	85%	86%
A2H027	2	134	254	359	487	703	826	993	42	113	188	287	463	636	851	218%	125%	91%	70%	52%	30%	17%
A2H029	2	80	153	216	293	423	497	597	6	17	31	51	94	145	220	1238%	798%	596%	474%	350%	243%	171%
B2H001	2	282	537	759	1029	1486	1746	2099	95	306	564	933	1645	2399	3394	197%	75%	35%	10%	-10%	-27%	-38%
T3H002	2	324	616	871	1181	1706	2005	2409	213	457	681	947	1372	1756	2203	52%	35%	28%	25%	24%	14%	9%
T3H005	2	360	685	969	1313	1896	2229	2679	150	552	1088	1906	3583	5453	8021	140%	24%	-11%	-31%	-47%	-59%	-67%
U2H013	2	122	232	329	446	643	756	909	45	91	131	178	250	314	387	172%	155%	151%	150%	157%	141%	135%
V6H003	2	125	237	336	455	657	773	928	96	171	232	300	402	490	589	30%	39%	45%	52%	64%	58%	58%
V6H004	2	181	345	488	661	955	1122	1348	103	204	293	395	551	689	846	76%	69%	66%	67%	73%	63%	59%
J3H004	3	301	695	1115	1619	2377	3014	3803	99	441	962	1830	3780	6123	9539	204%	58%	16%	-12%	-37%	-51%	-60%
L6H001	3	166	383	614	892	1309	1660	2095	80	339	722	1349	2726	4353	6692	107%	13%	-15%	-34%	-52%	-62%	-69%
P1H003	3	177	410	657	955	1402	1777	2243	25	101	212	393	792	1269	1957	609%	306%	210%	143%	77%	40%	15%
Q3H004	3	136	315	505	733	1076	1365	1722	52	172	322	540	968	1428	2039	162%	83%	57%	36%	11%	-4%	-16%

Table 38: MIPI design flood evaluation for region 4 to 7

Gauge ID	Region	Original MIPI design floods (m^3/s)							Probabilistic floods (m^3/s)							Difference in %						
		Recurrence intervals (yrs.)							Recurrence intervals (yrs.)							Recurrence intervals (yrs.)						
		2	5	10	20	50	100	200	2	5	10	20	50	100	200	2	5	10	20	50	100	200
B6H001	4	75	174	268	371	543	700	830	63	134	200	278	404	518	652	19%	30%	34%	33%	34%	35%	27%
S3H006	4	153	356	548	759	1111	1433	1698	58	152	252	380	606	826	1097	164%	134%	117%	100%	83%	73%	55%
T4H001	4	88	204	314	436	638	822	975	97	239	382	564	874	1169	1528	-9%	-14%	-18%	-23%	-27%	-30%	-36%
U2H004	4	165	384	590	818	1197	1544	1829	127	254	364	490	685	856	1051	30%	51%	62%	67%	75%	80%	74%
U3H002	4	62	144	222	308	450	580	688	39	98	158	234	365	491	645	59%	47%	40%	31%	23%	18%	7%
W2H005	4	207	480	738	1023	1497	1930	2288	302	712	1114	1612	2444	3223	4157	-32%	-33%	-34%	-37%	-39%	-40%	-45%
W3H001	4	126	293	450	624	913	1178	1396	90	302	569	959	1729	2559	3668	40%	-3%	-21%	-35%	-47%	-54%	-62%
W5H011	4	99	231	355	492	719	928	1099	17	39	59	83	122	158	200	484%	491%	501%	492%	490%	487%	450%
X2H008	4	44	103	158	219	320	413	489	30	72	115	170	262	351	457	47%	42%	37%	29%	22%	18%	7%
X2H031	4	53	124	190	264	386	498	590	30	106	206	355	656	987	1437	78%	17%	-8%	-26%	-41%	-50%	-59%
X3H001	4	43	101	155	215	315	406	481	14	27	39	52	72	89	109	210%	274%	298%	313%	337%	356%	341%
C1H001	5	209	507	813	1143	1656	2148	2648	277	614	930	1310	1928	2492	3156	-25%	-17%	-13%	-13%	-14%	-14%	-16%
C5H008	5	56	136	219	307	446	578	712	49	135	228	353	577	800	1079	15%	1%	-4%	-13%	-23%	-28%	-34%
C6H001	5	174	422	677	951	1378	1788	2203	401	919	1417	2025	3029	3959	5063	-57%	-54%	-52%	-53%	-54%	-55%	-56%
C7H005	5	172	418	671	943	1366	1772	2184	67	263	536	966	1875	2915	4372	157%	59%	25%	-2%	-27%	-39%	-50%
C8H003	5	65	159	255	358	519	674	830	49	120	190	280	431	575	750	34%	32%	34%	28%	21%	17%	11%
D1H001	5	113	274	440	618	896	1162	1432	99	280	465	695	1071	1415	1811	14%	-2%	-5%	-11%	-16%	-18%	-21%
D5H003	5	90	218	349	490	711	922	1136	60	160	268	410	662	910	1219	49%	36%	30%	20%	7%	1%	-7%
J2H016	5	301	732	1174	1650	2391	3101	3822	32	163	383	775	1713	2903	4714	841%	349%	207%	113%	40%	7%	-19%
L1H001	5	145	351	564	792	1148	1489	1835	159	393	642	974	1571	2176	2945	-9%	-11%	-12%	-19%	-27%	-32%	-38%
L2H003	5	78	189	304	427	619	803	990	35	104	185	298	509	726	1007	123%	82%	64%	43%	22%	11%	-2%
A2H004	6	20	58	104	162	259	343	427	6	19	34	55	95	136	189	230%	208%	207%	194%	172%	153%	126%
A7H001	6	149	439	784	1214	1941	2575	3199	64	229	460	831	1641	2609	4016	132%	92%	70%	46%	18%	-1%	-20%
C3H003	7	68	193	306	446	657	837	1031	118	268	420	615	954	1287	1702	-42%	-28%	-27%	-28%	-31%	-35%	-39%
D5H001	7	30	84	133	194	287	365	450	110	278	451	673	1056	1424	1875	-73%	-70%	-70%	-71%	-73%	-74%	-76%
D6H002	7	52	148	234	341	503	641	789	150	246	319	394	501	588	681	-65%	-40%	-27%	-13%	0%	9%	16%

Appendix D

Table 39: Evaluation of the Proposed MIPI updates for Region 1 to 3

Gauge ID	Region	Updated MIPI design floods (m^3/s)							Probabilistic floods (m^3/s)							Difference in %						
		Recurrence intervals (yrs.)							Recurrence intervals (yrs.)							Recurrence intervals (yrs.)						
		2	5	10	20	50	100	200	2	5	10	20	50	100	200	2	5	10	20	50	100	200
E2H002	1	950	1577	2055	2587	3410	4100	4495	263	535	775	1052	1486	1870	2309	261%	195%	165%	146%	129%	119%	95%
H1H006	1	314	521	679	854	1126	1354	1485	337	521	655	790	976	1123	1278	-7%	0%	4%	8%	15%	21%	16%
A2H012	2	168	433	735	1088	1572	2003	2464	119	254	391	566	876	1186	1576	42%	71%	88%	92%	80%	69%	56%
A2H013	2	114	293	498	737	1065	1357	1669	69	214	386	628	1089	1569	2196	65%	37%	29%	17%	-2%	-14%	-24%
A2H023	2	87	225	381	564	815	1038	1278	113	209	288	375	506	618	742	-23%	7%	32%	50%	61%	68%	72%
A2H027	2	63	162	275	407	588	749	922	42	113	188	287	463	636	851	50%	43%	46%	42%	27%	18%	8%
A2H029	2	38	97	165	245	354	450	554	6	17	31	51	94	145	220	531%	473%	434%	380%	276%	211%	152%
B2H001	2	133	342	581	860	1243	1583	1947	95	306	564	933	1645	2399	3394	40%	12%	3%	-8%	-24%	-34%	-43%
T3H002	2	153	393	667	987	1427	1817	2236	213	457	681	947	1372	1756	2203	-28%	-14%	-2%	4%	4%	3%	1%
T3H005	2	170	437	742	1098	1587	2020	2486	150	552	1088	1906	3583	5453	8021	13%	-21%	-32%	-42%	-56%	-63%	-69%
U2H013	2	58	148	252	372	538	686	843	45	91	131	178	250	314	387	28%	63%	92%	109%	115%	118%	118%
V6H003	2	59	151	257	380	550	700	862	96	171	232	300	402	490	589	-39%	-11%	11%	27%	37%	43%	46%
V6H004	2	86	220	374	552	799	1017	1251	103	204	293	395	551	689	846	-17%	8%	27%	40%	45%	48%	48%
J3H004	3	118	456	997	1877	3862	6270	9765	99	441	962	1830	3780	6123	9539	20%	3%	4%	3%	2%	2%	2%
L6H001	3	65	251	549	1034	2127	3454	5378	80	339	722	1349	2726	4353	6692	-19%	-26%	-24%	-23%	-22%	-21%	-20%
P1H003	3	70	269	588	1107	2278	3698	5759	25	101	212	393	792	1269	1957	179%	166%	177%	182%	188%	191%	194%
Q3H004	3	54	206	452	850	1749	2839	4422	52	172	322	540	968	1428	2039	3%	20%	40%	57%	81%	99%	117%

Table 40: Evaluation of the Proposed MIPI updates for Region 4 to 7

Gauge ID	Region	|Updated MIPI design floods (m^3/s)							Probabilistic floods (m^3/s)							Difference in %						
		Recurrence intervals (yrs.)							Recurrence intervals (yrs.)							Recurrence intervals (yrs.)						
		2	5	10	20	50	100	200	2	5	10	20	50	100	200	2	5	10	20	50	100	200
B6H001	4	62	159	235	340	503	647	820	63	134	200	278	404	518	652	-2%	19%	17%	22%	25%	25%	26%
S3H006	4	126	326	480	696	1030	1324	1677	58	152	252	380	606	826	1097	117%	114%	91%	83%	70%	60%	53%
T4H001	4	72	187	276	399	591	760	963	97	239	382	564	874	1169	1528	-25%	-22%	-28%	-29%	-32%	-35%	-37%
U2H004	4	136	351	517	750	1110	1426	1807	127	254	364	490	685	856	1051	7%	38%	42%	53%	62%	67%	72%
U3H002	4	51	132	195	282	417	536	679	39	98	158	234	365	491	645	31%	35%	23%	20%	14%	9%	5%
W2H005	4	170	439	647	938	1388	1784	2260	302	712	1114	1612	2444	3223	4157	-44%	-38%	-42%	-42%	-43%	-45%	-46%
W3H001	4	104	268	395	572	847	1089	1379	90	302	569	959	1729	2559	3668	15%	-11%	-31%	-40%	-51%	-57%	-62%
W5H011	4	82	211	311	451	667	857	1086	17	39	59	83	122	158	200	381%	441%	427%	443%	447%	443%	443%
X2H008	4	36	94	138	200	297	381	483	30	72	115	170	262	351	457	21%	30%	20%	18%	13%	9%	6%
X2H031	4	44	113	167	242	358	460	583	30	106	206	355	656	987	1437	46%	7%	-19%	-32%	-45%	-53%	-59%
X3H001	4	36	92	136	197	292	375	475	14	27	39	52	72	89	109	155%	242%	249%	279%	305%	321%	336%
C1H001	5	189	535	888	1335	2093	2704	3471	277	614	930	1310	1928	2492	3156	-32%	-13%	-4%	2%	9%	9%	10%
C5H008	5	51	144	239	359	563	728	934	49	135	228	353	577	800	1079	4%	7%	5%	2%	-2%	-9%	-13%
C6H001	5	157	445	739	1111	1742	2251	2889	401	919	1417	2025	3029	3959	5063	-61%	-52%	-48%	-45%	-43%	-43%	-43%
C7H005	5	156	442	733	1102	1727	2231	2864	67	263	536	966	1875	2915	4372	133%	68%	37%	14%	-8%	-23%	-34%
C8H003	5	59	168	279	419	656	848	1089	49	120	190	280	431	575	750	21%	40%	47%	50%	52%	48%	45%
D1H001	5	102	290	480	722	1132	1463	1878	99	280	465	695	1071	1415	1811	3%	3%	3%	4%	6%	3%	4%
D5H003	5	81	230	381	573	898	1161	1490	60	160	268	410	662	910	1219	35%	44%	42%	40%	36%	28%	22%
J2H016	5	273	773	1282	1928	3021	3904	5012	32	163	383	775	1713	2903	4714	752%	374%	235%	149%	76%	34%	6%
L1H001	5	131	371	616	926	1451	1875	2407	159	393	642	974	1571	2176	2945	-18%	-6%	-4%	-5%	-8%	-14%	-18%
L2H003	5	71	200	332	499	782	1011	1298	35	104	185	298	509	726	1007	102%	92%	79%	68%	54%	39%	29%
A2H004	6	9	31	63	114	226	358	552	6	19	34	55	95	136	189	42%	64%	84%	108%	138%	163%	192%
A7H001	6	64	234	470	858	1693	2684	4136	64	229	460	831	1641	2609	4016	0%	2%	2%	3%	3%	3%	3%
C3H003	7	193	319	428	630	973	1315	1743	118	268	420	615	954	1287	1702	64%	19%	2%	2%	2%	2%	2%
D5H001	7	84	139	187	275	424	573	760	110	278	451	673	1056	1424	1875	-23%	-50%	-59%	-59%	-60%	-60%	-59%
D6H002	7	148	244	328	482	745	1006	1334	150	246	319	394	501	588	681	-1%	-1%	3%	22%	49%	71%	96%

Appendix E

Table 41: Evaluation and updating of Q_S for slopes between 0 and 0.043 m/m

Gauge ID	Statistical Q_S (m^3/s)	Calculated Q_S (m^3/s)	Lumped Parameter M	Catchment Area (km^2)	MAP (mm)	Mean Catchment Slope (m/m)	Longest Watercourse (km)	Difference in percentage	Corrected Q_S (m^3/s)	Difference in percentage
T3H002	354	88	574	2109	776	0.010	84	-75%	150	-58%
T4H001	198	50	636	736	825	0.014	64	-75%	84	-57%
H1H006	402	110	1651	734	579	0.135	45	-73%	186	-54%
L1H001	296	84	332	3934	214	0.050	130	-72%	142	-52%
W3H001	300	87	746	1466	824	0.027	126	-71%	148	-51%
D5H001	156	51	288	2165	147	0.093	113	-68%	86	-45%
Q3H004	160	54	611	873	353	0.068	67	-66%	92	-42%
C1H001	419	143	373	8009	676	0.008	235	-66%	244	-42%
B2H001	221	88	703	1582	662	0.021	74	-60%	149	-33%
C5H008	87	35	483	608	505	0.020	54	-59%	60	-31%
J3H004	212	91	350	4292	189	0.068	130	-57%	155	-27%
W2H005	650	291	1589	3952	776	0.120	180	-55%	495	-24%
C6H001	618	279	1136	5645	596	0.115	238	-55%	473	-23%
A2H027	103	47	1002	367	691	0.045	41	-55%	79	-23%
A2H023	151	70	1009	688	674	0.053	62	-54%	119	-21%
V6H003	128	65	1687	295	826	0.085	35	-49%	111	-13%
D6H002	185	105	302	6898	279	0.023	163	-44%	178	-4%
E2H002	384	225	749	6784	306	0.112	154	-41%	383	0%
T3H005	322	198	1350	2578	786	0.079	136	-38%	337	5%
D1H001	207	131	852	2387	427	0.053	65	-37%	223	7%
V6H004	147	93	1500	659	840	0.087	70	-37%	159	8%
C8H003	83	60	730	869	668	0.090	222	-28%	101	22%
J2H016	275	199	321	17085	160	0.067	217	-28%	339	23%
A2H012	196	149	958	2345	664	0.043	100	-24%	254	30%

Table 42: Evaluation and updating of Q_S for slopes between 0.063 and 0.545 m/m

Gauge ID	Statistical QS	Calculated QS	Lumped Parameter M	Catchment Area (km2)	MAP (mm)	Mean Catchment Slope (m/m)	Longest Watercourse (km)	Difference in percentage	Corrected QS	Difference in percentage
A2H013	135	107	1138	1062	650	0.063	67	-21%	181	34%
X2H031	75	63	1856	263	905	0.096	37	-16%	107	42%
C3H003	204	179	394	11218	487	0.018	292	-12%	304	49%
A7H001	214	190	557	7704	423	0.033	167	-11%	323	51%
C7H005	186	188	702	5661	572	0.039	195	1%	319	72%
U2H013	68	85	2447	297	864	0.135	29	26%	145	115%
P1H003	79	110	993	1474	475	0.099	87	39%	187	137%
S3H006	99	158	1162	2207	440	0.135	91	59%	268	171%
A2H029	14	25	1015	124	693	0.052	27	77%	43	200%
W5H011	33	74	874	883	777	0.026	61	125%	126	282%
A2H004	14	32	1290	132	608	0.098	25	132%	54	295%
U3H002	70	112	3000	360	932	0.142	26	60%	81	17%
W1H004	10	22	3529	20	1125	0.154	7	122%	15	52%
X2H008	49	69	2738	187	956	0.162	27	39%	49	0%
L2H003	68	94	995	1152	321	0.167	59	39%	69	1%
U2H004	231	271	2040	2261	919	0.171	165	17%	199	-14%
B6H001	99	125	2605	514	991	0.189	62	26%	92	-8%
K4H003	32	34	2265	74	696	0.197	16	5%	24	-26%
D5H003	105	75	606	1487	213	0.197	94	-28%	54	-48%
X3H001	20	94	4157	178	1112	0.199	19	366%	68	239%
G1H004	267	84	7310	74	1513	0.407	15	-68%	143	-46%
J4H003	66	27	1371	92	423	0.219	20	-60%	45	-31%
L6H001	183	79	732	1287	232	0.219	79	-57%	135	-26%
R2H008	84	50	4220	68	951	0.406	17	-40%	85	1%
H7H004	20	13	3304	10	755	0.545	9	-36%	22	9%
G2H008	56	41	7647	22	1418	0.434	7	-28%	69	23%
B7H002	52	44	3687	62	878	0.224	10	-15%	74	44%
R2H012	18	26	5533	17	1012	0.435	6	48%	45	151%
R2H001	19	56	8553	31	1299	0.545	7	201%	95	411%

Appendix F

Table 43: Evaluation of the CAPA design floods for gauges within quaternaries A to C

Gauge ID	Original CAPA design floods (m^3/s)					Probabilistic floods (m^3/s)					Difference in %				
	Recurrence intervals (yrs.)					Recurrence intervals (yrs.)					Recurrence intervals (yrs.)				
	5	**10**	**20**	**50**	**100**	**5**	**10**	**20**	**50**	**100**	**5**	**10**	**20**	**50**	**100**
A2H004	30	45	64	96	121	19	34	55	95	136	57%	32%	17%	1%	-11%
A2H012	416	618	873	1293	1631	254	391	566	876	1186	64%	58%	54%	48%	38%
A2H013	289	431	609	904	1141	214	386	628	1089	1569	35%	12%	-3%	-17%	-27%
A2H023	318	472	666	985	1242	209	288	375	506	618	52%	64%	78%	95%	101%
A2H027	215	316	444	654	822	113	188	287	463	636	90%	68%	55%	41%	29%
A2H029	30	44	62	91	114	17	31	51	94	145	75%	42%	21%	-4%	-21%
A7H001	533	853	1267	1967	2556	229	460	831	1641	2609	133%	86%	52%	20%	-2%
B2H001	469	697	984	1457	1838	306	564	933	1645	2399	53%	24%	5%	-11%	-23%
B6H001	176	242	323	453	554	134	200	278	404	518	32%	21%	16%	12%	7%
B7H002	98	138	187	268	331	40	99	221	574	1124	144%	39%	-15%	-53%	-71%
C1H001	879	1300	1829	2699	3398	614	930	1310	1928	2492	43%	40%	40%	40%	36%
C3H003	483	756	1105	1691	2177	268	420	615	954	1287	80%	80%	80%	77%	69%
C5H008	204	317	461	701	901	135	228	353	577	800	51%	39%	31%	22%	13%
C6H001	1383	2108	3027	4552	5800	919	1417	2025	3029	3959	51%	49%	49%	50%	47%
C7H005	415	632	907	1363	1736	263	536	966	1875	2915	58%	18%	-6%	-27%	-40%
C8H003	175	259	366	541	681	120	190	280	431	575	46%	37%	31%	25%	19%

Table 44: Evaluation of the CAPA design floods for gauges within quaternaries D to Q

Gauge ID	Original CAPA design floods (m^3/s)					Probabilistic floods (m^3/s)					Difference in %				
	Recurrence intervals (yrs.)					Recurrence intervals (yrs.)					Recurrence intervals (yrs.)				
	5	**10**	**20**	**50**	**100**	**5**	**10**	**20**	**50**	**100**	**5**	**10**	**20**	**50**	**100**
D1H001	517	828	1229	1908	2479	280	465	695	1071	1415	85%	78%	77%	78%	75%
D5H001	578	1112	1869	3263	4560	278	451	673	1056	1424	108%	146%	178%	209%	220%
D5H003	338	608	978	1637	2229	160	268	410	662	910	111%	127%	139%	147%	145%
D6H002	543	937	1463	2384	3190	246	319	394	501	588	121%	194%	271%	376%	443%
E2H002	1143	1986	3116	5099	6844	535	775	1052	1486	1870	114%	156%	196%	243%	266%
G1H004	440	582	760	1045	1259	334	404	472	563	633	32%	44%	61%	86%	99%
G2H008	94	126	165	229	276	94	168	270	462	659	0%	-25%	-39%	-51%	-58%
H1H006	902	1377	1979	2979	3798	521	655	790	976	1123	73%	110%	150%	205%	238%
H7H004	40	58	81	118	148	26	42	63	101	141	55%	39%	29%	17%	5%
J2H016	991	1881	3133	5425	7540	163	383	775	1713	2903	508%	391%	304%	217%	160%
J3H004	712	1310	2136	3626	4978	441	962	1830	3780	6123	61%	36%	17%	-4%	-19%
J4H003	170	276	414	648	846	93	143	204	303	394	83%	93%	103%	114%	115%
K4H003	67	98	138	202	254	38	75	133	260	410	75%	31%	3%	-22%	-38%
L1H001	956	1726	2781	4664	6356	393	642	974	1571	2176	143%	169%	185%	197%	192%
L2H003	186	312	477	762	1007	104	185	298	509	726	79%	69%	60%	50%	39%
L6H001	574	1023	1632	2712	3676	339	722	1349	2726	4353	69%	42%	21%	-1%	-16%
P1H003	188	296	433	663	854	101	212	393	792	1269	87%	39%	10%	-16%	-33%
Q3H004	429	710	1078	1710	2252	172	322	540	968	1428	149%	120%	100%	77%	58%

Table 45: Evaluation of the CAPA design floods for gauges within quaternaries R to X

Gauge ID	Original CAPA design floods (m^3/s)					Probabilistic floods (m^3/s)					Difference in %				
	Recurrence intervals (yrs.)					Recurrence intervals (yrs.)					Recurrence intervals (yrs.)				
	5	**10**	**20**	**50**	**100**	**5**	**10**	**20**	**50**	**100**	**5**	**10**	**20**	**50**	**100**
R2H001	30	40	52	72	87	26	42	63	99	133	17%	-4%	-17%	-27%	-35%
R2H008	154	214	289	410	504	131	354	805	2032	3760	18%	-39%	-64%	-80%	-87%
R2H012	32	44	60	84	103	30	59	101	187	282	7%	-25%	-41%	-55%	-63%
S3H006	239	378	556	856	1106	152	252	380	606	826	58%	50%	46%	41%	34%
T3H002	711	1029	1427	2077	2594	457	681	947	1372	1756	55%	51%	51%	51%	48%
T3H005	637	917	1267	1837	2289	552	1088	1906	3583	5453	15%	-16%	-34%	-49%	-58%
T4H001	388	556	765	1107	1376	239	382	564	874	1169	62%	45%	36%	27%	18%
U2H004	432	607	824	1175	1449	254	364	490	685	856	70%	67%	68%	72%	69%
U2H013	129	183	249	358	443	91	131	178	250	314	42%	39%	40%	43%	41%
U3H002	129	181	245	348	429	98	158	234	365	491	32%	14%	5%	-5%	-13%
V6H003	248	354	486	700	869	171	232	300	402	490	45%	52%	62%	74%	77%
V6H004	285	407	558	804	998	204	293	395	551	689	40%	39%	41%	46%	45%
W1H004	17	23	30	42	51	13	28	53	109	176	31%	-18%	-43%	-62%	-71%
W2H005	1292	1865	2581	3749	4675	712	1114	1612	2444	3223	82%	67%	60%	53%	45%
W3H001	576	817	1118	1607	1991	302	569	959	1729	2559	91%	44%	17%	-7%	-22%
W5H011	66	95	131	191	238	39	59	83	122	158	68%	61%	58%	56%	51%
X2H008	93	131	178	255	315	72	115	170	262	351	29%	14%	5%	-3%	-10%
X2H031	142	201	273	390	482	106	206	355	656	987	34%	-3%	-23%	-41%	-51%
X3H001	34	46	60	84	101	27	39	52	72	89	26%	17%	16%	16%	14%

Appendix G

Table 46: Evaluation of the updated CAPA design floods within quaternaries A to C

Gauge ID	Updated CAPA design floods (m^3/s)						Probabilistic floods (m^3/s)						Difference in %					
	Recurrence intervals (yrs.)						Recurrence intervals (yrs.)						Recurrence intervals (yrs.)					
	5	**10**	**20**	**50**	**100**	**200**	**5**	**10**	**20**	**50**	**100**	**200**	**5**	**10**	**20**	**50**	**100**	**200**
A2H004	18	29	42	67	88	112	19	34	55	95	136	189	-3%	-15%	-23%	-29%	-36%	-41%
A2H012	264	411	606	959	1252	1604	254	391	566	876	1186	1576	4%	5%	7%	9%	6%	2%
A2H013	183	284	420	663	867	1110	214	386	628	1089	1569	2196	-15%	-26%	-33%	-39%	-45%	-49%
A2H023	203	317	467	739	965	1236	209	288	375	506	618	742	-3%	10%	25%	46%	56%	67%
A2H027	139	216	319	505	659	845	113	188	287	463	636	851	23%	15%	11%	9%	4%	-1%
A2H029	19	30	44	70	92	118	17	31	51	94	145	220	14%	-3%	-13%	-25%	-37%	-47%
A7H001	289	449	663	1048	1369	1755	229	460	831	1641	2609	4016	26%	-2%	-20%	-36%	-48%	-56%
B2H001	298	464	685	1083	1414	1812	306	564	933	1645	2399	3394	-2%	-18%	-27%	-34%	-41%	-47%
B6H001	134	208	308	486	635	814	134	200	278	404	518	652	0%	4%	11%	20%	23%	25%
B7H002	70	108	160	252	330	422	40	99	221	574	1124	2128	74%	9%	-28%	-56%	-71%	-80%
C1H001	566	880	1299	2053	2681	3435	614	930	1310	1928	2492	3156	-8%	-5%	-1%	6%	8%	9%
C3H003	275	429	633	1000	1306	1673	268	420	615	954	1287	1702	3%	2%	3%	5%	1%	-2%
C5H008	118	184	271	428	560	717	135	228	353	577	800	1079	-13%	-19%	-23%	-26%	-30%	-34%
C6H001	834	1298	1916	3029	3956	5068	919	1417	2025	3029	3959	5063	-9%	-8%	-5%	0%	0%	0%
C7H005	251	390	576	910	1189	1523	263	536	966	1875	2915	4372	-5%	-27%	-40%	-51%	-59%	-65%
C8H003	112	174	257	406	530	679	120	190	280	431	575	750	-7%	-8%	-8%	-6%	-8%	-9%

Table 47: Evaluation of the updated CAPA design floods within quaternaries D to Q

Gauge ID	Updated CAPA design floods (m^3/s)						Probabilistic floods (m^3/s)						Difference in %					
	Recurrence intervals (yrs.)						Recurrence intervals (yrs.)						Recurrence intervals (yrs.)					
	5	**10**	**20**	**50**	**100**	**200**	**5**	**10**	**20**	**50**	**100**	**200**	**5**	**10**	**20**	**50**	**100**	**200**
D1H001	280	436	643	1016	1327	1701	280	465	695	1071	1415	1811	0%	-6%	-7%	-5%	-6%	-6%
D5H001	210	327	483	764	998	1279	278	451	673	1056	1424	1875	-24%	-27%	-28%	-28%	-30%	-32%
D5H003	142	221	326	515	672	862	160	268	410	662	910	1219	-11%	-18%	-21%	-22%	-26%	-29%
D6H002	250	389	574	908	1186	1519	246	319	394	501	588	681	2%	22%	46%	81%	102%	123%
E2H002	518	807	1191	1882	2458	3149	535	775	1052	1486	1870	2309	-3%	4%	13%	27%	31%	36%
G1H004	360	560	827	1307	1707	2187	334	404	472	563	633	706	8%	39%	75%	132%	170%	210%
G2H008	76	118	174	275	360	461	94	168	270	462	659	915	-19%	-30%	-36%	-40%	-45%	-50%
H1H006	542	843	1245	1968	2570	3293	521	655	790	976	1123	1278	4%	29%	58%	102%	129%	158%
H7H004	27	42	62	98	128	164	26	42	63	101	141	192	4%	0%	-2%	-3%	-9%	-15%
J2H016	372	578	853	1349	1762	2258	163	383	775	1713	2903	4714	128%	51%	10%	-21%	-39%	-52%
J3H004	286	444	656	1036	1354	1734	441	962	1830	3780	6123	9539	-35%	-54%	-64%	-73%	-78%	-82%
J4H003	89	139	205	324	423	543	93	143	204	303	394	503	-4%	-3%	1%	7%	7%	8%
K4H003	43	67	99	157	205	263	38	75	133	260	410	626	14%	-10%	-25%	-40%	-50%	-58%
L1H001	399	621	916	1448	1891	2423	393	642	974	1571	2176	2945	2%	-3%	-6%	-8%	-13%	-18%
L2H003	92	143	211	333	436	558	104	185	298	509	726	1007	-12%	-23%	-29%	-34%	-40%	-45%
L6H001	247	385	568	897	1172	1502	339	722	1349	2726	4353	6692	-27%	-47%	-58%	-67%	-73%	-78%
P1H003	107	166	245	388	506	649	101	212	393	792	1269	1957	6%	-22%	-38%	-51%	-60%	-67%
Q3H004	216	336	496	784	1024	1313	172	322	540	968	1428	2039	26%	4%	-8%	-19%	-28%	-36%

Table 48: Evaluation of the updated CAPA design floods within quaternaries R to X

Gauge ID	Updated CAPA design floods (m^3/s)						Probabilistic floods (m^3/s)						Difference in %					
	Recurrence intervals (yrs.)						Recurrence intervals (yrs.)						Recurrence intervals (yrs.)					
	5	10	20	50	100	200	5	10	20	50	100	200	5	10	20	50	100	200
R2H001	25	39	58	91	119	152	26	42	63	99	133	175	-4%	-7%	-9%	-8%	-11%	-13%
R2H008	113	176	260	411	536	687	131	354	805	2032	3760	6620	-14%	-50%	-68%	-80%	-86%	-90%
R2H012	24	38	55	88	114	147	30	59	101	187	282	410	-20%	-36%	-45%	-53%	-59%	-64%
S3H006	134	208	307	485	634	812	152	252	380	606	826	1097	-12%	-18%	-19%	-20%	-23%	-26%
T3H002	479	744	1099	1737	2269	2907	457	681	947	1372	1756	2203	5%	9%	16%	27%	29%	32%
T3H005	434	676	997	1577	2059	2639	552	1088	1906	3583	5453	8021	-21%	-38%	-48%	-56%	-62%	-67%
T4H001	267	416	613	970	1266	1622	239	382	564	874	1169	1528	12%	9%	9%	11%	8%	6%
U2H004	312	485	716	1131	1478	1893	254	364	490	685	856	1051	23%	33%	46%	65%	73%	80%
U2H013	91	142	209	331	432	554	91	131	178	250	314	387	0%	8%	18%	32%	38%	43%
U3H002	94	147	216	342	447	572	98	158	234	365	491	645	-4%	-7%	-8%	-6%	-9%	-11%
V6H003	172	268	396	626	817	1047	171	232	300	402	490	589	1%	16%	32%	56%	67%	78%
V6H004	199	309	456	721	942	1207	204	293	395	551	689	846	-3%	6%	16%	31%	37%	43%
W1H004	13	21	31	48	63	81	13	28	53	109	176	273	3%	-26%	-42%	-56%	-64%	-70%
W2H005	877	1364	2014	3183	4157	5326	712	1114	1612	2444	3223	4157	23%	22%	25%	30%	29%	28%
W3H001	405	630	930	1470	1921	2461	302	569	959	1729	2559	3668	34%	11%	-3%	-15%	-25%	-33%
W5H011	44	69	102	161	211	270	39	59	83	122	158	200	14%	17%	23%	32%	33%	35%
X2H008	67	104	153	242	316	405	72	115	170	262	351	457	-7%	-10%	-10%	-8%	-10%	-11%
X2H031	102	159	234	370	483	619	106	206	355	656	987	1437	-4%	-23%	-34%	-44%	-51%	-57%
X3H001	27	42	62	98	129	165	27	39	52	72	89	109	0%	8%	20%	37%	45%	51%